DIELECTRIC STUDIES OF NOVEL POLYMERIC SYSTEMS

by

Ann Marie Walstrom Norris

Dissertation submitted to the Faculty of the
Virginia Polytechnic Institute and State University
in partial fulfillment of the requirements for the degree of

DOCTOR OF PHILOSOPHY

in

Materials Engineering Science

APPROVED:

Thomas C. Ward, Chairman

James E. McGrath

James P. Wightman

Harry W. Gibson

Halbert F. Brinson

March, 1987

Blacksburg, Virginia

DIELECTRIC STUDIES OF NOVEL POLYMERIC SYSTEMS

by

Ann Marie Walstrom Norris

Committee Chairman: Thomas C. Ward
Materials Engineering Science

(ABSTRACT)

This work combines many characterization techniques in an effort to enhance understanding of molecular motions of polymers and how they are influenced by structure. The primary characterization method was dielectric spectroscopy which utilizes an AC electric field as the stress field.

A variety of new, well controlled polymeric systems were studied. The first series included a number of radial starblock copolymers, styrene/isoprene, t-butyl-styrene/isoprene, and t-butylstyrene/butadiene. These ABA copolymers consisted of hard and soft blocks, with the soft block comprising 75% by weight. The effect of microstructure of the soft block, casting solvent, hydrogenation, and chemical composition of the hard block were some of the variables studied. The amount of phase separation and the molecular motions occuring will be influenced by these parameters. Hydrogenation of the soft block increased the phase separation.

Another system investigated included some stereospecific poly(alkyl methacrylates) which were

synthesized anionically. In this series the alkyl group was systematically changed in order to study the effects of the bulkiness of the substituent and the tacticity on the α and β transitions. The β transition associated with side chain rotations was only observed in the case of the methyl and ethyl substituents. The Havriliak-Negami data analysis was used to evaluate the breadth and the skewness of the distribution of relaxation times.

Finally, some high temperature thermoplastic polymers were evaluated with dielectric spectroscopy. The effect of the backbone composition, moisture, and fillers on the β transition was looked at. These studies showed that moisture and fillers play an important role on the magnitude and temperature of the observed β transition.

ACKNOWLEDGEMENTS

The author would like to express sincere graditude and appreciation to Dr. Thomas C. Ward for guidance and encouragement throughout the pursuit of this research and degree. Appreciation is also extented to Drs. James E. McGrath, James P. Wightman, Harry Gibson, David Dwight, and Hal Brinson for agreeing to serve as my committee members.

The author also would like to acknowledge all of the PMIL faculty and their students. The cooperative research and academic efforts that result from this inter-departmental program are extremely beneficial.

A special thanks to , and for their synthetic efforts and helpful discussions. Appreciation is also extended to and for the GPC results and Dr. Raj Subramanian for the NMR and DSC results.

Also, I would like to acknowledge the financial support provided by the Dow Corning Corporation through the form of a four year fellowship awarded to me.

A special thanks to the Polymer Physical Chemistry and Polymer Synthesis Groups for their friendship and research cooperation.

Lastly, I need to thank my family who's encouragement kept me going; and my husband, , who was always there providing support when I needed it the most.

Table of Contents

LIST OF FIGURES

LIST OF TABLES

CHAPTER I

INTRODUCTION

The molecular motions occuring in polymeric materials are important to understand because they influence many properties. Amorphous regions in polymers undergo an α transition at the glass transition temperature (Tg) and, depending on the structure, β, γ, etc. transitions may be observed at lower temperatures. It is well accepted that the α transition is associated with micro-Brownian type main chain mobility as the polymer passes from a glassy to a rubbery state. The sub-glass transition relaxations (β, γ, etc.) have been identified as side-group rotations or other more localized main chain motions.

Molecular movements occuring in polymers can be monitored by various methods, the most common being listed in Table 1 (1). It is important to note that to observe all the motions which exist in polymers eleven or twelve decades of frequency are required. In this work dielectric spectroscopy will be used in addition to dynamic mechanical analysis. The dielectric technique has proven to be a powerful tool in recent years for the study of polymer solids and solutions (1-5). Although solution studies provide important information on molecular conformations, only the application to solid polymeric materials will be discussed here. Dielectric spectroscopy utilizes an

Table 1

MEASUREMENT OF MOLECULAR MOVEMENT (1)

Phenomenon	Constraint Varied	Property Observed
Dynamic mechanical (0.01-100 Hz)	Stress, strain	Strain, stress, modulus
Viscoelastic relaxation (0.1-50 Hz)	Shear stress & rate	Dynamic η, shear modulus
Dielectric relaxation (50 Hz-100 KHz)	Electric field	Electric Polarization Capacitance, loss
NMR, ESR (60-600 MHz)	Magnetic field	Nuclear and electron polarization

alternating electric field as the stress source to study transitions in a polymer as a function of temperature and frequency. These transitions detected correlate to the rotation of permanent electric dipoles or induces dipoles.

In general, when two unlike atoms are chemically bonded a permanent electric dipole moment results, due to their difference in electronegativity. With polymers the bond moments vectorially sum up to molecular or segmental moments of many molecular configurations and/or conformations. Polymers, due to their net moments, can be polarized by an electric field. The measurement of the polarization induced in such dielectrically active polymers has proven to be an extremely useful method of probing polymer structure (6).

In this work a number of new polymers were analyzed utilizing dielectric spectroscopy and other thermal analytical techniques. One investigation involved two series of radial starblock copolymers. These series of copolymers were synthesized anionically giving very well controlled chemical composition. The variable in the first series was the microstructure of the polybutadiene soft block; the hard block, poly(t-butylstyrene), was kept constant. In the second series the hard block was either polystyrene or poly(t-butylstyrene), with the soft block being polyisoprene. The effect of casting solvent on the observed transitions was also investigated with the second series. In all cases the polymers were elastomeric, with

the soft block comprising 75 percent and the hard block comprising 25 percent of the overall weight. Although the dynamic mechanical analysis has been utilized to study microphase separation in block copolymers, the dielectric technique has been, for the most part, overlooked. Therefore this technique was chosen to supplement the dynamic mechanical information on these new radial starblock copolymers.

Another system studied was a series of stereospecific poly(alkyl methacrylates). These polymers were synthesized anionically to have high syndiotactic and atactic triad microstructure. The alkyl substiuent was systematically changed to investigate the effect of the bulkiness of the side group on the α and β transitions. It is well known (5a) that any steric hinderance which increases the barriers to rotation (decrease the overall chain flexibility) can increase the glass transition temperature and, hence, the α and possibly the β transitions will also be effected.

The last system studied was a series of high performance thermoplastics. These polymers have excellent thermal and hydrolytic stability, they also exhibit high impact strength which is partly due to a very prevalent β transition. In this new series of polymers we systematically altered the chemical structure of the backbone and compared the properties to that of the commercially available UDEL^{TM}.

In all of the polymers studied the synthetic chemistry techniques employed resulted in very well-defined materials for investigating structure/property relationships. The theory and instrumentation involved in such a challenge will be presented.

CHAPTER II

GENERAL BACKGROUND AND THEORY

A. Introduction

The theory behind dielectric relaxation studies was first applied to the study of low molecular weight compounds (7,8). It has become increasingly important in the study of polymeric solids. The technique of dielectric spectroscopy involves exposing the polymer to an alternating electrical field. Any electrical dipoles present, located either along the backbone or on side chains, try to align with the field. Their ability to align will be a function of the temperature and frequency of the experiment as well as polymer structure.

In this chapter the background of the dielectric technique and the phenomenological models will be discussed. The experimental details, the analogy to dynamic mechanical analysis, and the applicability of the technique for polymer characterization will also be covered.

B. Fundamentals and Phenomenological Models

1. Introduction to Theory

In order to present a complete picture of the dielectric properties of materials some basic concepts follow. Consider first a parallel plate capacitor. If a voltage, V_o, is applied in vacuum, a charge, q_0, will build up.

$$V_0 = \frac{q_0}{C_0} \tag{1}$$

where $C_0 = A/4\pi d$, with A being the area of the plates and d the separation between the two plates. After inserting a dielectric between the plates the capacitance increases to C.

$$V_0 = \frac{q_1}{C} \tag{2}$$

The dielectric constant, or relative permittivity, ϵ, is defined as follows:

$$\epsilon = \frac{C}{C_0} = \frac{q_0}{q_1} \tag{3}$$

The value q_0 is known as the true charge and is the charge actually placed on the capacitor, whereas q_1 is the free charge and is the proportion of the true charge which contributes to the voltage. The difference in the charges, $(q_0 - q_1)$, is known as the bound charge. The polarization of the dielectric is defined as:

$$P = \frac{1}{A} (q_0 - q_1) \tag{4}$$

The electric field, E, generated by the free charge is defined as:

$$E = \frac{4\pi q_1}{A} \tag{5}$$

and the electric displacement, D, is defined as:

$$D = \frac{4\pi q_0}{A} \tag{6}$$

The dielectric constant is related to these quantities by the following relationship:

$$D = \epsilon * E \qquad (7)$$

Up to this point in the discussion it has been assumed that the dielectric constant was time independent, however, there is a time dependency. Because of the nature of polymeric solids the application of a constant electric field (E_0) leads to an increase in polarization, hence, a time dependent dielectric constant:

$$\epsilon(t) = \frac{D(t)}{E_0} \qquad (8)$$

At short times (or high frequency), $\epsilon(t)$ tends toward the value ϵ_u (or ϵ_0) the unrelaxed dielectric constant. At long times (or low frequencies) $\epsilon(t)$ tends toward ϵ_R (or ϵ_∞), the relaxed dielectric constant; this time dependency is shown in Figure 1. Also, E_0 is analogous to σ_0, the mechanical stress, whereas D(t) is analogous to $\gamma(t)$, the mechanical strain. The dielectric constant is equivalent to the compliance, J(t), in the mechanical experiment.

2. Viscoelastic Models

Attempts have been made to model the response of a viscoelastic polymeric system to mechanical and electrical deformations (9-11). A reasonable representation results from various combinations of dissipative viscous elements (dashpots or resistors) and elastic elements (springs or

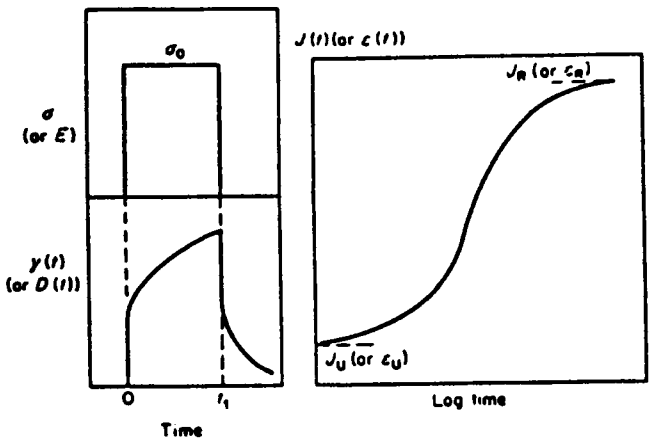

Figure 1. Time dependence of compliance and permittivity (2)

capacitors). Resistance is defined by Ohm's law as R = V/I where the current (I) and capacitance (C) are defined as follows: I = dQ/dt, and C = Q/V.

A Maxwell model (Figure 2A) puts the capacitance and resistance together in parallel whereas the springs and dashpots are combined in series. This case, for the electrical measurements, would yield the following relationship (3):

$$\frac{dQ}{dt} = C\frac{dV}{dt} + \frac{V}{R} \qquad (9)$$

The time dependence of the voltage in the Maxwell model would be:

$$V(t) = V_0 \exp(-\frac{t}{RC}) \qquad (10)$$

This equation describes the discharge of the capacitor through the resistor; the relaxation time is $\tau_e = R * C$. Typically the discharge current is what is actually measured:

$$I(t) = I(0) \exp(\frac{-t}{\tau_e}) \qquad (11)$$

Another well known model is the Voight-Kelvin (Figure 2B). In this model the resistor and the capacitor are combined in series. The electrical measurements would yield the following relationship (3):

$$V(t) = R*I + \frac{Q}{C} \qquad (12)$$

$$V(t) = \frac{Q}{C} + R\frac{dQ}{dC} \qquad (13)$$

$$C*V = \tau_e \frac{dQ}{dt} + Q \qquad (14)$$

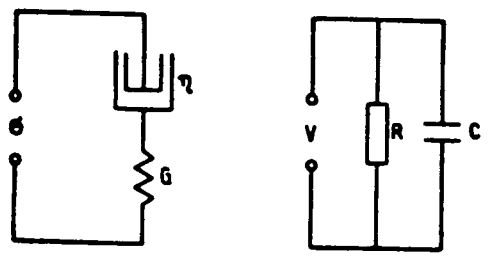

(a)

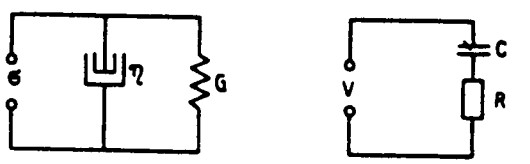

(b)

Figure 2. Proposed models for electrical and mechanical measurements (a) Maxwell model (b) Kelvin-Voight model (3)

The solution to equation (8) yields:

$$\frac{dQ}{dt} = \frac{CV}{RC} - \frac{Q}{RC} \qquad (15)$$

$$\frac{dQ}{dt} = \frac{V}{R} - \frac{Q}{RC} \qquad (16)$$

$$\frac{dQ}{dt} = \frac{V_0}{R} * \left(\exp\left(-\frac{t}{\tau_e} \right)\right) \qquad (17)$$

This analysis would describe an electric charge experiment in which current at constant voltage is measured.

Because these two models alone do not adequately describe the viscoelastic response of polymers, a combination of these models must be used. The simplest is shown in Figure 3; however, others have been proposed.

3. Application of sinusoidal stress

In the actual dielectric or dynamic mechanical analysis the stress field is not a step-type function (Figure 1), but rather is a sinusoidal function as shown in Figure 4 (12). In the dielectric analysis the AC electric field is applied as a sinusoidal stress. Polymers are viscoelastic, thus, the stress and strain or current and voltage will be out of phase by an angle δ (Figure 5). This phase lag is a result of the time necessary for dipoles to align with the field.

More quantitatively, the dielectric behavior can be described utilizing the Boltzmann superposition principle. The electrical displacement D(t) at any given time is defined as (2):

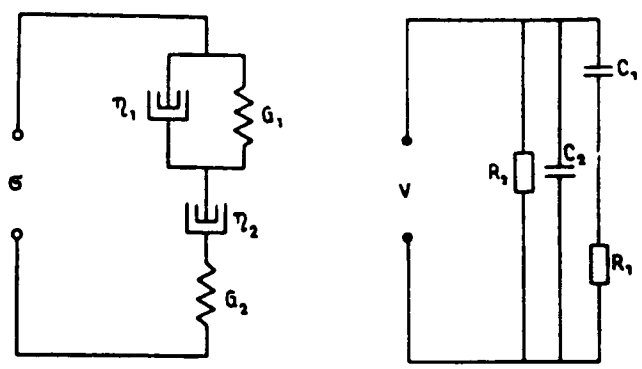

Figure 3. Combined model for a viscoelastic fluid (mechanical and dielectric) (3)

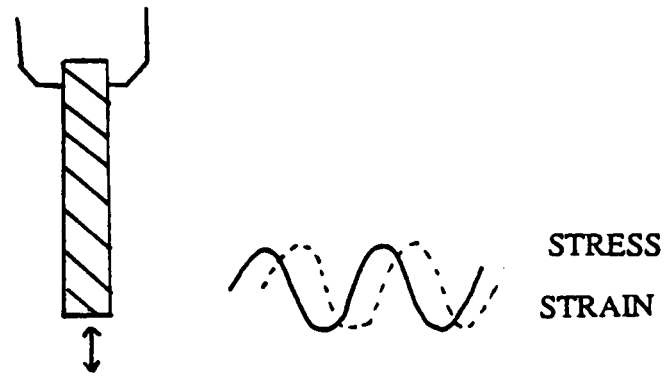

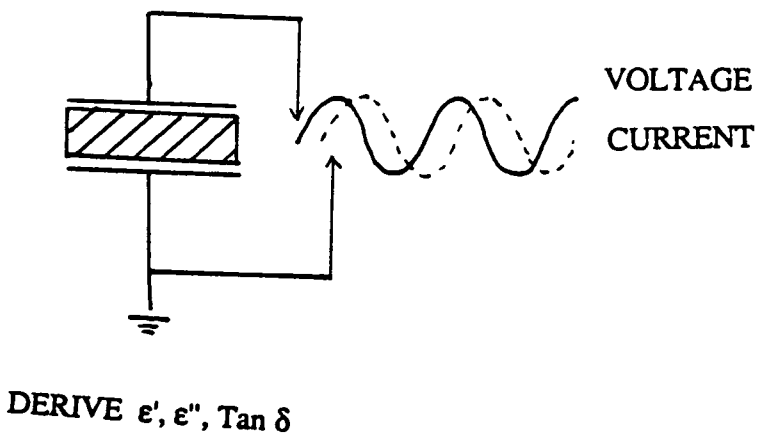

Figure 4. Sinusoidal mechanical and electrical stress (12)

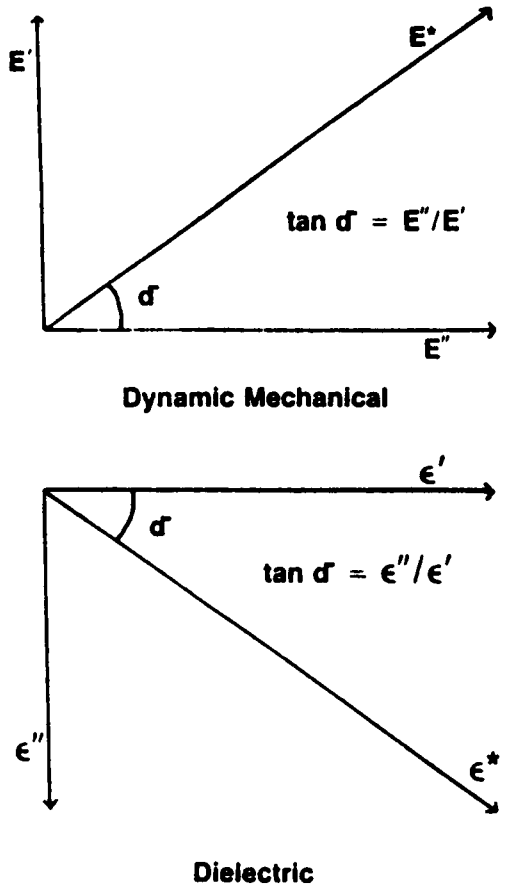

Figure 5. Relationship between storage and loss modulus and storage and loss permittivity (12)

$$D(t) = \epsilon_u E(t) + (\epsilon_R - \epsilon_u) \int E(u)\alpha_E(t-u)du \qquad (18)$$

Where $\alpha(t)$ is the dielectric decay function which describes the approach of D(t) to equilibrium in the presence of a constant field (2). This equation shows that the displacement is the sum of previous displacements arising from the incremental fields applied prior to time t. Use of a single relaxation time model for dielectric relaxations results in the following differential (2):

$$\tau \frac{dD(t)}{dt} + D(t) = (\tau * \epsilon_u) * \frac{dE(t)}{dt} + \epsilon_R * E(t) \qquad (19)$$

The complex electric field (E^*) and displacement (D^*) are defined as:

$$E_* = E_0 \exp(i\omega t) \qquad (20)$$

$$D^* = D_0 \exp(i\omega t - \delta) \qquad (21)$$

Applying these equations, the complex permittivity which results is:

$$\epsilon^*(\omega) = \epsilon_u + \frac{(\epsilon_R - \epsilon_u)}{1 + i\omega\tau} \qquad (22)$$

τ is the dielectric relaxation time and ω is the angular frequency. The complex dielectric constant can be defined as:

$$\epsilon^*(\omega) = \epsilon' - i\epsilon'' \qquad (23)$$

Thus, the following relationships can be obtained (8):

$$\epsilon' = \epsilon_u + \frac{(\epsilon_R - \epsilon_u)}{1 + \omega^2\tau^2} \quad (24)$$

$$\epsilon'' = (\epsilon_R - \epsilon_u) * \frac{\omega\tau}{1 + \omega^2\tau^2} \quad (25)$$

The dielectric loss tangent is given by

$$\text{Tan } \delta = \frac{\epsilon''}{\epsilon'} \quad (26)$$

The equations 24-26 are plotted in Figure 6 as a function of frequency. The difference (ϵ_R-ϵ_u) is known as the magnitude of the relaxation. Typically, the permittivity of the material will be higher the greater the polarizability of the molecules. In non-polar materials the polarizability arises from two effects (13):

a) Electronic polarization, which is the displacement of the electrons relative to the nuclei in each atom.

b) Atomic polarization, which is the displacement of the atomic nuclei relative to one another

In polar molecules a third process contributes to the total polarizability:

c) Orientation polarization, where the applied field causes a net orientation of the dipoles parallel to the field.

At low frequencies the storage permittivity, ϵ', is an asymptotically high value because the dipoles can follow the field very easily. At high frequencies the dipoles can no longer follow the field and ϵ' reaches an asymptotically low

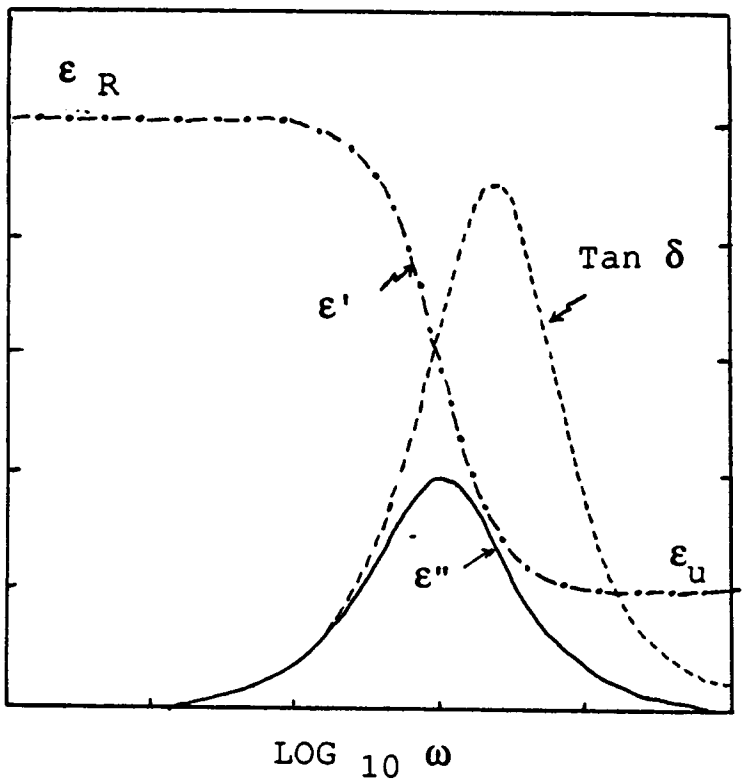

Figure 6. Tan δ, ε', ε" as a function of frequency (9)

value. Also, at low and high frequencies the loss permittivity, ϵ'', is small because the dipoles can either follow the field completely or not at all. At some intermediate frequency ϵ'' goes through a maximum, indicating that the dipoles of the polymer only partially follow the field so heat is generated as the current and voltage become more out of phase. For the single relaxation time model tan δ goes through a maximum at the frequency where $\omega\tau=1$.

4. Application to Polymeric Materials

Dielectric relaxation studies are very useful when studying polymer solids and solutions. The theories discribed previously for low molecular weight organic compounds need only be modified slightly to extend this analysis to high molecular weight materials. There are many desirable results which come from dielectric measurements in polymers; the overall magnitude of the polarization, the dielectric constant, and the determination of the thermal dependence of molecular motions from tan δ measurements are just a few.

When polymers are placed in an electric field at a given temperature and frequency the ease at wich the dipoles can align to the field is a function of many parameters, e.g., chain mobility, steric hindrance, inter- and intramolecular forces, as well as others. To observe a dielectric relaxation in a material it must possess a dipole

somewhere within the sample. However, even polymers which typically are considered nonpolar (i.e., polyethylene) will exhibit dielectric relaxations due to polar endgroups, oxidation products, or impurities. The quantities ϵ', ϵ'', and tan δ are all greatly effected by molecular structure, chain stiffness, crosslinking, plasticizers, polar impurities, tacticity and many other factors. The dynamic dielectric properties of polymers are related to molecular structure in much the same way as are the mechanical properties of storage modulus and tan δ. Studies by Heijboer (14) and others (2) discuss many of these important relationships between chemical structure and the 'transitions' observed.

In amorphous polymers the transitions discribed above can be associated with the either glass transition or sub-glass transition relaxations. These transitions, however, are not the typical first order thermodynamic phase transitions. Glass transitions are thought to be pseudo-second order transitions which may be detected by a change in Cp (heat capacity at constant pressure) on heating. These transitions are said to be pseudo-second order because they are dependent on heating direction and rate; in addition, they are also sensitive to thermal pretreatment (3). The sub-Tg transitions are too small to observe thermodynamically but can be detected numerous other ways, one being dielectric spectroscopy.

The response of a polymer to an applied mechanical or electrical stress field does not adhere to the single relaxation time models proposed. Rather, polymers must be modeled by a broad distribution of relaxation times in order to fully describe their behavior. In an isothermal experiment a wide range of frequencies are necessary to observe a particular transition (i.e., α, β, or γ). Dielectric spectroscopy has this capability, which is one of its advantages over dynamic mechanical analysis. Table 2 summarizes the various dielectric techniques available for a specific frequency range (9). The work described in this thesis was performed using frequencies between 10^1 to 10^7 Hz. The following three sections contain important concepts for understanding the application of dielectric analysis to polymers.

a. Stereospecificity and Chemical Structure

The configuration and conformation of a molecule are two factors which help define its static stereochemistry; that is, the spatial arrangement of the atoms of the molecule (15). Polymerization of some monomers (e.g. methyl methacrylate) which yield tactic structures (either isotactic or syndiotactic) are called stereospecific polymerizations. Stereoregular polymers exhibit large differences in stereochemical configurations.

Configuration relates to the arrangement in space of

Table 2

METHODS FOR DIELECTRIC MEASUREMENT (9)

Method	Frequency Range (hz)
DC Transient	10^{-4} to 10^{-1}
Ultra-low frequency bridge (Harris bridge)	10^{-2} to 10^{2}
Schering bridge; Transformer ratio arm bridge	10 to 10^{7}
Resonance circuits; Q meter	10^{5} to 10^{8}
Coaxial (slotted) line; reentrant cavity	10^{8} to 10^{9}
Coaxial line and waveguide	10^{9} to $3*10^{9}$

the substituents about a particular atom. Bonds must be broken to change a polymer's configuration. The simplest regular arrangement of successive groups along a chain is the isotactic structure (Figure 7a); in which all the R substiuents are located on the same side of the zigzag planar representation of the chain. In the syndiotactic arrangement the R groups alternate from side to side (Figure 7b). In the atactic arrangement the R groups appear at random on either side of the zigzag plane.

Another type of isomerism occurs in polymers having unsaturation in the main chain. Since carbon atoms linked together by double bonds are not free to rotate about the chain axis, repeating units in polymers, such as polyisoprene, can exist as two geometric isomers, cis and trans (16).

Conformation is concerned with the overall shape of the macromolecule. Any conformational changes occur by rotation about single bonds. Most physical properties of polymers, such as Tg, can be at least qualitatively be considered in terms of chain conformational flexibility (15). Subsituents which tend to decrease the barriers to rotation about the backbone chain atoms will tend to give the polymer increased conformational flexibility. However, polar interactions between chains and H-bonding will decrease chain flexibility.

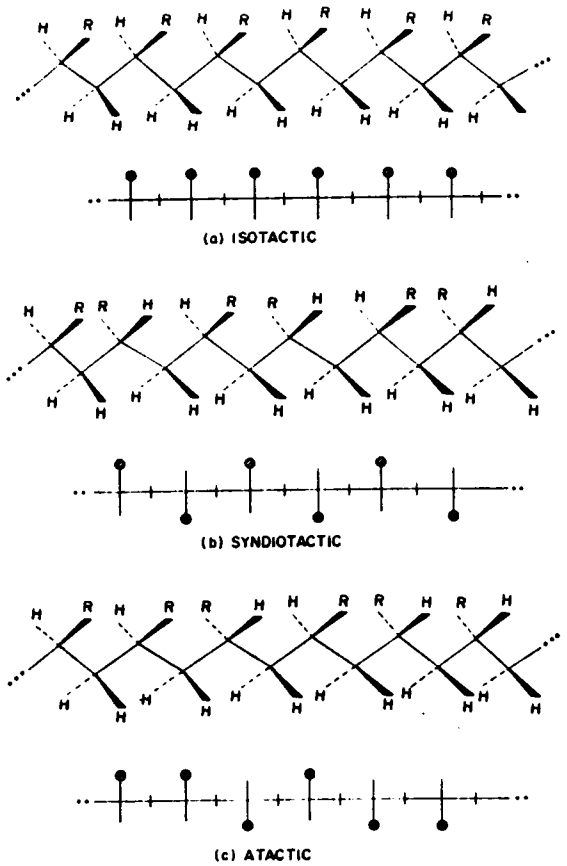

Figure 7. Stereochemical configurations of polymer chains (a) isotactic (b) syndiotactic (c) atactic (16)

b. The Effect of Temperature and Frequency

The effect of temperature and frequency of dielectric measurements must always be considered. As the frequency of the experiment is increased the temperature at which a dispersion is observed also increases. At higher frequencies a higher temperature is necessary for the dipoles to align with the field; hence, more kinetic energy is required. When a sample is analyzed at various frequencies the activation energy of a transition can be obtained. This is done by plotting $1/T_{max}$ (temperature in Kelvin at which tan δ goes through a maximum) against the log of the frequency of the analysis. The activation energy from this Arrhenius type plot is obtained from the following relationship:

$$\omega=\omega_o*\exp(-Ea/R*T) \qquad (27)$$

This equation was first shown by Arrhenius (17) to describe the influence of temperature on the velocity of chemical reactions. In this equation Ea is the Arrhenius activation energy and ω_0 is the pre-exponential term which is related to the probability of the reaction occuring at any given temperature When applied to polymeric solids it indicates that the influence of changing frequencies on an observed dispersion will depend on the absolute temperature of Tg and its energy of activation, ΔH. The ΔH reflects the relative magnitude of the energy barriers that need to be overcome to undergo the conformational changes required to

observe a given transition. The activation energy of a glass transition is typically of the magnitude of 100 Kcal/mole. This relaxation (α) is due to large scale, co-operative movements of the main chain. For secondary relaxations, those associated with side-group rotations or very localized main chain motions, the E_a is more on the order of 10 kcal/mole. This means that the peaks in tan δ associated with secondary transitions will shift more with frequency than those of the main transition. Eventually, the two transitions will merge at high frequencies resulting in a single ($\alpha\beta$) transition.

Both dielectric and dynamic mechanical data of polymers are often analyzed in terms of the Arrhenius equation and a constant activation energy. In some cases this can be regarded as only an approximate treatment due to the limited range of experimental frequencies available. Also, for this treatment to be valid the data must fall on a straight line in a plot of Log frequency versus 1/temperature (K).

Another important principle in polymer analysis is based on the concept of time-temperature superposition. This principle in its simplest form implies that the viscoelastic behavior at one temperature can be related to that at another temperature by a shifting of the time scale only (11). This is a well known method for analyzing both dynamic mechanical and dielectric data. The values of ϵ', ϵ'', and tan δ are first determined as a function of log

frequency at various isotherms. By shifting the curves horizontally until they overlap a mastercurve can be constructed. This superposing of curves allows for the prediction of data at a given temperature over a wide range of frequencies, even frequencies which are not actually used experimentally.

c. Arc Diagrams

Another important method of analyzing data resulting from dielectric studies is the construction of arc diagrams. These diagrams, first developed by Cole and Cole (18), are obtained by plotting ϵ'' against ϵ' for various frequencies. In the ideal, single relaxation case the Debye equations (24) and (25) can be rearranged to the equation of a semicircle (9):

$$[\epsilon' - (\frac{\epsilon_R + \epsilon_u}{2})]^2 + \epsilon''^2 = (\frac{\epsilon_R - \epsilon_u}{2})^2 \qquad (28)$$

Plots of this equation produce the semicircle shown in Figure 8a, with a radius of $(\epsilon_R - \epsilon_u)/2$.

Modifications must be made in this type of analysis when considering polymers as a consequence of their broad distribution of relaxation times. As explained previously the circular arc equations are derived from the single relxation time model. This model predicts that if equation 25 is plotted as a function of $\log(\tau\omega)$ for a given ϵ_R and ϵ_u, then ϵ'' goes through a maximum at $\log(\tau\omega)=1$. Also, the

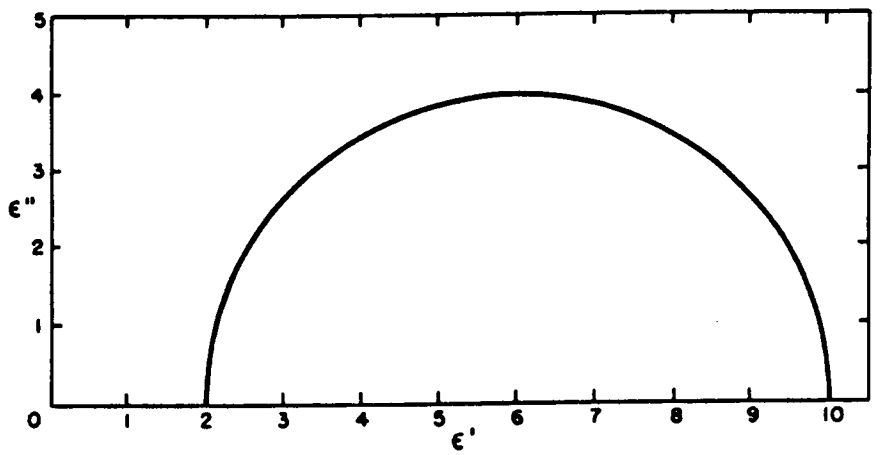

(a)

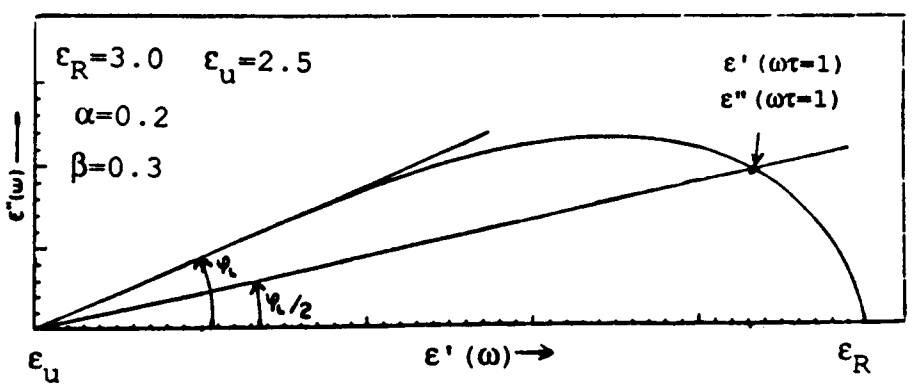

(b)

Figure 8. Arc diagrams for dielectric analysis (a) single-relaxation time model, proposed by Cole-Cole (9) (b) polymeric materials, model proposed by Havriliak-Negami (20)

ϵ' versus temperature (or time) curve shows an inflection point at $\log(\tau\omega)=1$. With polymers it has been shown that this model does not fit experimental data (2).

From Figure 8 it is obvious that the observed curve is broader than the predicted curve; hence, several or, in the limit, a distribution of relaxation times are neccessary to describe the behavior.

The Debye equations alone are not sufficient to model the plot of ϵ' versus ϵ'' of polymers. A skewed arc diagram which is linear at high frequencies and circular at low frequencies is actually observed. The single relaxation time equations were first modified (18) to the following:

$$\epsilon^*(\omega)=\epsilon_u + \frac{(\epsilon_R-\epsilon_u)}{1+(i\omega\tau)^b} \qquad (29)$$

Where b is a parameter, $0<b\leq 1$. A plot of log ϵ'' versus ω has a slope of b at low frequencies and -b at high frequencies. For b=1 the Debye equation is obtained.

The equation required further modification (19) to explain the high frequency data:

$$\epsilon^*=\epsilon_u+ \frac{(\epsilon_R-\epsilon_u)}{(1+i\omega\tau)^y} \qquad (30)$$

Where y is a parameter, $0<y\leq 1$.This form of the equation fits the 'skewed' behavior slightly better.

The most accurate prediction of the skewed arc diagram behavior of polymers is obtained by combining equations (29) and (30). This complex plane analysis (Figure 8b) was first developed by Havriliak and Negami (20-22).

$$\epsilon^*(\omega) = \epsilon_u + \frac{\epsilon_R - \epsilon_u}{(1+(i\omega\tau)^{(1-a)})^b} \qquad (31)$$

Where "a" describes the breadth of the distribution, the breadth increases as "a" goes from 0 to 1. b describes the skewness, which increases as b goes from 1 to 0. These parameters may be obtained graphically as described in Appendix B.

C. Dielectric Instrumentation-General Radio Bridge

1. Equipment

The dielectric experiments were performed using a type 1620-A Capacitance Measuring Assembly purchased from General Radio Company of West Concord, Massachusetts. This bridge is equipped with a type 1311-A audio oscillator and the type 1232-A tuned amplifier and null detector. A high degree of accuracy is achieved through the use of precisely wound transformer ratio arms and very stable standards. This instrument has eleven frequencies available between 50 Hz and 10 KHz and can be used in either the 2- or 3- terminal mode, measuring capacitances of 10^{-5}pF to 11.1 MF. Both capacitance and dissipation factor can be determined on digital lever-type switches (Figure 9).

A Three-Terminal Research Cell (Model LD-3) purchased from Gilian and Company of Watertown, Massachusetts, was used to contain the sample. It is a liquid-tight, three-

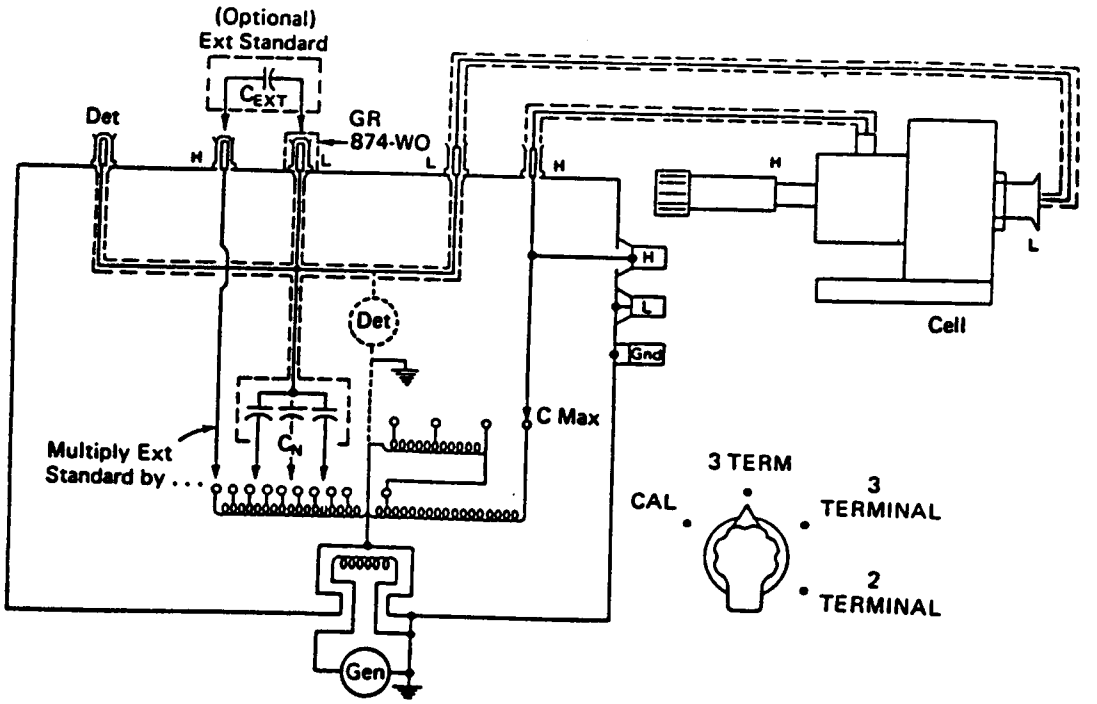

Figure 9. Bridge circuit for 3-terminal coaxial measurement of test cell (25)

terminal cell with a 6.35cm diameter guarded electrode. Variable spacing from 0 to 0.8cm can be achieved via a micrometer fixed to one end. It can be operated at temperatures up to 200°C and frequencies up to 1 MHz. This cell was contained in a Delta Design Environmental temperature chamber (Model 2850) obtained from Delta Design Inc. of San Diego, California. Temperature was regulated to ± 0.1°C in the range from -150°C to +300°C.

2. Fundamentals of Operation

In the frequency range of 10^1 to 10^6Hz the most common method of dielectric analysis utilizes the transformer ratio-arm bridge. In general, the capacitance measurements are made by the null method involving a modified Wheatstone bridge (23) as shown in Figure 10. The capacitance of the unknown C_x is balanced by a calibrated, variable, standard capacitor and variable ratio arm such as R_a. By the introduction of the transformer ratio arms, as shown in Figure 11, higher accuracy, resolution and stability of capacitance measurments can be achieved. This configuration is important because it allows the voltage ratio at balance to be determined almost entirely by the ratio of turns in the transformers, N_X/N_N. This means that stray capacitances from the point H (high voltage, low impedence) to the guard or ground point 6 will not affect the balance point (6). This technique is reviewed in much greater detail in various

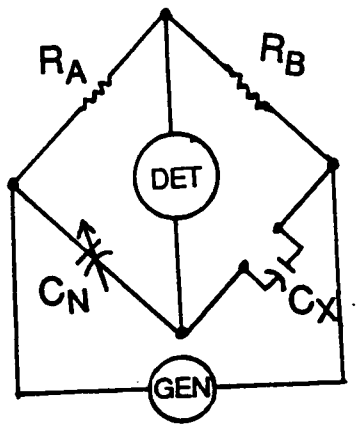

Figure 10. Basic ratio bridge (23)

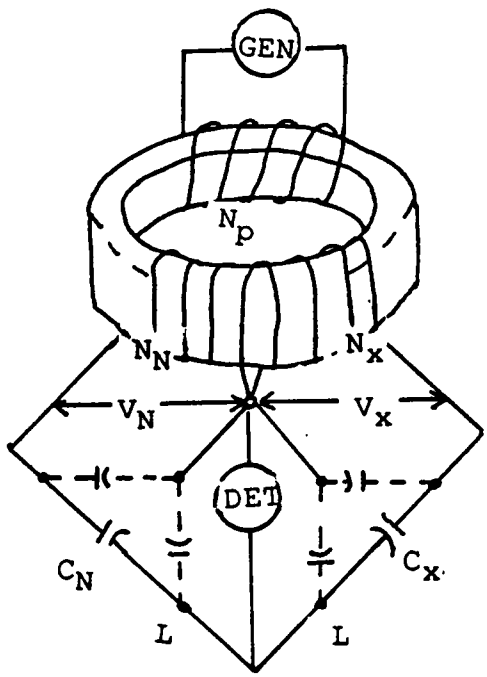

Figure 11. Transformer ratio arm bridge (23)

references (6,24).

The use of a three-terminal guarded electrode, as shown in Figure 12, eliminates lead capacitance and confines the measurement to a fairly well defined portion of the sample (6).

3. Measurement Methods

The experiment was typically conducted by first cooling the system down to the minimum temperature (T_{min}) with the sample in place and a thermocouple fixed to the electrode. A cover was placed over the cell which had a gas inlet; while the system was cooling to T_{min}, there was a constant purge of N_2. The data of capacitance and dissipation factor at the desired frequencies were collected as the system warmed at a slow rate (<2°C/minute).

In the determination of the complex permittivity components ϵ' and ϵ'' and the tan δ values at each temperature and frequency, three methods are available with this cell (25,26).

a) Contacting Electrodes Method

This method utilizes the definition of dielectric constant, $\epsilon_r = C_1/C_F$, where C_1 is the capacitance of a test cell with the unknown sample between the two electrodes, and C_F is the capacitance of the cell containing only a vacuum, or air. Tan δ may be obtained by multiplying the

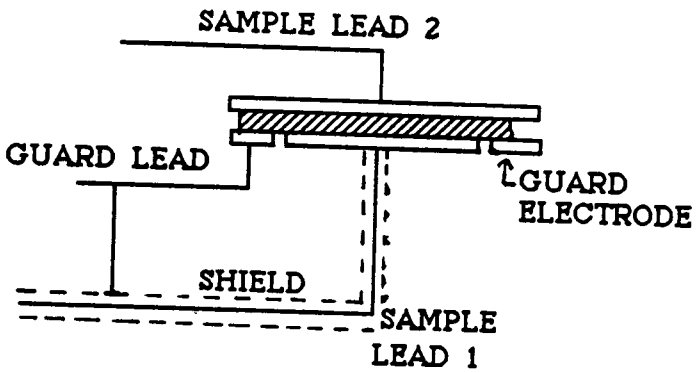

Figure 12. Dielectric sample cell equipped with guard ring (6)

dissipation factor value by the frequency in kHz (Figure 13). There is a problem with this approach, samples can not be made perfectly uniform in thickness; thus, this method may not give accurate ϵ' values because the entire surface of the polymer is not in contact with the electrodes. It has been observed that this error can be significantly reduced if a thin layer of silicone grease is placed on the film (27).

b) Air-Gap Method

In this technique the electrodes are opened to a known separation of ~ 0.01 to 0.02 cm greater than the film thickness. By using this method a non-uniform thickness can be more easily tolerated and the result is a higher degree of accuracy. First the capacitance and dissipation factor, C_F and D_F, are measured for a separation of h_o with air between the plates. The film is then inserted and the new values of C_1 and D_C are measured (Figure 14). The values of ϵ', ϵ'' and tan δ are calculated from the following equations (25):

$$\epsilon' = \frac{1}{1 - \frac{(C_1 - C_F)}{C_1}\,\frac{h_0}{h}} \qquad (32)$$

$$\text{Tan } \delta = D_C + \left(\frac{h_0}{h} - 1\right) \epsilon_r (D_C - D_F) \qquad (33)$$

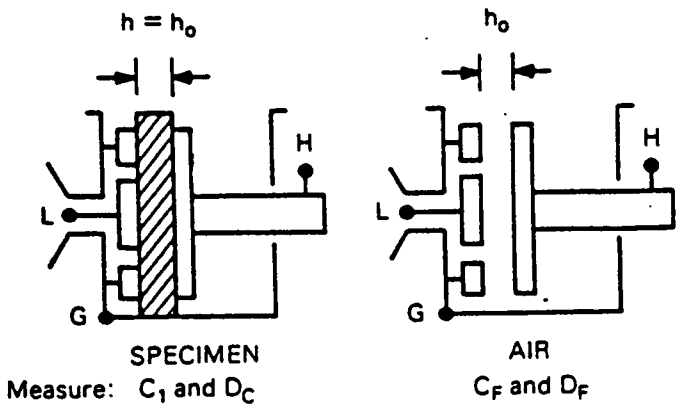

Figure 13. Contacting electrode method for the determination of capacitance and dissipation factor (25)

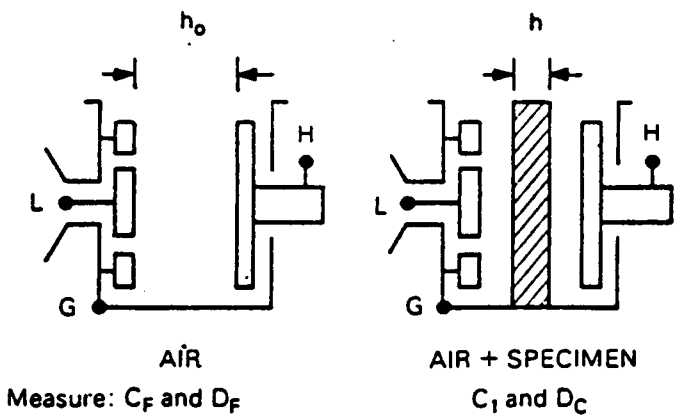

Figure 14. Air-Gap method for the determination of capacitance and dissipation factor (25)

c) Two-Fluid Method

The third method is useful for samples whose thickness is difficult to measure because they are too thin or too soft and for measurements where extremely high accuracy is desired. In this determination four capacitance and dissipation factor values are required (Figure 15). The first two measurements involve fluid one (usually air) followed by fluid one with the sample in place. The second two measurements involve fluid two and fluid two with the specimen in that second fluid. For polymeric films this second fluid should be non-sorbing and low viscosity, such as fluorocarbons or silicon fluids. The equations needed for these calculations are as follows (25):

$$\epsilon_r = \epsilon_{F1} + \frac{C_2\Delta C_1(\epsilon_{F2} - \epsilon_{F1})}{C_2\Delta C_1 - C_1\Delta C_2} \qquad (34)$$

$$\frac{\epsilon_{F2}}{\epsilon_{F1}} = \frac{C_{F2}}{C_{F1}} \qquad (35)$$

$$D_x = D_{C2} + \frac{\epsilon_r C_v - C_2}{\Delta C_2} \quad \Delta D_2 \qquad (36)$$

$$C_v = \frac{C_{F1}}{\epsilon_{F1}} \qquad (37)$$

Values of ϵ', ϵ'' and tan δ at each temperature and frequency were obtained from computer solutions of the equations. Different programs were written for the different methods used to measure capacitance and dissipation factors. It should be noted that due to the

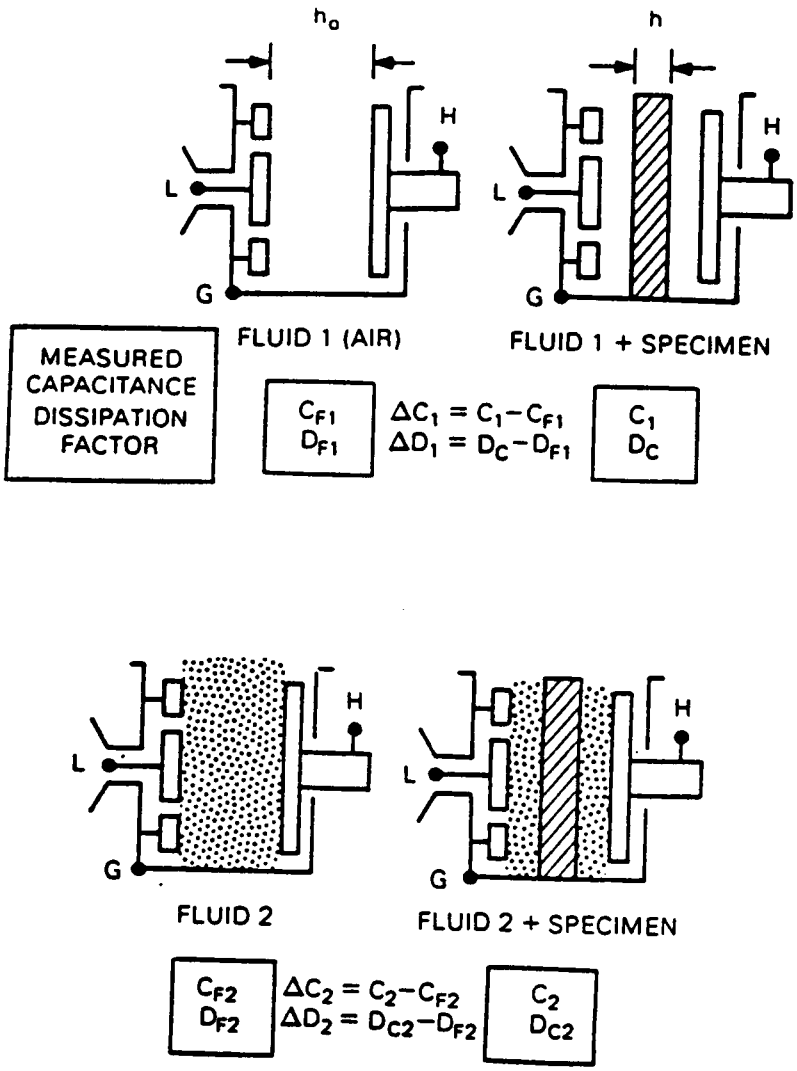

Figure 15. Two-Fluid method for the determination of capacitance and dissipation factor (25)

cell design is was difficult to determine accurate ϵ' values as a function of temperature. It was determined that the plates were changing their separation as temperature was changed due to normel thermal expansion and contraction. Because of this uncertainty, only tan δ could be determined accurately with this equipment except for isothermal room temperature measurements conditions.

D. Dielectric Instrumentation-Polymer Laboratory DETA

The Dielectric Thermal Analyzer (DETA) from Polymer Laboratory Ltd. of England was used to obtain some of the dielectric data. This instrument provides a more accurate determination of ϵ' and ϵ'' when scanning temperatures; and, therefore, further data analysis can be performed. The instrument can be run in a manual mode or automated by interfacing it to a computer for the data acquistion. Analysis measurements can be made over the range of 20 Hz to 100 kHz using any of the preset 500 frequencies. The liquid or solid sample can be scanned over the range of -150°C to 300°C at rates of 0.1 degrees/minute up to 8 degrees/minute.

The instrument consists of three components (28):

1) Dielectric Spectrometer Head

2) Microprocessor Based Analyzer

3) Temperature Programmer

The analyzer determines the ϵ' and tan δ values of the

sample for a given temperature and frequency via the contacting electrode method (see previous section). The microprocessor controls the measurement sequence from programs in read only memory (ROM) via operator selection available from the keyboard. The temperature programmer is designed for accurate control and programming of linear variations of temperature with time. The temperature of the furnace is determined by a platinum thermocouple which is located close to the sample. The spectrometer head consists of two circular electrodes mounted horizontally on a ceramic base. The bottom electrode is fixed by a locking screw. The top electrode is held down onto the sample by a spring which can either be locked into place or remain free to expand or contract with the sample. The electrodes are 33 mm in diameter and can accommodate film thicknesses of 0.1 to 2 mm. The chamber can be evacuated or filled with an inert atmosphere if desired. Liquid nitrogen is used as the coolant for subambient temperatures. Up to five frequencies can be scanned simultaneously during a single temperature ramp.

E. Dynamic Mechanical Analysis-Polymer Laboratory DMTA

The Polymer Laboratory Dynamic Mechanical Thermal Analyzer (DMTA) was used to measure the dynamic properties of storage and loss modulus (E' and E") and the tan δ as a function of temperature and frequency. In this analysis, as

mentioned previously in this chapter, a small sinusoidal stress is applied to the sample and the resulting strain is detected (see Figure 4a).

The instrument is comprised of four components (29,30):

1) The Measuring Mechanical Head

2) The Dynamic Analyser

3) The Temperature Programmer

4) The Micro-computer

The measuring head holds the sample and subjects it to small amplitudes of sinusoidal oscillation at a constant temperature. The measurement can be made in either a two or three point bending mode giving Young's modulus or in a shear mode giving a shear modulus. The dynamic analyzer computes the storage and loss modulus and the tan δ for a fixed strain level at the desired frequencies. The frequency range available is 0.033 Hz to 90 Hz and three controlled strain levels covering a 16 fold range. The temperature programmer provides accurate control for linear temperature scans as well as isothermal analyses. Temperature is sensed by a platinum resistance thermometer lying behind the sample. Temperatures in the range of -150°C to 500°C can be scanned at rates of 1 to 10°/minute. If desired the samples can be analyzed in an inert atmosphere. Liquid nitrogen is used as the coolent for sub-ambient work. By interfacing the instrument to a micro-computer complete automation can be obtained with the data

being acquired and stored on disks. The theory of dynamic mechanical analysis parallels that behind the dielectric experiment and will not be discussed here. It is reviewed in great detail in other sources (2,9-11).

CHAPTER III

ANALYSIS OF RADIAL STARBLOCK COPOLYMERS

A. Introduction

A great deal of interest in the polymer community has centered around radial starblock copolymers recently, due to their desirable thermoplastic elastomeric properties and their rheological behavior. These polymers are of a "star" topology with many arms linked together by a central hub. The arms are typically composed of a "hard" and "soft" molecular block, as described in terms of the relative ease of rotational conformational changes at room temperature. Most often such polymers have a microphase separated morphology.

In this study the dielectric properties of two series of radial starblock polymers were analyzed. The first class of materials consisted of four polymers having poly(t-butylstyrene) as the hard block and poly(butadiene) as the soft block, with the microstructure of the butadiene also being a variable. The influence of hydrogenation of the poly(butadiene) soft block was also investigated.

The second radial starblock series was comprised of two polymers in which the soft block, poly(isoprene), was identical while the hard block was either poly(styrene) or poly(t-butylstyrene). The casting solvent necessary for film preparation was also a variable.

B. Background

A thermoplastic elastomer (TPE) behaves as an elastomer at ambient temperatures, yet can be molded into desirable shapes at elevated temperatures (31-33). The most common commercially available TPE is Kraton^{TM} which is an ABA triblock copolymer, where the A block is polystyrene and B is polybutadiene. Given that the blocks are high enough in molecular weight, and of different chemical composition and interaction parameters, microphase separation occurs (Figure 16a). Theories of the microdomain formation have been proposed by Meier (34,35). The model which Meier proposes states that criteria for phase separation arise from three factors (36):

1) The restriction of the position of the A-B covalent bonds between the domains, resulting in an entropy decrease termed the placement entropy.

2) A reduction in entropy due to the requirement that A segments remain in the domain space of A and that B segments remain in the B domain, termed the restricted volume entropy.

3) The perturbation of chain dimensions in the micro-domains away from the normal random-flight values, termed the elasticity entropy.

When the soft block comprises ~75% by weight of the overall composition, as is typical of the TPE's, the morphology has usually been found to be a continuous rubbery

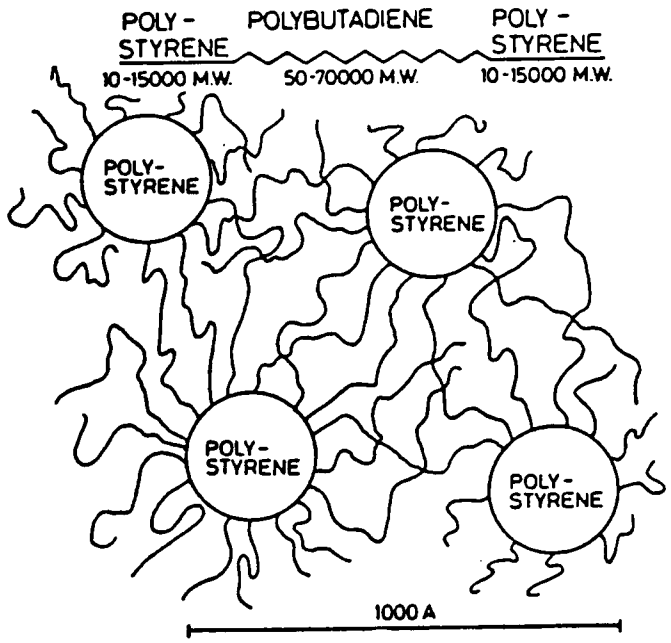

(a)

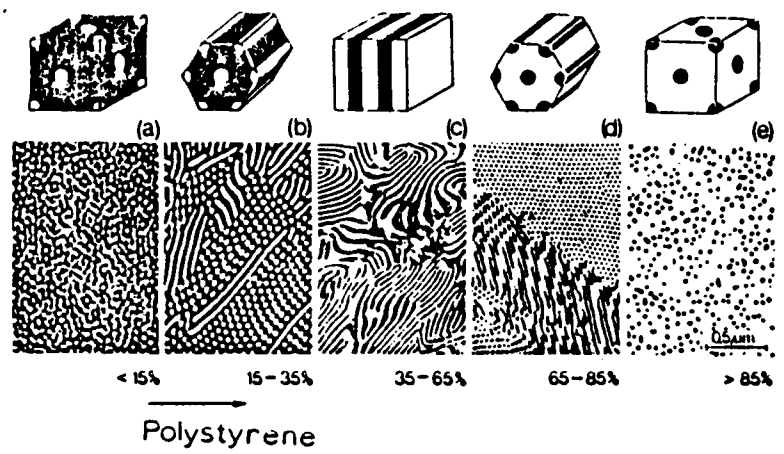

(b)

Figure 16. Microphase separation, (a) ABA block copolymers (b) ABA block copolymers with varying percentages of polystyrene hard block (3).

phase with hard, glassy spheres dispersed in the soft phase. If the chemical compositition tends more toward equal percentages of the two components, the microstructure will be more lamellae like. If the soft block composition is decreased to 25% a phase inversion occurs, resulting in a glassy matrix with rubbery spheres dispersed in it (Figure 16b).

Both dielectric and dynamic mechanical analyses have proven to be quite useful in studying microphase separated copolymers (37-39). Using these techniques if microphase separation occurs two tan δ maxima should be observed due to the glass transition temperatures of the two components. The mechanical analysis has the added advantage that the modulus-temperature curves can also be obtained, typically showing a modulus plateau between the Tg's of the individual components.

Dielectric analysis has been successfully employed for the study of two phase polymer systems. Some investigations have focused on the Maxwell-Wagner-Sillars (MWS) (40-42) interfacial polarization which usually developes in heterogeneous dielectrics, typically at low frequencies (0.01 Hz) and usually at high ϵ' and ϵ'' values (43-46). Because the frequencies necessary for this polarization to be observed are lower than what could be obtained with the instrumentation used in the present research such interfacial polarization could not be studied. However,

other important factors effecting phase separation in these radial starblock copolymers were examined.

C. Experimental

1. Synthesis

The anionic synthesis of the radial starblock copolymers was performed by Mr. James M. Hoover in Prof. J. E. McGrath's laboratories at Virginia Polytechnic Institute and State University. Recent publications have described the starblock synthesis and properities (47-52). The anionic polymerization of these materials offers many advantages. Some of these are, i) controlled microstructure, ii) a highly variable chemical composition, and iii) narrow molecular weight distributions.

These polymers were synthesized under a nitrogen atmosphere at 50°C in a modified Chemco glass bowl/stainless steel reactor (53). Purified cyclohexane was used as the polymerization solvent, the styrene or substituted styrene was added to the solvent with a syringe. The initiator, secondary butyllithium (1.37 M in hexane) was added dropwise. This was allowed to react for ~1 hour, resulting in a "living" poly(styrene) chain. The purified isoprene or butadiene was then added to the reactor and allowed to polymerize for ~2 hours. This procedure produces an A-B type diblock copolymer.

The final step was the addition of purified divinyl-

benzene (DVB) in hexane (0.72 M) to the reactor. The DVB acts as a linking agent that hooks the polymer chains to a central point, resulting in the "star". The DVB was syringed into the reactor, producing a red color within several minutes. This reaction was allowed to proceed for 2 hours at 60°C. After this linking reaction the living system was terminated with 0.5 ml HPLC grade, degassed methanol.

Measurements made by Gel Permeation Chromatography (GPC) indicate that 8-10 arms were linked into the star. The molecular weights of the blocks and overall composition was controlled via initiator concentration and molar amounts of the monomers. Molecular weights between blocks were independently determined in all cases. The polymer was isolated by precipitation from an appropriate nonsolvent or simply by pulling the solvent off under vacuum.

Films for the dielectric and dynamic mechanical analysis were prepared by casting the polymer from a desired solvent. When dealing with a phase separated block copolymer the solvent that the sample is cast from can effect the final morphology which develops. If a solvent is categorised as non-selective it will be equally "good" or "poor" for both blocks, whereas a selective solvent will be "good" for one block yet "poor" for the other.

Star block copolymers of styrene and isoprene with 30 weight percent of polystyrene have been reported in the

literature to have an ordered bicontinuous type morpholgy (54,55) with both phases being continuous. This complex morphology was also found by Mr. Jim Scott (51) for the polymers described here.

2. Instrumentation

The capacitance and dissipation factor measurements of the polymers were made on the General Radio 1620A Capacitance Bridge assembly and the Polymer Laboratory Dielectric Thermal Analyzer (DETA) (see Chapter 2). The analyses were performed as a function of temperature over the frequency range of 100 Hz to 100 kHz and a temperature range of -100°C to 200°C.

The dynamic mechanical measurements were performed in the shear mode on the Polymer Laboratory Dynamic Mechanical Thermal Analyzer (DMTA) (see Chapter 2). A test frequency of 1 Hz over a temperature range of -150°C to 200°C at 5°C/minute was utilized.

The glass transition (Tg) temperatures were determined on the Perkin Elmer Model 2 Differential Scanning Calorimeter (DSC-II) at a heating rate of 10°C/minute. In this work the glass transition temperatures quoted were determined from the midpoint of the observed thermogram baseline shifts.

A Waters 150C Gel Permeation Chromatograph operating at 30°C with THF and fitted with 5 Ultrastyragel^{TM} columns was

used to obtain molecular weight information. The GPC was equipped with a Waters refractive index detector.

D. Results and Discussion

1. T-Butylstyrene/Butadiene Radial Starblocks

In this study four polymers were anionically synthesized according to the previous discussion. The soft block consisted of 75 weight percent poly(butadiene) and the hard block was 25 weight percent poly(t-butylstyrene). In this investigation the hard block was kept as a constant; however, the microstructure of the soft block was varied so as to contain various percentages of the 1,2- microstructure. This was achieved by varying the temperature of the polymerization and by keeping a 1:1 mole ratio of dipiperodinoethane (DIPIP) to lithium. In polymerizations at 60°C the microstructure was 10 mole % 1,2-, whereas, 10°C produced 92 mole % 1,2-microstructure (47,49).

As shown in Figure 17, the samples contained either 100% 1,2-, 70% 1,2-, or 50% 1,2- of the butadiene microstructure with the remaining composition being 1,4-variety. The 1,4-microstructure polymer was determined by FTIR and FT proton NMR to be 60% cis and 31% trans. For the 50% 1,2- and the 70% 1,2- samples there was a random distribution of the 1,2- and the 1,4- microstructure along the chain. Also, catalytic hydrogenation of the 50% 1,2-sample (50%-1,2 H) was accomplished by first synthesizing

Hard Block: Poly(t-butyl styrene)

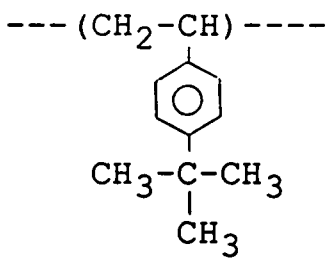

Soft Block: Poly(butadiene)

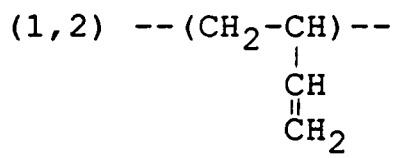

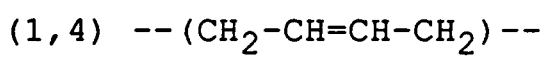

(1) 100% (1,2)

(2) 70% (1,2)

(3) 50% (1,2)

(4) 50% (1,2)H

Molecular Weight ~450,000
Polydispersity <1.2

Figure 17. Radial starblock copolymer chemical composition, for the first series

the polymer then purging the system well with H_2. The hydrogenation catalyst, a TEA/Ni(Oct)$_2$ complex, was then added, while maintaining the H_2 pressure at 50 psi. The catalyst was prepared by adding 0.228 g of nickel octoate, 15 ml of purified cyclohexane, and 1.13 ml (1.65 mmol) of triethylaluminum into a bottle sealed with a syringe. The catylst was added to the reactor at 50°C via a syringe (47). The effect of hydrogenation on the phase separation will also be discussed. Samples were prepared by casting from a cyclohexane solution (20 weight percent) onto Teflon sheets and drying under vacuum near the Tg of the hard block.

a. Dynamic Mechanical Thermal Analysis

Dynamic Mechanical Thermal Analysis (DMTA) was employed to access the mechanical behavior of these four polymers. Figure 18 shows the DMTA trace for the 50% 1,2- polymer at 1 Hz and a scan rate of 5°C/minute; this behavior was typical for all the polymers. It is evident from the two peak maxima in the tan δ curve that phase separation has occured. The soft block has a fairly sharp transition at 0°C and the hard block has a broader transition at 130°C. The storage modulus, E', is high ($1*10^{8.5}$ Pa) at low temperatures which is representative of a glassy material. Above 20°C the modulus drops off to $1*10^{6}$ Pa which is representative of an elastomer. There is evidence of partial phase mixing due to the broadness of the upper tansition; however, phase

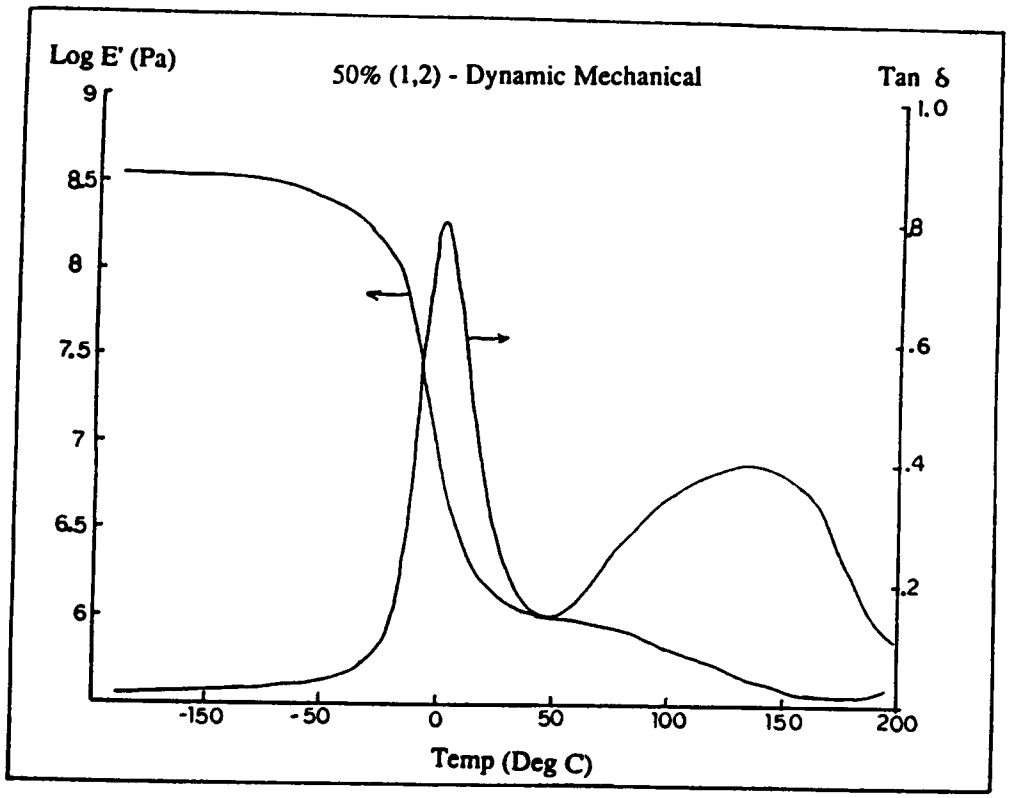

Figure 18. Dynamic mechanical analysis of the 50 %-1,2 radial starblock, 1Hz and 5°C/minute

separation was observed in all the polymers.

b. Dielectric Analysis

The films cast from cyclohexane were analyzed on the GenRad Capacitance Bridge from 100 Hz to 10 kHz. Only the low temperature transition was studied because, in this series, the hard block was not altered. In Figure 19 is a typical dielectric scan for the polybutadiene block. As expected, the observed transition shifts to higher temperatures as the test frequency increased. The other three samples showed similar responses. For comparison, the tan δ curves of the three polymers of differing microstructure are shown in Figure 20. As the percent 1,2-content of the butadiene was increased the tan δ curve also was detected at higher temperatures.

In Table 3 the tan δ maxima are listed in addition to the DSC information. The glass transition temperatures drop as the percent 1,2- decreases. This is expected because the Tg of pure 1,2-polybutadiene is 0°C, whereas the Tg of pure 1,4-polybutadiene is -80°C. Also, as expected, the tan δ maxima from both the dielectric and dynamic mechanical analysis correlate directly with the glass transition temperature. Typically the tan δ observed in a mechanical experiment (i.e. DMTA) the tan δ maxima (at 1 Hz) is expected to be 5 to 10 degrees higher than the glass transition observed on the DSC (12). In the block

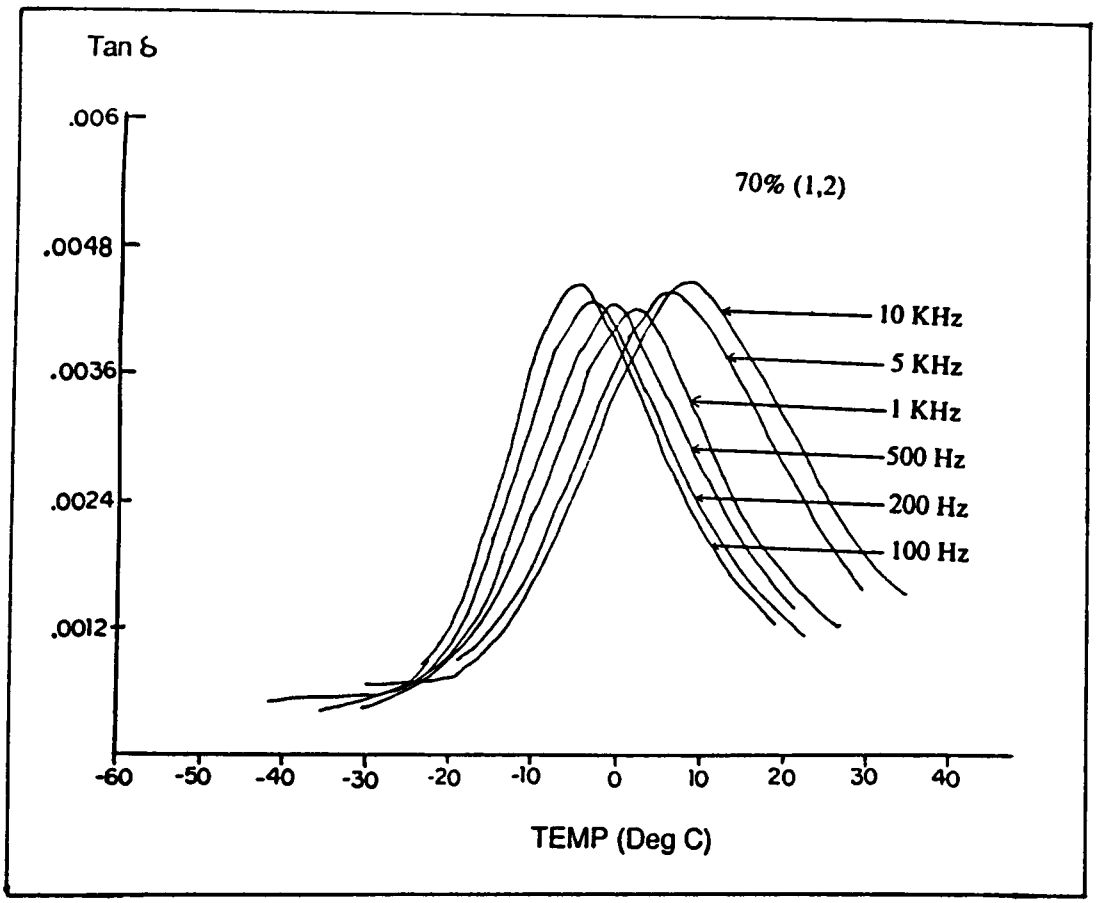

Figure 19. Dielectric analysis (tan δ) of 70%-1,2 radial starblock at various frequencies

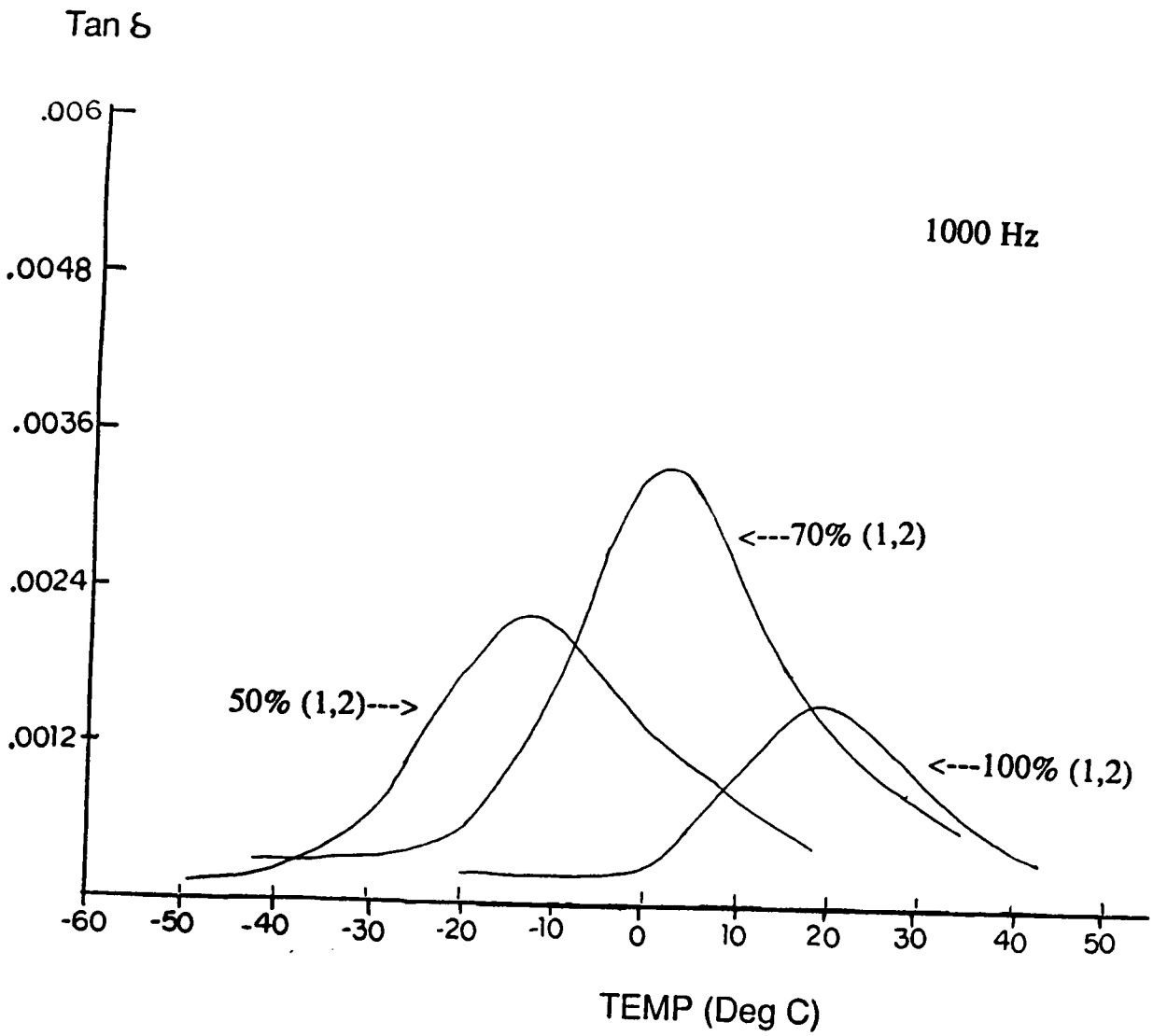

Figure 20. The effect of microstructure, %-1,2 content, on the tan δ curves

Table 3

COMPARISON OF THERMAL ANALYSIS WITH
DIELECTRIC AND DYNAMIC MECHANICAL DATA

Sample	DSC Tg(°C)	Tmax (°C) of Tan δ Dielectric(1kHz)	DMTA(1Hz)	Ea ± 3
100%-1,2	4* (-11,17)	18.1	23	63.7
70%-1,2	-18* (-43,2)	1.3	6	54.0
50%-1,2	-26* (-43,-6)	-12.5	0	46.5
50%-1,2 H	-47* (-58,33)	-15.7	-7	--

Ea in Kcal/mole calculated from dielectric data

*Mid point of the transition, entire range of the transiton is listed below each midpoint

copolymers studied here the difference is as high as 40 degrees. We believe this is because the transitions for the soft block are so broad; the breadth of the transitions are listed in parentheses in Table 3.

The tan δ maxima and the glass transition temperature of the hydrogenated 50% 1,2- are all lower in temperature than found for the unhydrogenated species. This indicates an increase in the degree of phase separation was produced by hydrogenation. This is very important because many of the polymer's mechanical properties such as ultimate strength, stress-strain response, mechanical damping, and others will all be influenced by the degree of phase separation.

An important observation arises from the data in Table 3. Even though the dielectric analysis was performed at a higher frequency, the tan δ peak detected occured at a lower temperature than the mechanical tan δ in all cases. If the two techniques are responding to the same relaxation mechanism, then the higher frequency experiment should result in a dispersion observed at a higher temperature. It is postulated that the dielectric experiment was responding to more localized motions rather than the large scale micro-Brownian type mainchain motion being detected in the DMTA.

Also shown in Table 3 are the activation energies for the three polymers, these values were obtained from Arrhenius plots (see Chapter 2) of the dielectric data. The

activation energies correlate directly with the glass transition temperatures, such that, as the 1,2- content decreased so did the activation energy. It is postulated that the presence of the alkene side group allows the polymer chains to pack better than the cis-1,4- microstructure, thereby accounting for the higher Ea value.

In Figure 21 the dielectric loss data for the 50% 1,2- microstructure were replotted as a function of log frequency. It was impossible to determine the exact shape of the curves because only five frequencies were analyzed, however, a good representation was obtained. Plotting the data in this fashion enables a horizontal shifting of the curves with respect to one isotherm in order to produce a mastercurve (Figure 22). This representation of the data via a mastercurve is important because it generates a prediction of properties (ϵ', ϵ'', and tan δ) outside the frequency range of the instrument. It is well known that phase separated block copolymers are thermorheologically complex (57). This means that superpositioning across both transitions can not be performed, however, nearby each individual transition this technique can be applied.

From this mastercurve a Williams-Landel-Ferry (WLF) (58) treatment was applied to the data, resulting in a graph of log a_T (the shift factor) versus (T-Tg) (Figure 23). This type of plot allows one to calculate the C_1 and C_2 values of the WLF equation:

50%(1,2)

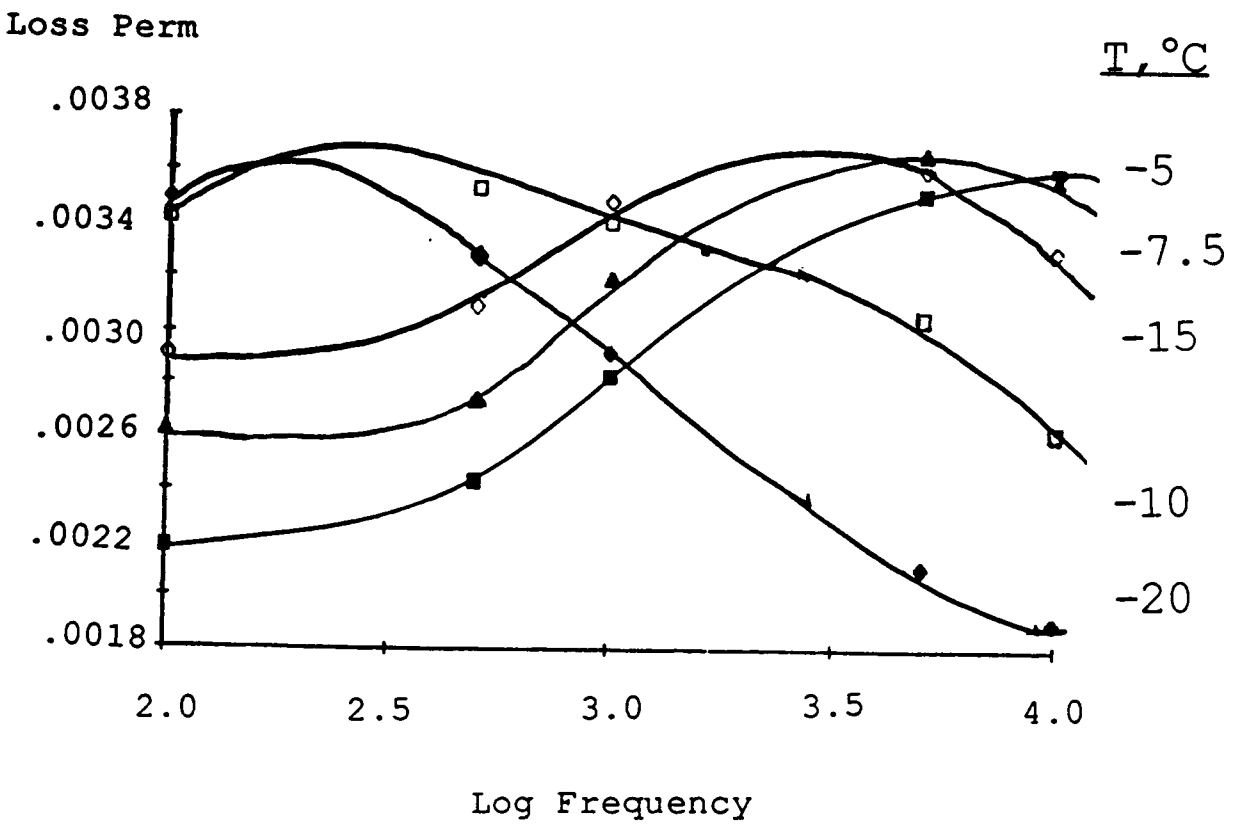

Figure 21. Effect of temperature on ε" (loss permittivity) versus log frequency at 1000 Hz

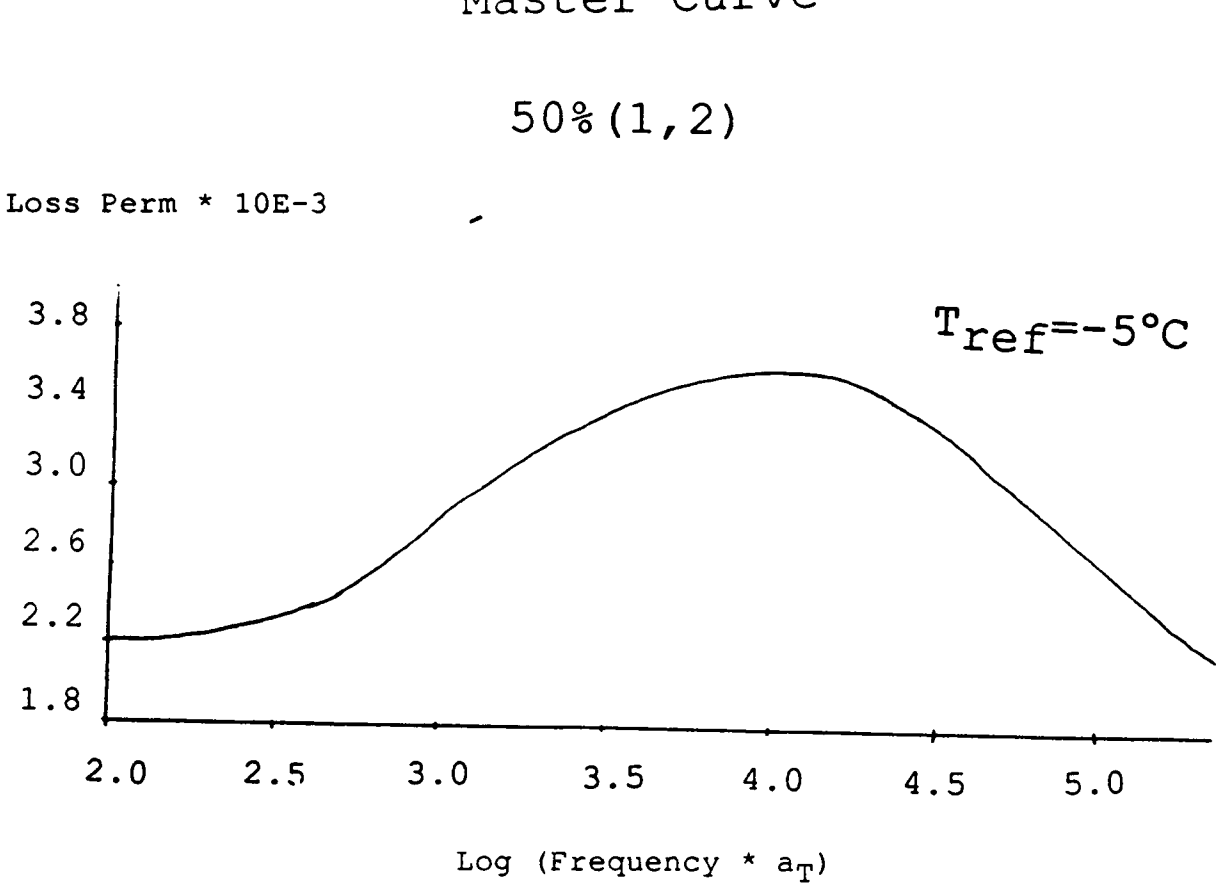

Figure 22. Mastercurve obtained by horizontally shifting curves in Figure 21

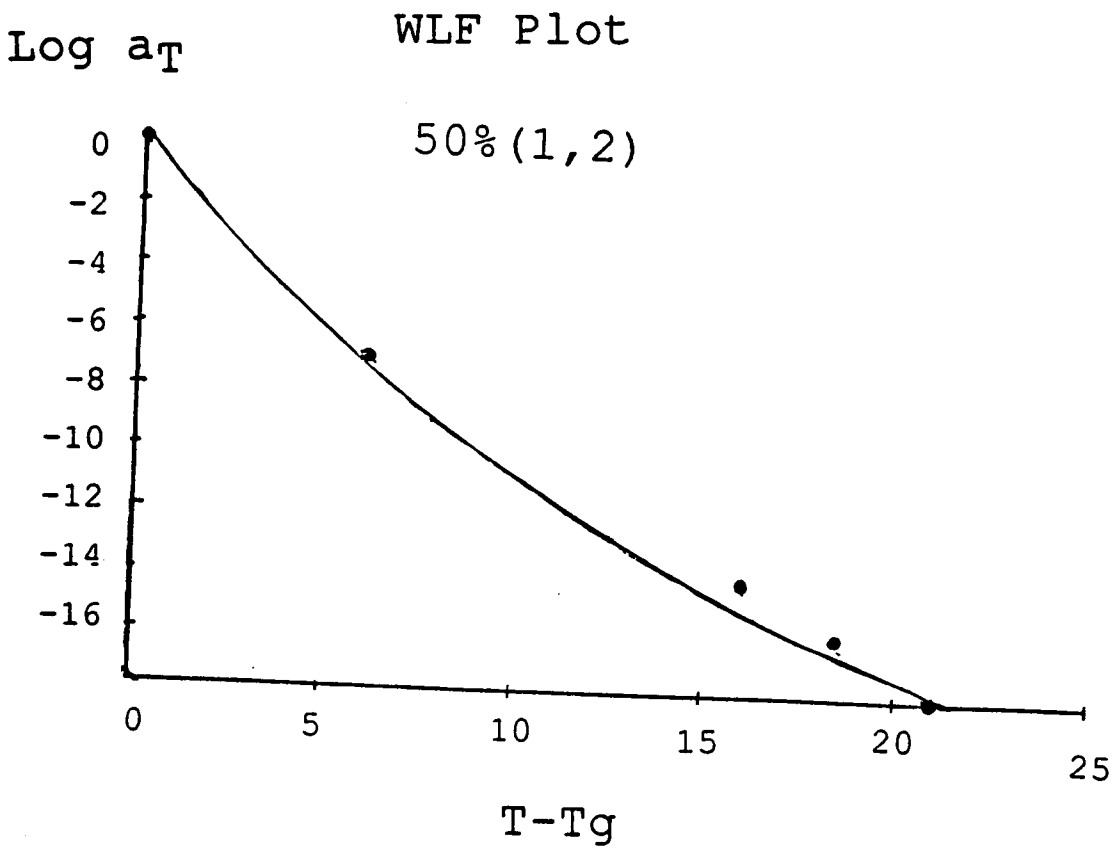

Figure 23. WLF plot of the 50%-1,2 polymer, obtained from the Mastercurve in Figure 22

$$\log a_T = \frac{-C_1(T-Tg)}{C_2+T-Tg} \qquad (38)$$

For polybutadiene, C_1 has been quoted as 11.2 and C_2 as 60.5 (8). From these values the activation energy can be calculuated from the following equation:

$$E_a = 2.303RC_1Tg^2/C_2 \qquad (39)$$

From this equation we obtained an E_a of 51.7 Kcal/mole was obtained which compares closely to the E_a of 46.5 Kcal/mole calculated using the Arrhenius equation.

2. T-Butylstyrene/Isoprene and Styrene/Isoprene Starblocks

For this study two radial starblocks were synthesized according to the previous discussion. These polymers contained poly(isoprene) as the soft block. FTIR and FT proton NMR analysis showed that the isoprene microstructure was 70% cis-1,4, 22% trans-1,4 and, 5% 3,4-microstructure (47). The hard block was either polystyrene or poly(t-butylstyrene). In both cases the soft block was 75 percent by weight and the hard block 25 percent by weight (Figure 24). Both samples were determined by GPC to have an overall molecular weight of 1,000,000 g/mole (47).

As mentioned previously the casting solvent used for film preparation can influence the type and amount of phase separation if it is selective for one of the two components.

Hard Block: 1) Poly(t-butyl styrene)

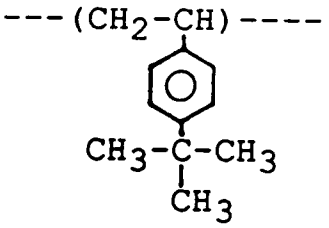

2) Poly(styrene)

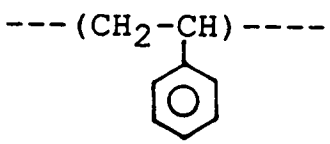

Soft Block: Poly(isoprene)

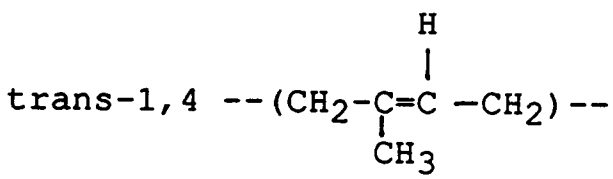

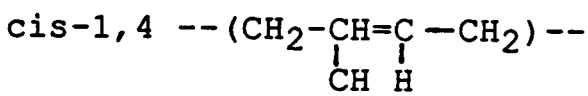

Figure 24. Radial starblock copolymer chemical composition, for the second series

The important factors governing selectivity can be estimated by the solubility parameters (δ) of the solvent and polymer. The solubility parameter of a given material can be calculated either from the cohesive energy, or from the molar attraction constant (59). These samples were cast from two solvents, cyclohexane (C) (δ= 8.2 $(cal*cm^{-3})^{1/2}$), which is preferential to the soft block (δ=7.9-8.2 $(cal*cm^{-3})^{1/2}$) and dichloroethane (DCE) (δ=9.2 $(cal*cm^{-3})^{1/2}$), which is preferential to the hard block (δ=8.1 $(cal*cm^{-3})^{1/2}$ for TBS and δ=9.4 $(cal*cm^{-3})^{1/2}$ for poly(styrene)) (19). The two polymers each cast from two solvents led to four samples which were analyzed with the Polymer Laboratory DETA and DMTA.

The DMTA trace for 25S75I (25% styrene and 75% isoprene), in cyclohexane, is shown in Figure 25. It is evident that phase separation has occured as indicated by the presence of the two transitions. This was also observed for the other polymers. Again, a rubbery plateau modulus is seen in between the two transitions.

The dielectric analysis was performed from -75°C to 175°C at frequencies of 1, 5, 10, 50, and 100 kHZ on the DETA. Figure 26 shows the dielectric relaxation spectra (tan δ versus temperature) for 25TBS75I in DCE. A transition was observed for both the hard and soft block in all cases; however, in some experiments the high temperature transition was not as easy to detect. This is thought to

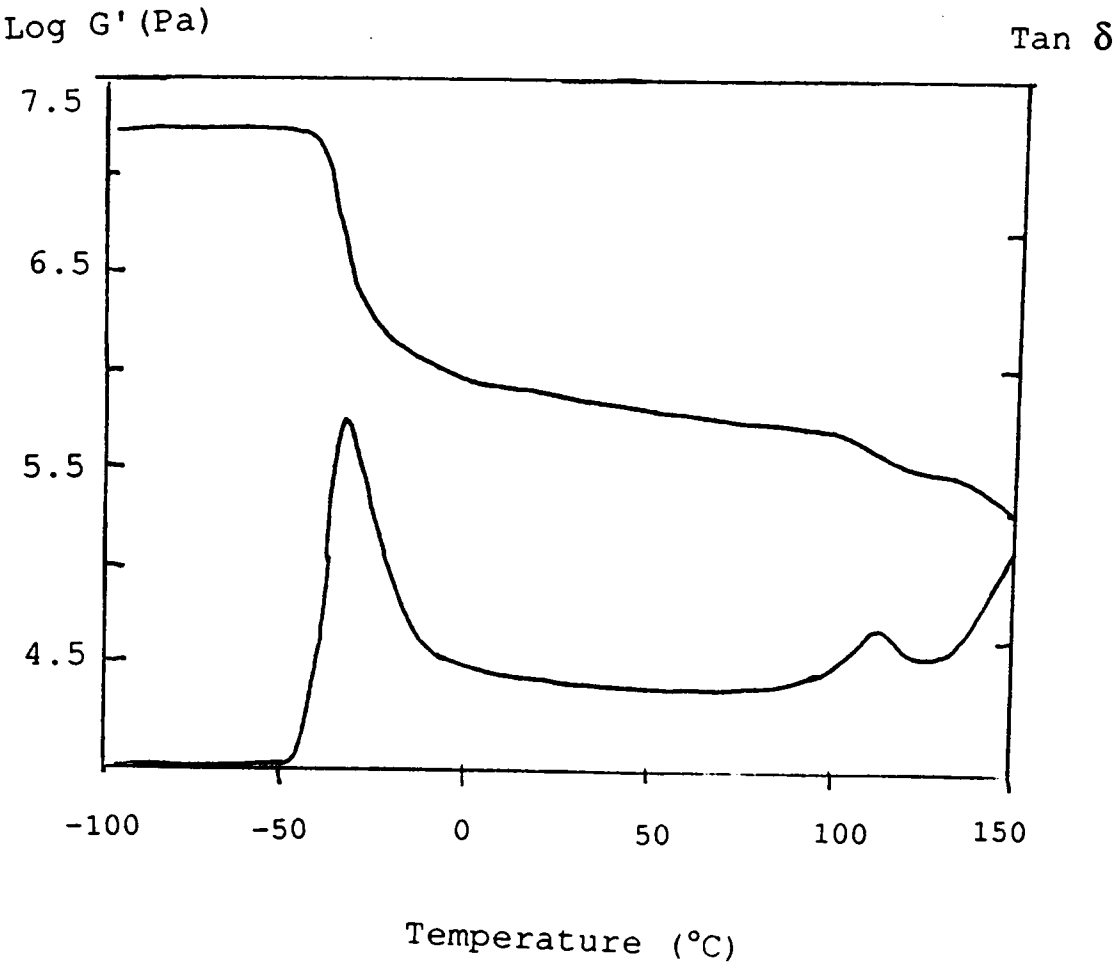

Figure 25. Dynamic Mechanical Analysis of the 75% isoprene/ 25% styrene in the shear mode at 1 Hz, 4°C/minute

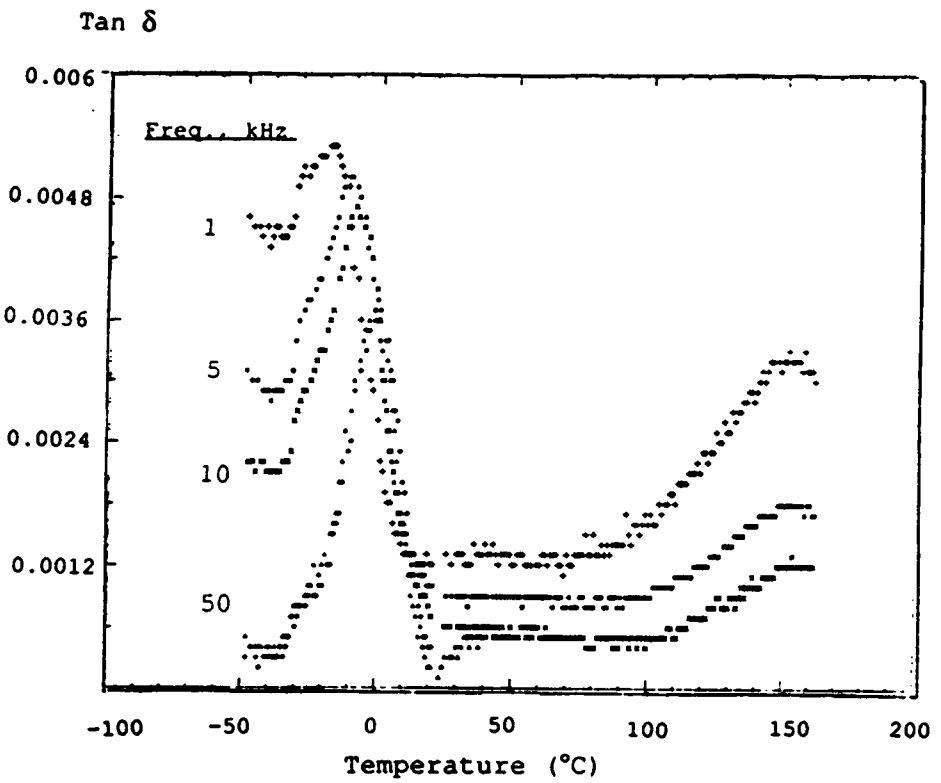

Figure 26. Dielectric analysis (tan δ vs. temperature) of the 25% TBS/75% isoprene cast from DCE at 1, 5, 10, and 50 KHz and 4°C/min. heating rate.

result from the fact that there was partial phase mixing of the two phases and also because the hard block only comprises 25 percent of the polymer.

The low temperature dielectric tan δ peak maxima for the styrene/isoprene at 1 kHz were -23°C and -28°C when cyclohexane (Figure 27) and dichloroethane were the solvents repectively. The low temperature tan δ peak maxima for the t-butylstyrene/isoprene at 1 kHz were -11°C and -19°C when cyclohexane and dichloroethane were chosen as solvents, respectively. These values indicate that for both copolymers the DCE increased the phase separation, because the transition was shifted to lower temperatures, toward the pure homopolymer transition. Also, the poly(styrene) is more phase separated than the poly(t-butylstyrene) when cast from either DCE or cyclohexane. From the dielectric data acquired on the Polymer Lab's DETA the activation energies for the low temperature transitions were calculated and are shown in Table 4. Within the experimental error only the 25% TBS cast from cyclohexane is significantly greater then the others, hence, requiring more energy to observe the low temperature transition.

The storage permittivity (ϵ') of the four samples are plotted as a function of temperature in Figure 28. When the ϵ' or dielectric constant of homopolymers are plotted as a function of temperature the value of ϵ' will initially be an asymptotically low value and increase dramatically to an

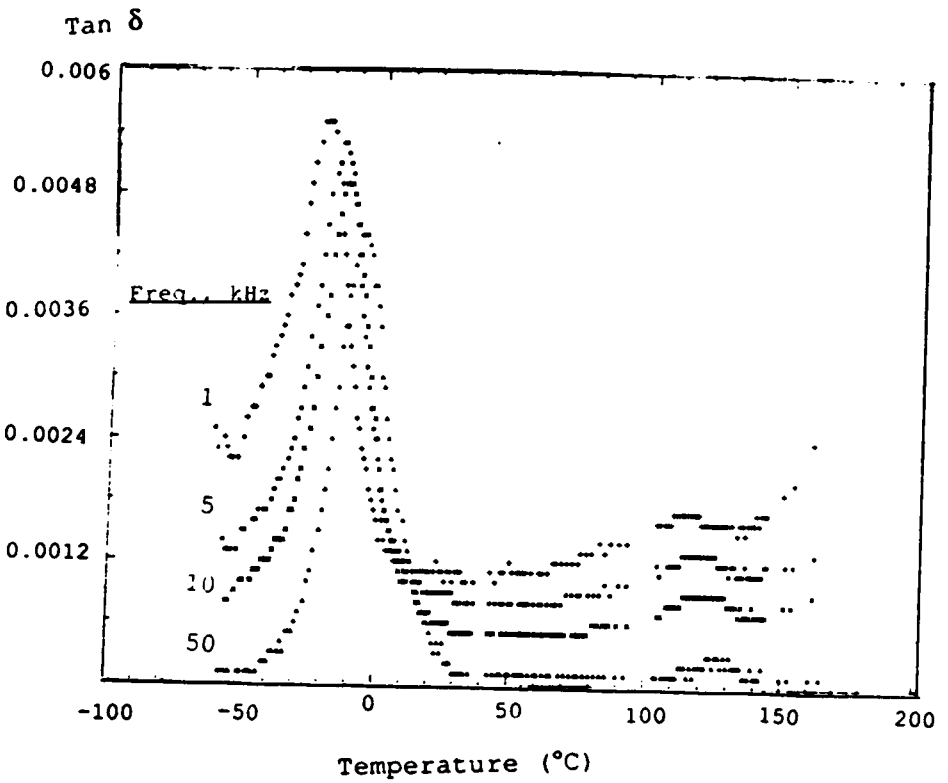

Figure 27. Dielectric analysis (tan δ vs. temperature) of the 25% styrene/75% isoprene cast from cyclohexane at 1, 5, 10, and 50 KHz and 4°C/min. heating rate.

Table 4

ACTIVATION ENERGIES FOR RADIAL STARBLOCK COPOLYMERS

Sample	Ea ± 3 Kcal/mole	Soft block Tan δ max
25S75I *	30.7	-23°C
25S75I **	28.7	-28°C
25TBS75I *	55.8	-11°C
25TBS75I **	33.8	-19°C

* Cyclohexane

** Dichloroethane

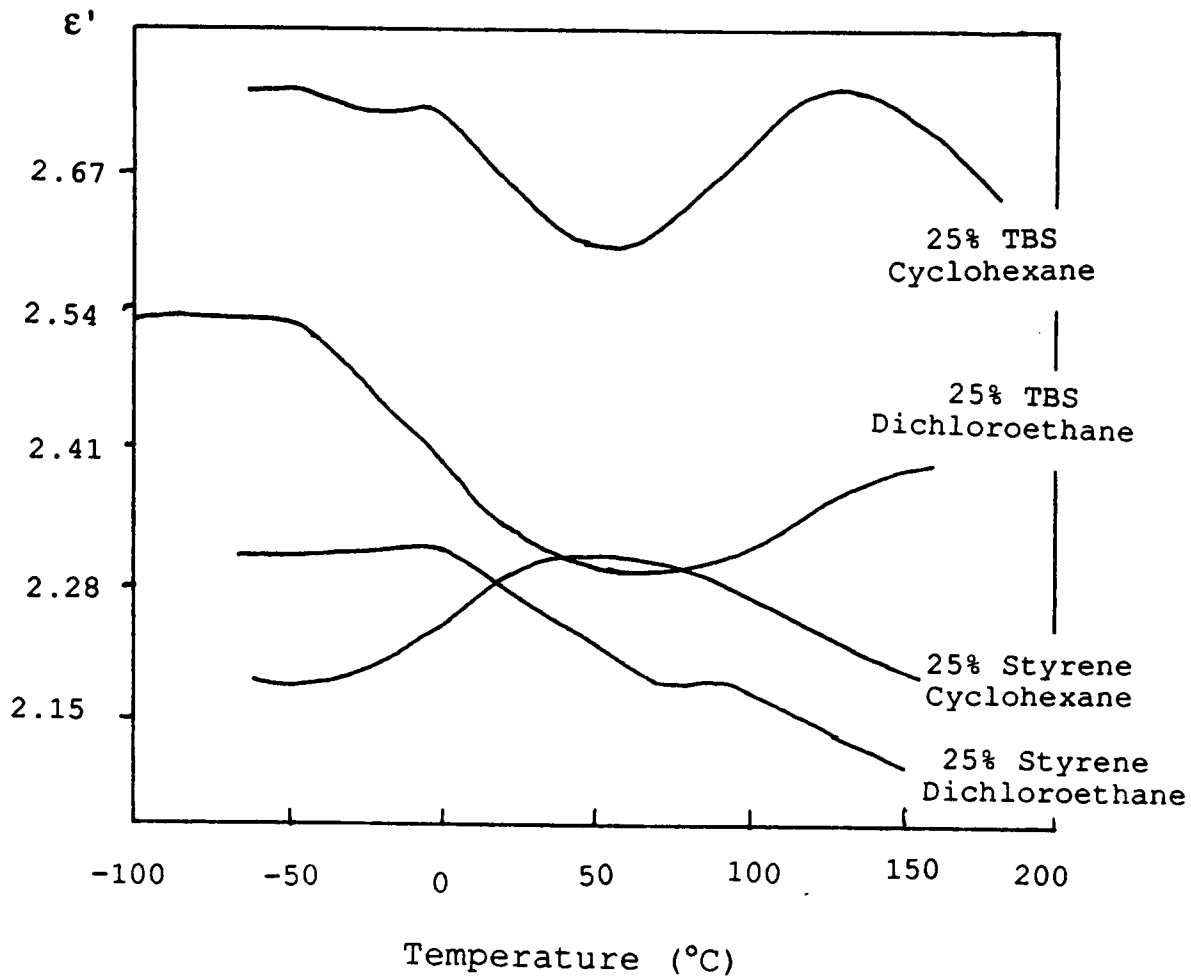

Figure 28. Dielectric analysis (storage permittivity versus temperature) of the two polymers cast from the two solvents

asymptotically high value at the glass transition temperature. In these copolymers this was not observed; rather, there is some amount of mixing of the dielectric constants of the two blocks. L. E. Nielsen (60) discusses mixture effects of a two-phase system with one being the continuous phase (i.e. block copolymers). According to Nielson, the dielectric constant is just one of many properties effected by the amount of mixing and the volume fractions of the two components. The dielectric constants of the blocks were determined to be as follows (61): poly(styrene) 2.49-2.55 and poly(isoprene) 2.37-2.45, no literature value was found for poly(t-butylstyrene). Because of the limited time on the Polymer Labs' DETA no quantitative analysis on the amount of mixing could be estimated. However, future work may involve isothermal studies of the polymers at different volume fractions to determine how the mixing is changing as a function of temperature and composition by monitoring the dielectric constant. Also comparing this data to the homopolymers at the same conditions will be helpful.

E. Conclusions

This work discusses some new and unique radial starblock copolymers synthesized under very well controlled conditions. The effects of phase separation, chemical composition, and microstructure were studied primarily by

dynamic mechanical thermal analysis and dielectric thermal analysis. With poly(butadiene) as the soft block if the %-1,2 microstructure decreased (%-1,4 increased) the phase separation increased, hence, the tan δ maximum, Tg and activation energy all decreased. Another very significant discovery was that hydrogenation of the soft block increased the phase separation which will effect the mechanical behavior as well as other properties.

The second series the radial starblocks were comprised of poly(isoprene) as the soft block and the hard block was either poly(styrene) or poly(t-butylstyrene). In this study it was observed that the poly(styrene) copolymer was more phase separated and that casting solvent for film preparation influenced the amount of phase separation. Dielectric analysis may prove to be a useful method to monitor phase mixing. Knowing the dielectric constants of the blocks and the volume fraction of each as estimate should be possible.

CHAPTER IV

ANALYSIS OF POLY(ALKYL METHACRYLATES)

A. Introduction

For this investigation a series of narrow molecular weight distribution, stereospecific poly(alkyl methacrylates) which were anionically synthesized were obtained. These were characterized by dielectric, and dynamic mechanical and other thermal analytical and solution techniques. The alkyl methacrylate side group was systematically increased in size from methyl to tertiary butyl. The effects of the bulkiness of the side group and the tacticity on the molecular transitions and other properties were of interest. The results showed that steric factors and stereoregularity influence the positions of the transitions observed and also their temperature dependence.

B. Background

Numerous physical studies have been undertaken in the past on a variety of poly(alkyl methacrylate) solid materials. However, the majority of these polymers were synthesized by free radical techniques resulting primarily in a syndiotactic microstructure with a fairly broad molecular weight distribution (M_w/M_n=3-5). In the following discussion a summary will be given of earlier researches which been reported in the literature on the stereoregular

and atactic poly(alkyl methacrylates).

One of the earliest investigations (62) of the effect of tacticity on the glass transition temperatures in poly(methyl methacrylate) (PMMA) reported a syndiotactic Tg of 115°C and an isotactic Tg of 45°C. In a more recent study the effects of the percent syndio- and isotactic triads were correlated to the glass transition temperatures (63). The difference in the Tg values has been shown to be due to a large difference in energy levels between rotational isomers in the syndiotactic chains (64).

The first studies of poly(n-alkyl methacrylates) performed by Rogers and Mandelkern (65) led to the glass temperatures of a series which consisted of PMMA through poly(n-dodecyl methacrylate), all synthesized free radically. The Tgs and number of carbon atoms on the side chain were inversely related. This has also been examined by others (2); it is thought that the longer n-alkyl group lowers the glass temperature due to an internal plasticization effect, or higher free volume. The longer n-alkyl chains increase the free volume available to the polymer chains through inefficient chain packing and hence decrease the Tg. The discontinuity in the expansion coefficient of glasses at Tg corresponds to the sudden onset of expansion in free volume and therefore allows an increased number of cooperative molecular motions in the chain backbone to occur (11).

If instead of lengthening the alkyl side chain, its bulkiness is increased, such as, replacing n-hexyl with cyclohexyl, the Tg will increase, from -5°C to 90°C (2) in this example. The effect of sustituent bulkiness, which is discussed in this thesis, has not been investigated in much detail for the stereoregular poly(alkyl methacrylates).

The initial dielectric studies on stereoregular poly(alkyl methacrylates) centered on PMMA (66-68). The reported tan δ curves plotted as a function of temperature indicate that the syndiotactic form has an α transition at 130°C and a β transition at 35°C (28Hz). The magnitude of the β tan δ peak was larger than that of the α peak, due to the high polarity of the ester side group. The conventional free radically synthesized form exhibited nearly identical relaxations to those of the syndiotactic PMMA, this is expected because NMR studies show the tactictiy of free radical PMMA to be largely syndiotactic.

It is well accepted that the β relaxation of methacrylate polymers is due to motion of the -COOR side groups (69). Also, the γ relaxation in these polymers has been associated with the rotation of the α-methyl group (70,71). More recent studies, at frequencies less than 1 Hz, were conducted to separate the β transition from the α in poly(alkyl methacrylates) (72). Other low temperature investigations dealt with the effects of moisture (73) on the β and γ transitions.

C. Experimental

1. Synthesis

The anionic synthesis of the poly(alkyl methacrylates) was performed by Mr. Tim Long in Prof. J. E. McGrath's laboratories at Virginia Polytechnic Institute and State University and has been discussed in many recent publications (74-77). This synthetic method results in narrow molecular weight distributions with predictable molecular weights. Other advantages to this synthetic scheme are that block copolymers may be produced by sequential addition, controlled tacticity is available, and there is functional termination capability. In anionic synthesis, the polymerization solvent plays a large role in the tacticity and microstructure obtained. Polar solvents, such as ethers, produce a syndiotactic microstructure, whereas nonpolar solvents, such as hydrocarbons, tend to produce the isotactic form (78). When considering various alkyl methacrylate monomers, the size of the alkyl group also influences the tacticity.

The polymerization solvents, tetrahydrofuran (THF) and toluene, were first purified by distillation. The initiator, diphenylhexyl lithium (DPHL), was formed by reacting sec-butyl lithium and 1,1-diphenyl ethylene (DPE). The sec-butyl lithium was used as received (1.35 M in cyclohexane) and DPE was purified by vacuum distillation from sec-butyl lithium. The alkyl methacrylate monomers

were first distilled from CaH_2. Immediately prior to use, the monomers were distilled from trialkyl aluminum reagents (25 weight percent solutions in hexane). Recent work has involved the extension of this technique to the purification of branched alkyl methacrylate monomers (79).

The polymerization scheme is shown in Figure 29. First the initiator is formed in the desired solvent under dry nitrogen. In hydrocarbons the initiator is formed at room temperature (1 to 2 hours). The reactor is then cooled to-78°C; however, with polar solvents the initiator is formed at -78°C. The purified monomer is slowly added to the initiator solution; the temperature is maintained at -78°C to prohibit any undesirable exotherms. The polymerization time is a function of both the solvent and the reaction temperature, typically 20 to 30 minutes for polar solvents and several hours in hydrocarbon solvents. The polymerization is terminated with degassed HPLC-grade methanol. All polymers were isolated by precipitation into an appropriate nonsolvent determined by the polymers solubility characteristics. Films of the polymers were prepared either by solution casting or compression molding. In the case of solution casting a 20 weight percent solution of the polymer in THF was cast onto a sheet of Teflon. The film was dried under vacuum near its glass transition temperature for 24 to 48 hours. The compression molding was done at ~50°C above the glass transition temperature. Films

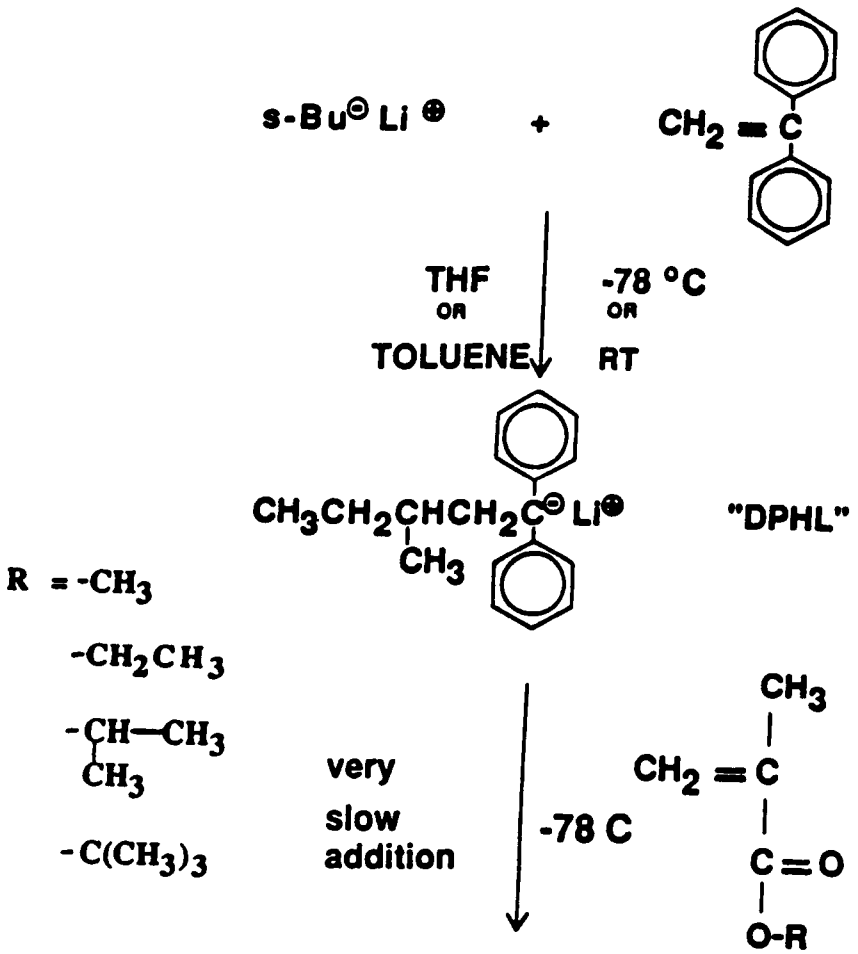

Figure 29. Anionic polymerization of Alkyl Methacrylates

were typically 0.1 to 0.4 mm in thickness.

2. Instrumentation

The capacitance and dissipation factor measurments of the polymers were made on the General Radio Bridge 1620A capacitance bridge assembly and the Polymer Laboratory Dielectric Thermal Analyzer (DETA) (see Chapter 2). The analyses were performed as a function of temperature over the frequency range of 100 Hz to 100 kHz and a temperature range of -100°C to 200°C.

The dynamic mechanical measurements were performed in the two point single cantilever beam mode on the Polymer Laboratory Dynamic Mechanical Thermal Analyzer (DMTA). A geometry constant, based on sample dimensions, is entered into the analyzer. The microprocessor adjusts the drive current to give a constant strain level. The signal amplitude and phase are detected as a function of temperature and frequency (29). A frequency of 1 Hz over a temperature range of -150°C to 200°C at 5°/minute was utilized.

The glass transition temperatures were determined on the Perkin Elmer Model 4 Differential Scanning Calorimeter (DSC-4) at a heating rate of 10°C/minute. In this work the glass transition temperatures quoted were determined from the midpoint of the observed transition. Typically, the glass transition temperature quoted is reproducible to

within ±1°C.

The tacticites were determined on a high resolution 50 MHz C-13 NMR (in $CDCl_3$) using a Bruker WP 200 SY spectrometer. Inverse-gated proton decoupling in combination with the addition of a small amount (0.1 M) of $Cr(AcAc)_3$ to the samples assured quantitative accuracy of the data. Typically 1000 free induction decays with a recycle delay of 5.0 seconds and a flip angle of ~40° were accumulated and Fourier transformed.

The molecular weight and other solution properties were determined on the Waters 150C Gel Permeation Chromatograph (GPC) at 30°C in THF, and a flow rate of 1 ml/minute with five Ultrastyragel™ columns. The GPC was equipped with a Waters refractive index detector and a Viscotek™ (Model 100) differential viscosity detector. Polymer Laboratory poly(styrene) standards were used to construct a universal calibration curve. This method of determining absolute molecular weight uses the hydrodynamic volume ($[\eta]M$) as the calibration parameter (80).

D. Results and Discussion

A series of eight polymers were synthesized according to the polymerization scheme shown in Figure 29. The monomers utilized were methyl methacrylate (MMA), ethyl methacrylate (EMA), isopropyl methacrylate (IPMA), and tertiary-butyl methacrylate (TBMA). All monomers were

synthesized in both the syndiotactic and isotactic forms. Also, a syndiotactic block copolymer of PMMA-PTBMA was synthesized. Some of these characterization results have been previously published (81).

Many factors influence molecular motions in polymeric solids; steric hindrance and stereospecificity, in particular, will be focused on here. If a large bulky group is directly attached to the main chain, it will decrease the mobility of the main chain. In general, this effect will increase both the activation energy and the characteristic relaxation times. If the large bulky group is attached to a side chain it has been proposed (13) that the main chain mobility would again be decreased by steric hindrance. However, adjacent polymer chains may be forced further away and hence can increase the overall mobility of the main chain. The main chain relaxation will thus depend on the relative magnitudes of these two effects.

The stereochemistry determines the position and conformation of sidegroups. This will play a large part in determining the overall modility of the mainchain due to steric factors, rotational degrees of freedom, and the packing ability of chains.

1. Tacticity and Thermal Analysis

The tacticity distributions were determined by triad measurements of the carbonyl and quaternary carbon regions

Table 5

MICROSTRUCTURAL CHARACTERIZATION OF
POLY(ALKYL METHACRAYLATES)

SAMPLE	PZN. SOLVENT	%TACTICITY ISO	HETERO	SYNDIO
PMMA	THF	1	21	78
	TOL	82	15	3
PEMA	THF	2	21	77
	TOL	90	10	0
PIPMA	THF	6	29	65
	TOL	83	17	0
PTBMA	THF	2	46	52
	TOL	99	1	0

with ^{13}C NMR (Table 5). In Figure 30 these two carbon regions for PTBMA are shown. Typically, the tacticity measurements of PMMA utilize ^{1}H NMR. However, with higher alkyl esters there are overlapping signals in the α-methyl region, thus ^{13}C was choosen. Comparison of the ^{1}H and ^{13}C tacticity calculations of PMMA agreed to within 2%.

From Table 5 it is evident, for the syndiotactic polymers, that as the bulkiness of the side-group is increased the overall percent syndiotactic structure decreases. It is thought that the bulkiness of the group hampers the formation of the desired microstructure. In all cases the toluene polymerizations resulted in a higher percentage of the desired tacticity; this is consistent with the literature (82).

In Table 6 the glass transition (T_g) temperatures are listed for the eight polymers. It is interesting to note the wide range of T_g's which can be obtained depending on the structure. Isotactic PEMA was an elastomer while most of the others were glassy polymers at room temperature. One can also observe that the T_g drops from methyl to ethyl due to an increase in the free volume as the chain is lengthened. However, from ethyl to tertiary butyl the glass transition temperatures either stay the same or increase, due to an increase in the bulkiness of the side groups. It is important to point out that the glass transition temperature is influenced by the percent of the desired

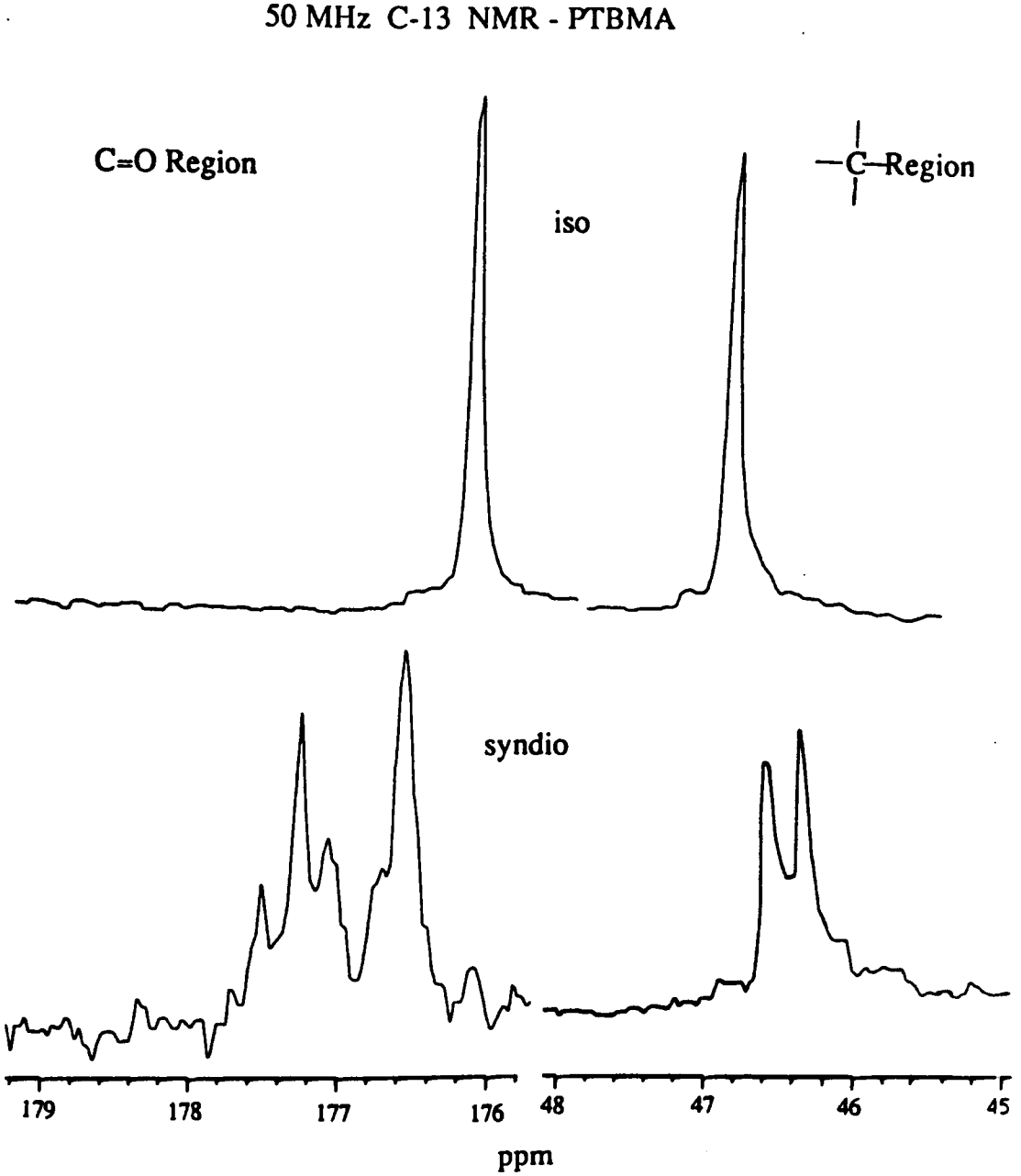

Figure 30. 50 MHz C-13 NMR of iso and syndio PTBMA, the carbonyl and quarternary carbon regions

Table 6

GLASS TRANSTION TEMPERATURES

	T_g (°C) [a]		Theoretical T_g (°C) [b]	
SAMPLE	SYN	ISO	SYN(100%)	ISO(100%)
PMMA	130	54	160	43
PEMA	86	6	120	8
PIPMA	86	34	139	27
PTBMA	118	84	145	84

a. Experimentally determined
b. Theoredically calculated, see ref 64 PTBMA calculated from extrapolated values (77)

microstructure incorporated into the polymer. Table 6 also gives the theoretical Tg's of these polymers if they were 100% syndio- or isotactic (64). The deviations from the theoretical values are due the microstructure obtained.

2. Gel Permeation Chromatography

The molecular weight information on the eight polymers is shown in Table 7. This table lists the molecular weight distribution (MWD), weight average molecular weight ($<M_w>$), and number average molecular weight ($<M_n>$). All of the polymers are high molecular weight and above the reported critical molecular weight ($<M_c>$) of ~27,000 g/mole for PMMA (83). The critical molecular weight is not the same for all polymers, it will increase in magnitude as the intermolecular forces in the polymer decrease. At the M_c the slope of the log melt viscosity versus log MW increases from 1.0 to 3.4 due to the presence of chain entanglements. If the polymers are well above the critical molecular weight the physical properties measured should be independent of molecular weight.

The MWD's of the syndiotactic polymers are all very narrow; however, the isotactic microstructure polymerizations resulted in a broader MWD. Figure 31 shows a chromatogram for S-PTBMA, one curve is the viscosity trace and the other is the refractive index trace. The hydrocarbon solvent polymerizations do not produce a true

Table 7

SOLUTION BEHAVIOR OF POLY(ALKYL METHACRYLATES)

	Mw/Mn		$Mw*10^{-5}$		$Mn*10^{-5}$	
SAMPLE	Iso	Syn	Iso	Syn	Iso	Syn
PMMA	4.73	1.29	8.57	2.67	1.81	2.07
PEMA	2.45	1.46	6.99	2.17	2.85	1.49
PIPMA	3.09	1.25	7.05	3.63	2.29	2.91
PTBMA	1.14	1.13	3.70	.632	3.24	.562

*All measurements at 30°C in THF and in g/mol

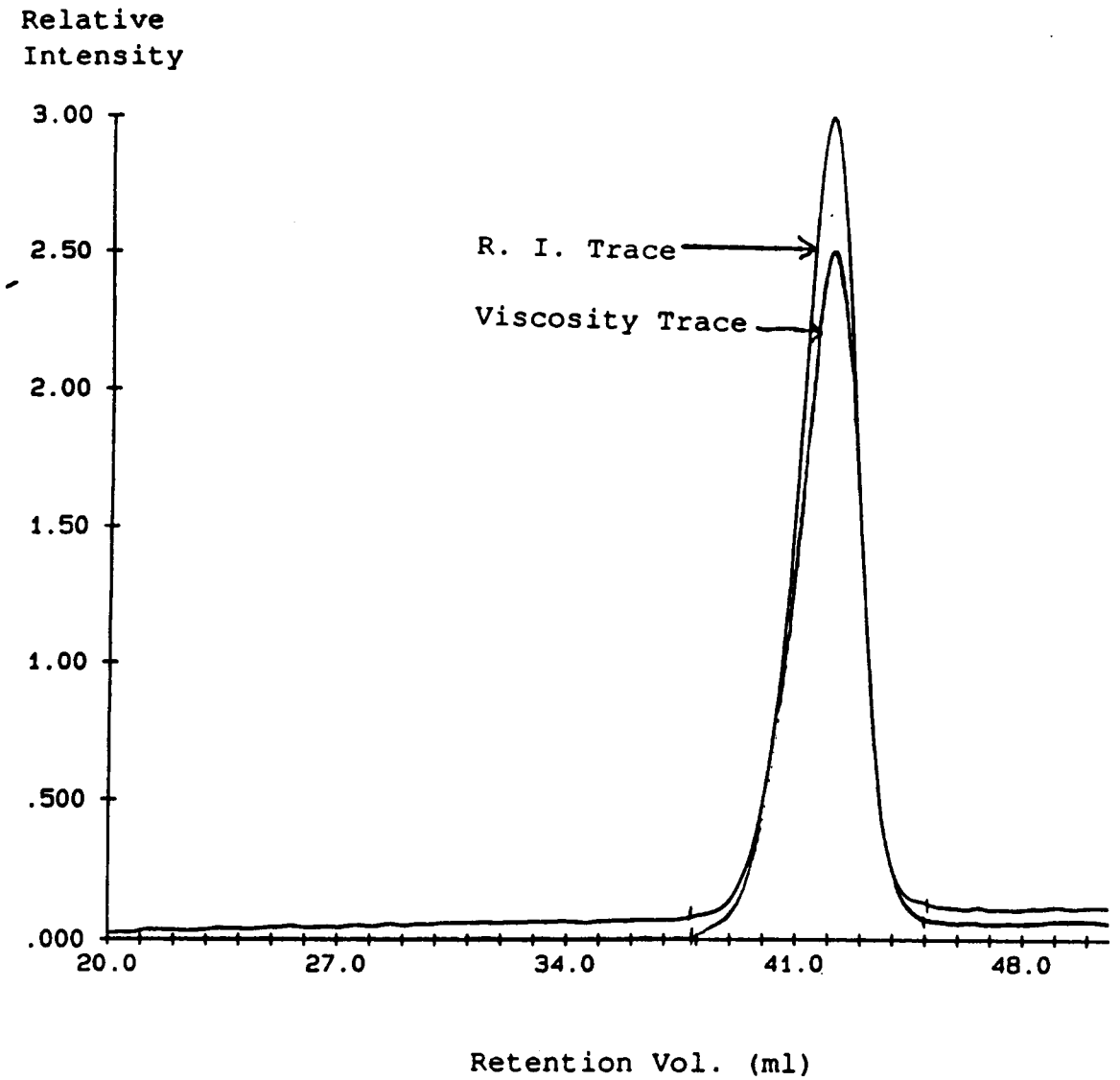

Figure 31. Dual chromatogram of S-PTBMA, the refractive index and differential vicosity curves

"living" polymer chain as do the other anionic syntheses due to the enolate instability, therefore their MWD's tend to be broader. In the case of PTBMA, both the iso and syndio forms are narrow in MWD. Apparently the bulkiness of the side group inhibits undesirable side reactions.

Table 8 lists other solution properties obtained via the Viscotek^{TM} detector attached to the GPC (84,85). The parameters of Log k and a are from the well known Mark-Houwink equation which relates the intrinsic viscosity to the viscosity average molecular weight ($<M_V>$):

$$\eta = K * M_V^{a} \qquad (40)$$

The parameter a has a range of -2 to +2 (86), however, it usually does not go below 0. The value of a provides information on the polymer's conformation in solution. The K's and a's will differ for each polymer/solvent combination. A value of 0.5 is obtained for a random coil, as a gets larger the polymer chains become more extended (rod like). It appears from Table 8 that there is no difference in the average conformations between the syndiotactic and isotactic forms of either PMMA and PEMA. However, the syndiotactic forms of PIPMA and PTBMA appear to be more extended that the corresponding isotactic microstructures (in solution).

The intrinsic viscosity values, shown in Table 8, appear to correlate with the $<M_W>$ as expected.

Table 8

SOLUTION BEHAVIOR OF POLY(ALKYL METHACRYLATES)

	- Log K (dl/g)		a		η	
SAMPLE	Iso	Syn	Iso	Syn	Iso	Syn
PMMA	3.724	3.789	.663	.665	1.253	.654
PEMA	3.157	3.311	.583	.589	1.621	.636
PIPMA	3.878	4.08	.685	.703	1.211	.674
PTBMA	3.612	3.738	.622	.677	.712	.318

*All measurments at 30°C in THF

3. Dielectric and Dynamic Mechanical Analysis

In Figure 32 the storage modulus (E') and Tan δ are plotted for both the isotactic and syndiotactic forms of PMMA. The modulus at low temperatures is indicative of a glassy material, as the temperature approaches the Tg of the PMMA the modulus drops off to a value indicative of a rubbery material. The tan δ represents the damping ability, as the temperature increases tan δ goes through a maximum representing the temperature at which the polymer has the greatest energy absorbing capability. A low temperature β relaxation was seen in the syndiotactic form at 20°C, however, the scale had to be enlarged to observe the transition mechanically. The isotactic PMMA does not exhibit any β relaxation.

In Figure 33 the mechanical properties of PTBMA are plotted against temperature. In this experiment there was no detectable low temperature relaxation. A β relaxation was detected for the S-PEMA, however, it was slightly merged into the α transition. It is well accepted that the β relaxation observed mechanically for poly(alkyl methacrylates) is associated with the rotation of the ester side-group.

The dielectric data were gathered on both the GenRad Capacitance Bridge and the Polymer Lab's DETA. Good agreement of the data from each instrument was found (see Appendix A). The dielectric analyses for syndiotactic PMMA

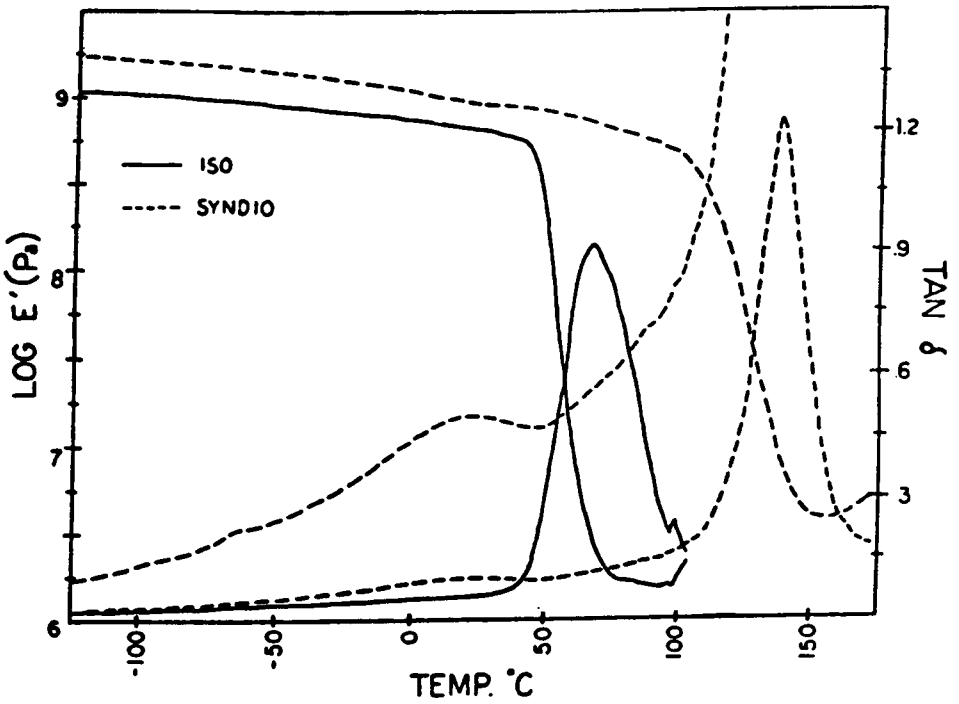

Figure 32. Dynamic mechanical analysis of iso and syndio PMMA at 1 Hz (E' and tan δ versus temperature)

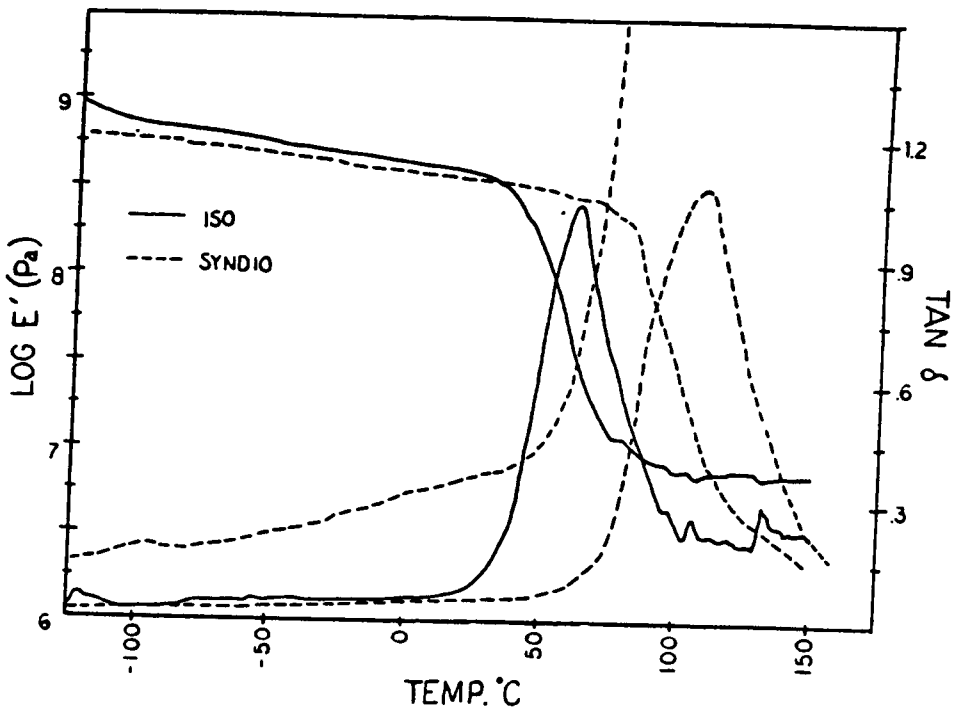

Figure 33. Dynamic mechanical analysis of iso and syndio PTBMA at 1 Hz (E' and tan δ versus temperature)

are shown in Figure 34. The tan δ values for three frequencies, 100 Hz, 1000 Hz, and 10,000 Hz are shown as a function of temperature. The magnitude of the β peak is much larger than the α peak. This was not the case in the mechanical analysis; rather, the α was much larger than the β. This is because the overall dipole moment of the side group is greater than the main chain. Hence, the β relaxation (in the dielectric experiment) is more prominent because of the strong coupling with the electric field. This fact emphasizes one advantage of dielectric analysis over dynamic mechanical testing, the former method is more sensitive if one can take advantage of polar substituents. Another important point is that at 100 Hz the α and β peaks are separated, at 1000 Hz the α peak is just a shoulder and by 10,000 Hz the two peaks are totally merged.

The dielectric spectrum for the isotactic form of PMMA is shown in Figure 35. Only a small shoulder for the β transition is detected at 100 Hz which merges with the α peak at 1000 Hz. This is due to two factors: first, the isotactic α transition has shifted down in temperature relative to a more syndiotactic polymer, thus overlapping with the β region. This merging of dispersions is also verified by noting that the α transition obtained at 10,000 Hz is much broader than that from the 100 Hz test. The second important factor is the tacticity effect. It has been postulated that the β relaxation observed in the

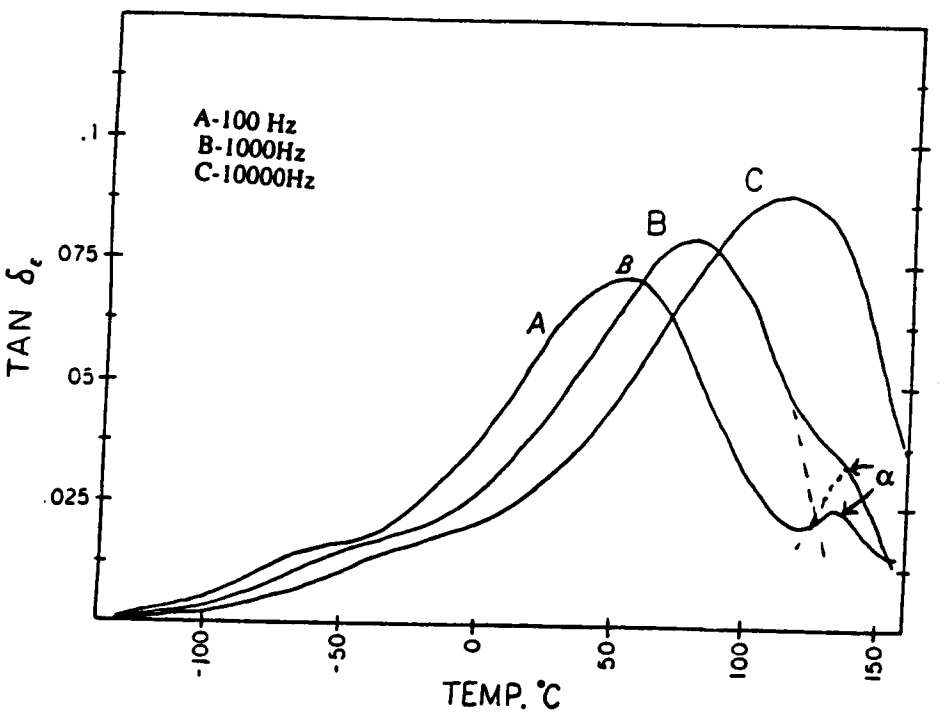

Figure 34. Dielectric tan δ curves of syndiotactic PMMA at 100, 1000, and 10,000 Hz

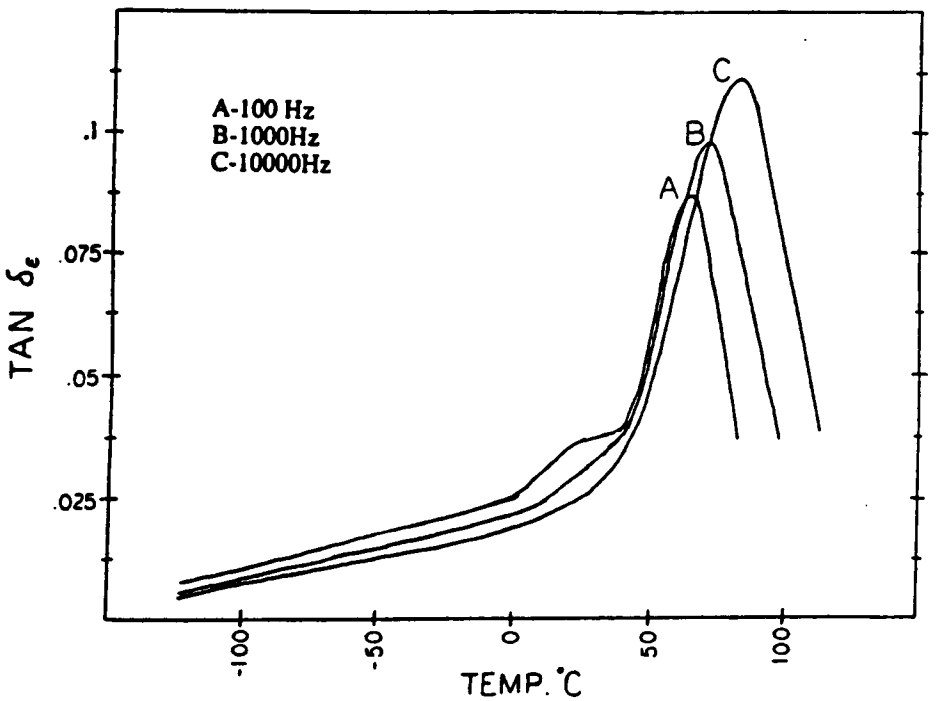

Figure 35. Dielectric tan δ curves of isotactic PMMA at 100, 1000, and 10,000 Hz

syndiotactic microstructure is due to the steric hindrance of the ester group with the main chain methyl group of the adjacent repeat unit (2). In the isotactic structure these interactions are not present. Another fact which reinforces this point is that syndiotactic poly(methyl acrylate), which does not contain the above mentioned methyl group, does not exhibit any β relaxation.

Figure 36 shows the dielectric analysis of S-PEMA. Here a large β relaxation was observed during tests at 100 Hz; but, this feature merges into the α at 1000 Hz test frequencies. The activation energy for the β relaxation of the S-PEMA was calculated to be 22 kcal/mole, very close to that of the S-PMMA. Figure 37 shows the dielectric spectrum for isotactic PTBMA, where no β relaxation was observed. Both tacticity effects and the steric factors mentioned above probably are responsible for this lack of a β-dispersion in isotactic PTBMA. The dielectric scan for the syndiotactic PMMA-PTBMA block copolymer is shown in Figure 38. This polymer's composition was 75 weight percent PMMA with <Mw> of 50,000 and, therefore, the dielectric relaxation closely resembles that of the homopolymer syndiotactic PMMA.

An Arrhenius plot for the syndiotactic PMMA is shown in Figure 39. From the slopes of these curves the activation energies were calculated to be 117.5 kcal/mole and 19.4 kcal/mole for the α and β transitions, respectively, which

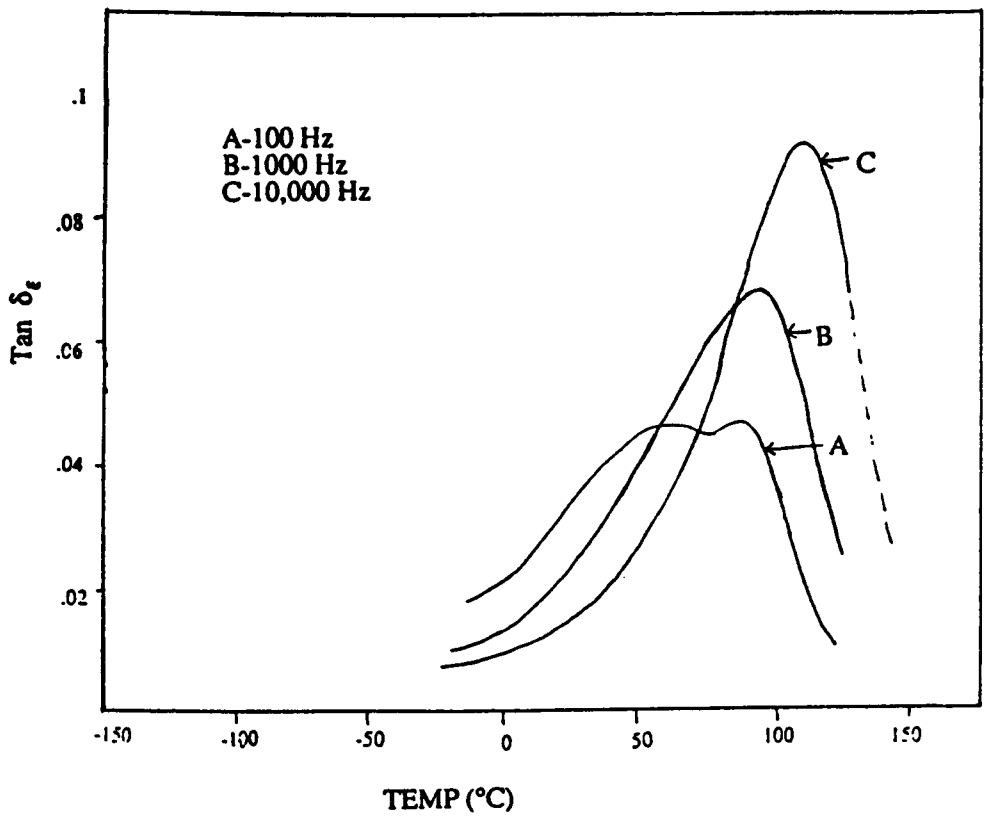

Figure 36. Dielectric tan δ curves of syndiotactic PEMA at 100, 1000, and 10,000 Hz

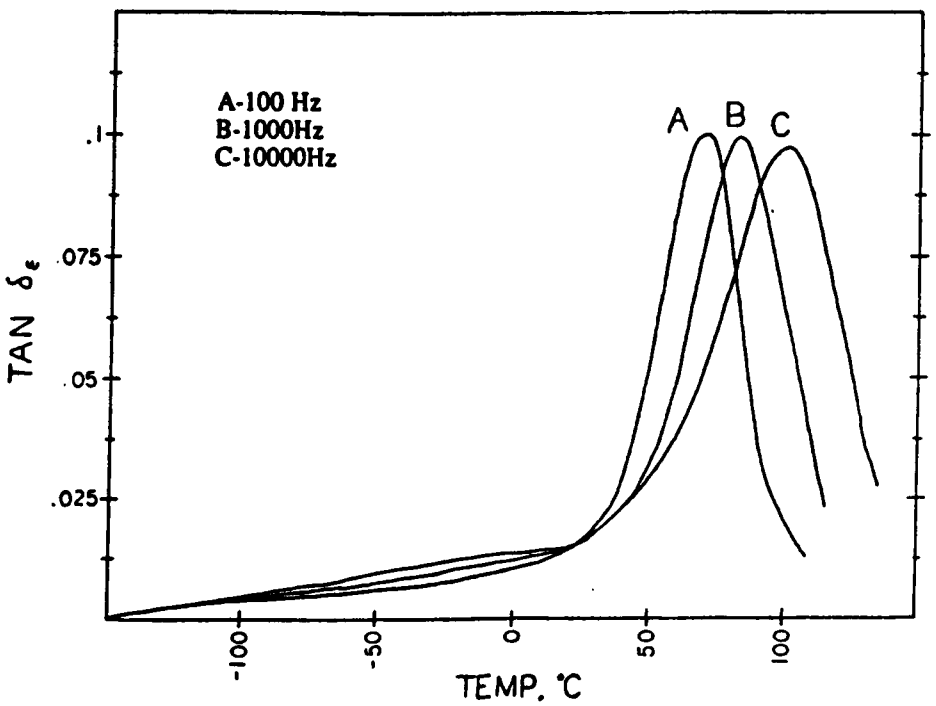

Figure 37. Dielectric tan δ curves of isotactic PTBMA at 100, 1000, and 10,000 Hz

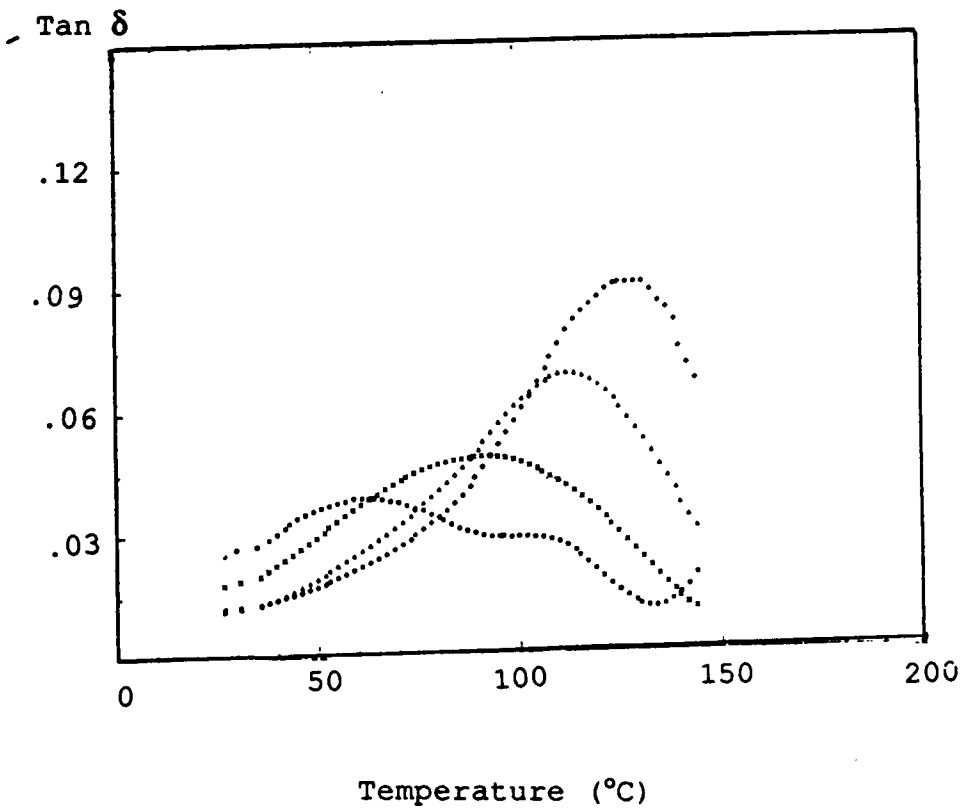

Figure 38. Dielectric tan δ curves of PTBMA-PMMA block copolymer at 200, 2000, 20,000, and 100,000 Hz

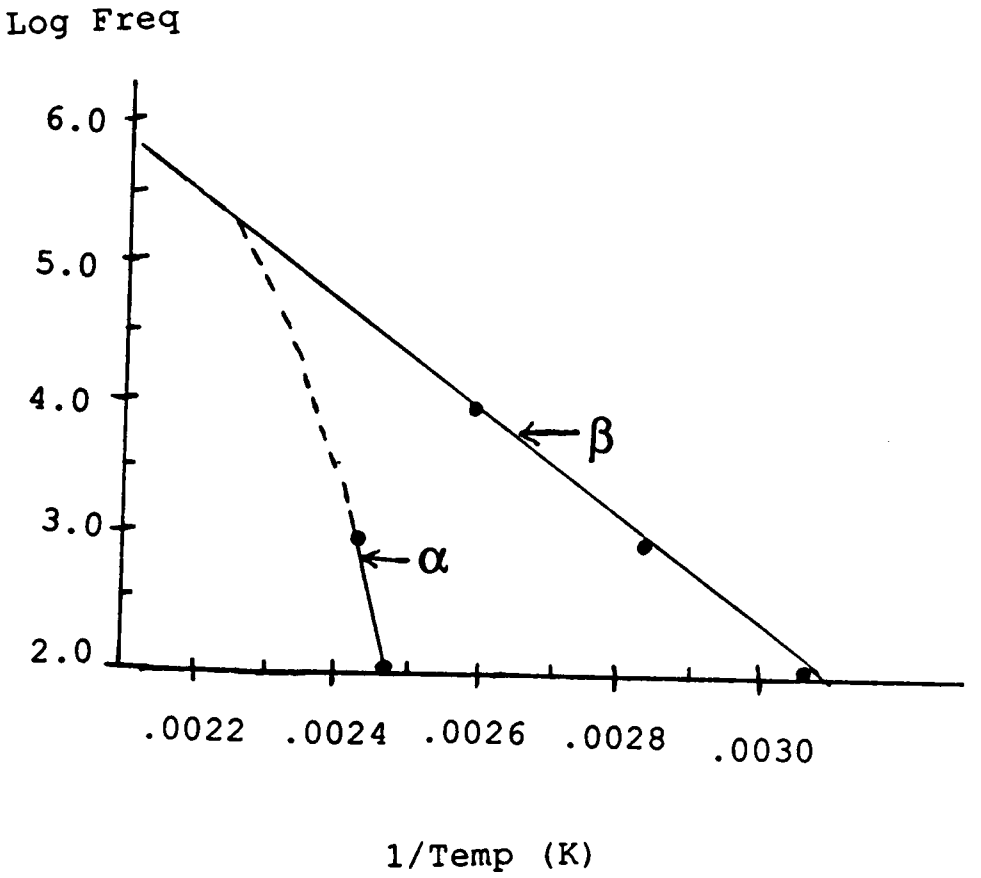

Figure 39. Arrhenius plot of syndiotactic PMMA

is in good agreement with the literature (2). The calculated activation energies for the α transitions of the eight polymers studied are shown in Table 9. These values, interestingly enough, do not correlate directly with the glass transition temperatures. It appears that from methyl to isopropyl there is an increase in the free volume due to chain lengthening, hence, the chain becomes more flexible and E_a drops. The bulkiness of the t-butyl group causes the activation energy to increase in both the isotactic and syndiotactic polymers, where it is postulated that the steric effect is the overriding factor effecting the activation energy.

a. Cole-Cole Analysis

The complex plane representation of dielectric relaxation processes, otherwise known as arc diagrams, result by plotting ϵ' versus ϵ'' over a wide range of frequencies at a given temperature (see Chapter 2). The Havriliak-Negami equation is given as follows:

$$\epsilon^*(\omega) = \epsilon_u + \frac{\epsilon_R - \epsilon_u}{(1+(i\omega\tau)^{(1-a)})^b}$$

This equation describes dispersions in such a way that a linear form results at high freqencies and a circular arc at low frequencies. The details involved in the following

Table 9

COMPARISON OF GLASS TRANSITION TEMPERATURES TO ACTIVATION ENERGIES

	T_g(°C)		*Ea ± 3.5	
SAMPLE	SYN	ISO	SYN	ISO
PMMA	130	54	117.5	59.0
PEMA	86	6	59.8	32.6
PIPMA	86	34	38.7	29.5
PTBMA	118	84	52.5	37.9

*E_a in Kcal/mole determined from dielectric measurements of α transition

discussion are listed in Appendix B.

In this study the following polymers were analyzed using the Havriliak-Negami equation: S-PMMA, S-PTBMA, I-PTBMA, and a syndiotactic PMMA-PTBMA block copolymer. First the dielectric ϵ' and ϵ'' were determined on the Polymer Laboratory DETA. Measurements were made as temperature was scanned at 4°C/minute, at frequencies of 1, 5, 10, 50, and 100 kHz. After these data were accumulated the Cole-Cole plots (ϵ' versus ϵ'') were constructed at different temperatures for all the polymers. Figure 40 shows a plot for syndiotactic PTBMA at three temperatures. From this plot it is evident that the high frequency value of ϵ_u was quite easy to obtain, however, there was some error in determining the low frequency ϵ_R. Also, from this plot the high frequency limiting angle ϕ_L and its bisector $\phi_L/2$ were determined. The relaxation time τ was calculated from the value of $1/\omega$ where $\phi L/2$ intersects the arc (Figure 41).

Next it was necessary to determine numerical values for a and b as discussed in Appendix B. From the five parameters a, b, ϵ_u, ϵ_R, and τ theoretical values of ϵ' and ϵ'' at any frequency can be calculated. In Figure 42 the calculated and experimental points are plotted, good agreement was seen between these values.

Table 10 lists the parameters of a, b, τ, and $(\epsilon_R-\epsilon_u)$ for the above discussed polymers. Since it is postulated that the isotactic form is more extended then syndiotactic

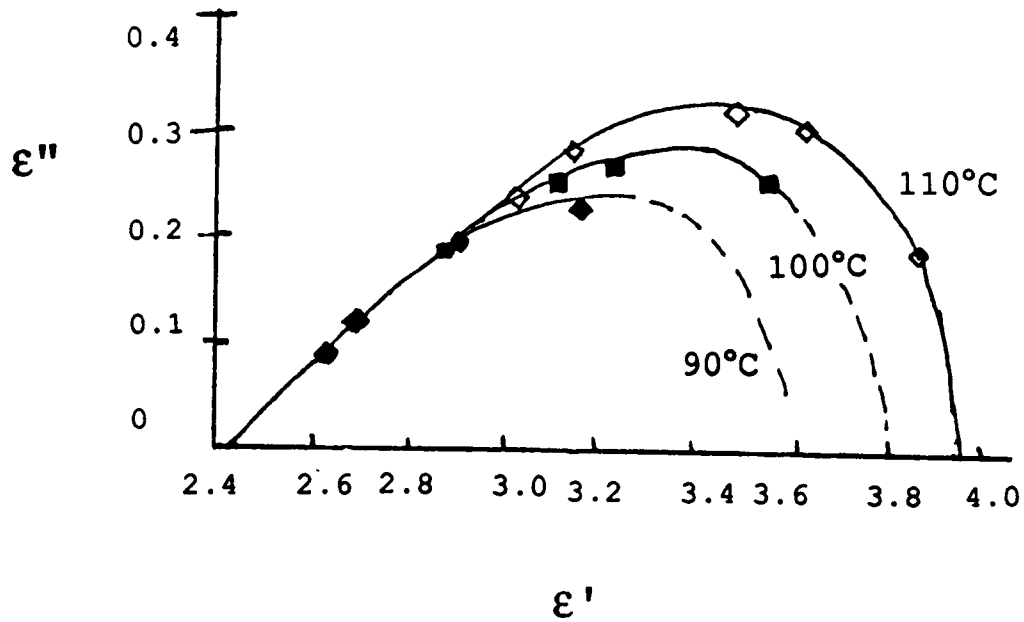

Figure 40. Cole-Cole plots of syndiotactic PTBMA at various temperatures

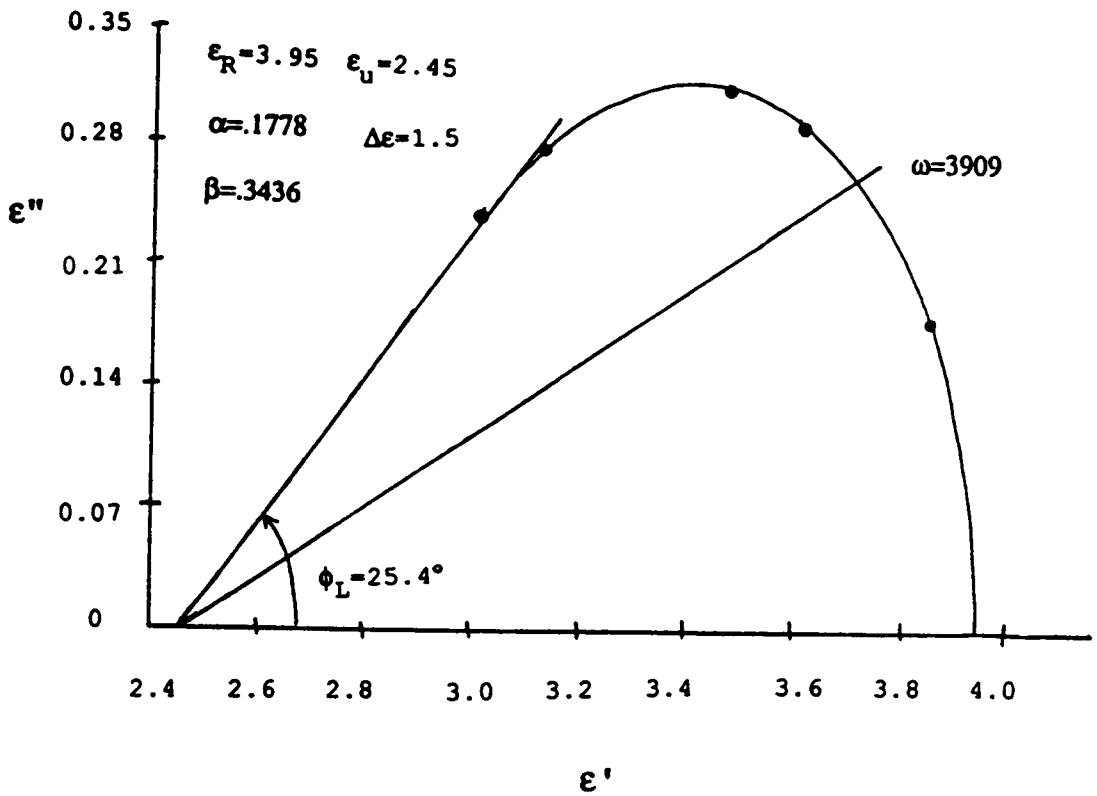

Figure 41. Evaluation of Havriliak-Negami parameters from the curve at 110°C in Figure 40

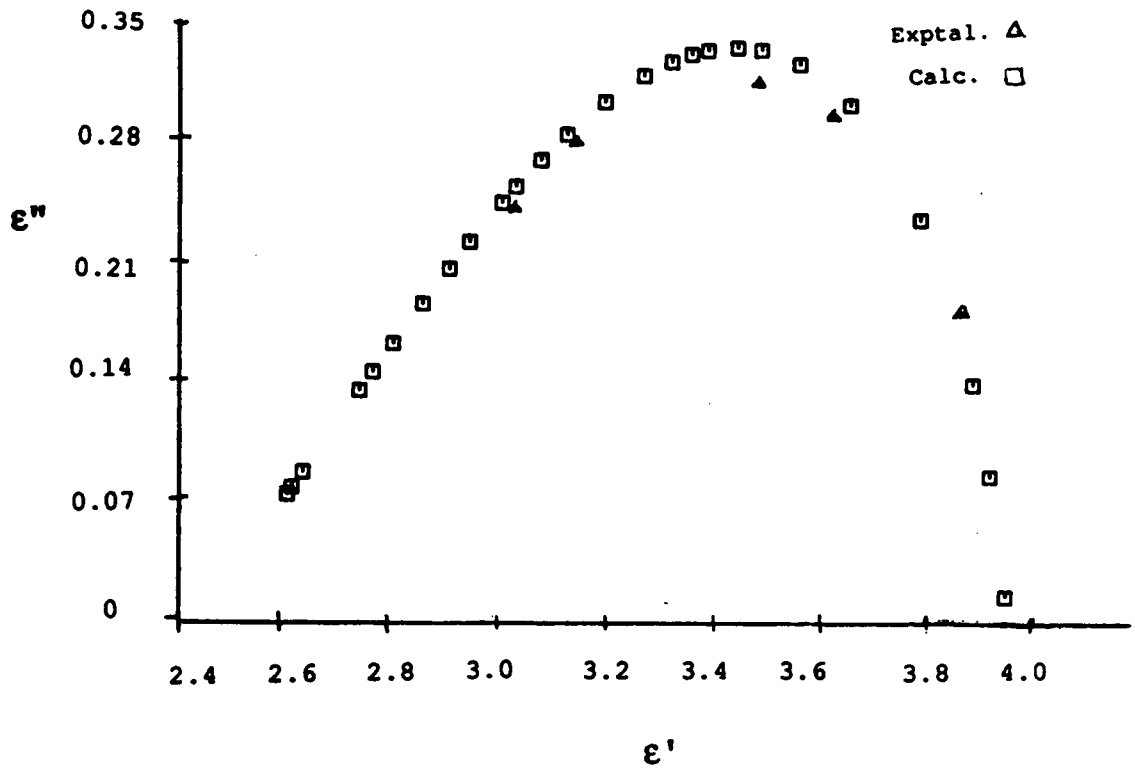

Figure 42. Comparison of the calculated and experimentally obtained values of ε'and ε"

Table 10

SUMMARY OF COLE-COLE ANALYSIS

Polymer	α	β	$\varepsilon_R - \varepsilon_u$	τ
S-PMMA	.245	.284	2.6-1.65	.000259
S-PTBMA	.178	.344	3.95-2.45	.000256
I-PTBMA	.318	.359	3.6-2.35	.000345
PMMA-PTBMA	.507	.434	2.75-1.75	.0002

it seems reasonable that I-PTBMA has a broader distribution of relaxation times (larger a). It also seems reasonable that the block copolymer would have the largest distribution because of the two components. The b parameter is more indicative of localized, short range motions and describes the skewness of the relaxation (smaller b, more skewed). The S-PMMA has the largest β relaxation, hence smallest b value.

E. Conclusions

In this study a series of well-controlled, stereospecific, anionically synthesized poly(alkyl methacrylates) were investigated. The techniques of dielectric and dynamic mechanical thermal analysis, as well as other characterization methods were used.

The β transition, associated with motions of the ester side group, was only observed in the syndiotactic PMMA and PEMA. The dielectric analysis was more sensitive to these motions due to the strong polarity of the ester group. As the alkyl side group increased in bulkiness the β transition decreased in size, indicating a weaker coupling with the applied fields. Due to the large and bulky groups in the isopropyl and t-butyl containing polymers, steric henderance prohibits this coupling from occuring. In all cases the α and β transitions merge at high frequencies. A wide range of glass transitions were observed depending on the

tacticity and the structure of the alkyl group.

When the ϵ' and ϵ'' data were plotted in a Cole-Cole fashion a skewed arc was observed. The breadth of the distribution of relaxation times increased in the following way: S-PTBMA < S-PMMA < I-PTBMA <PMMA-PTBMA block copolymer. However, this Cole-Cole analysis was somewhat tentative due to the limited number of frequencies investigated.

CHAPTER V

ANALYSIS OF ENGINEERING THERMOPLASTICS

A. Introduction

Engineering thermoplastics are becoming increasingly important due to their desirable stress/strain mechanical properties, toughness, and high temperature characteristics (87). It is well accepted that the high impact strength of polysulfone is strongly related to the low temperature β transition (14,88-90). This transition is observed at approximately -90°C at 1 Hz in a dynamic mechanical experiment and -75°C at 100 Hz in a dielectric experiment.

The purpose of this work was to study the effect of the chemical composition of the polymer backbone on the β transition in materials similar to polysulfone. Initially, UDEL^{TM}, a polysulfone purchased from Union Carbide, was characterized quite extensivly. These results were then compared to a series of poly(arylene ether sulfones) and poly(arylene ether nitriles) synthesized within Virginia Polytechnic Institute and State University. The structures of the UDEL^{TM} and the PEEK^{TM}, along with the other materials investigated, are shown in Figure 43. In addition to these homopolymers two copolymers shown in Figure 44 were also analyzed and compared to UDEL^{TM}. The effects of fillers and moisture was also studied for the UDEL^{TM} polysulfone case.

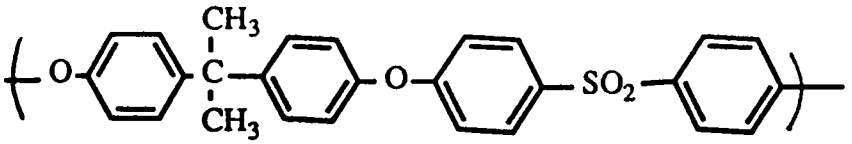

UDEL

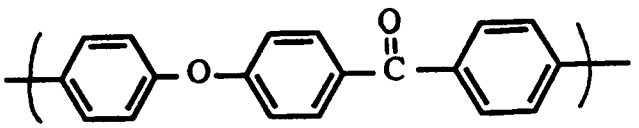

PEEK

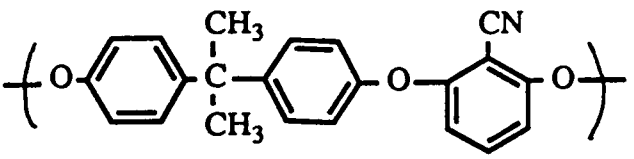

Poly(arylene ether nitrile)

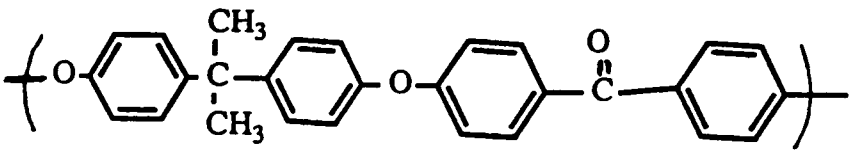

Bis-A-polyetherketone

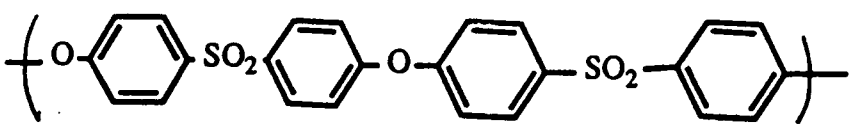

Bis-S-polysulfone

Figure 43. Engineering thermoplastic polymers investigated

50% Hydroquinone/50% Biphenol polysulfone

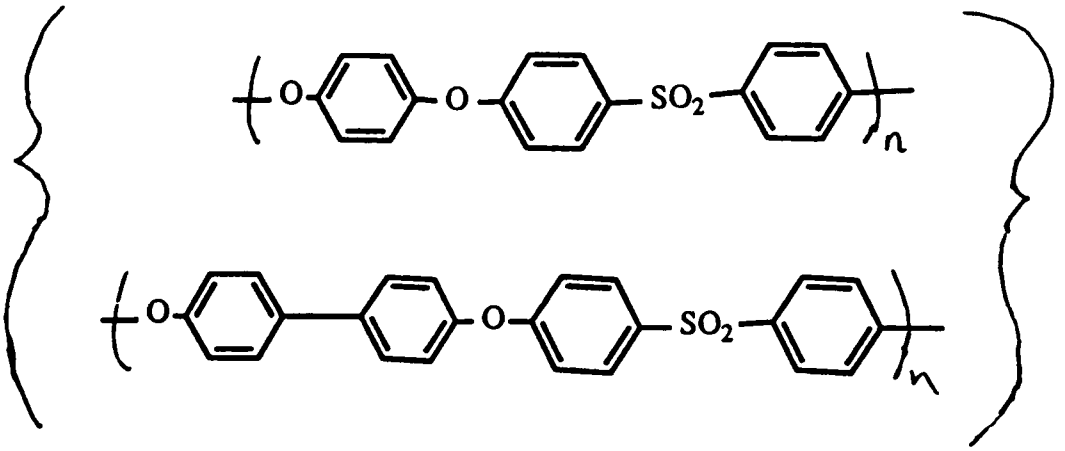

50% Bis-A/50% Biphenol polysulfone

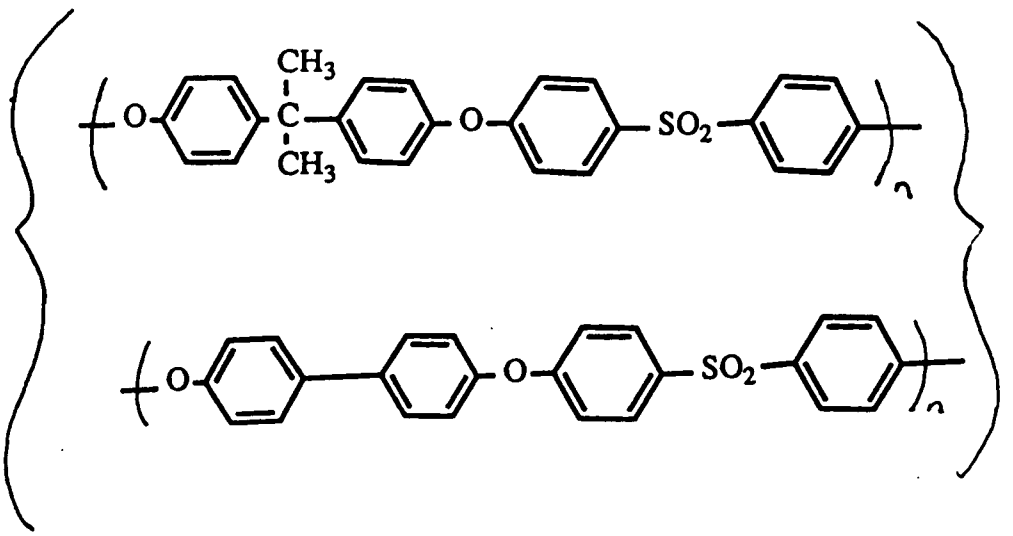

Figure 44. Engineering thermoplastic copolymers investigated

Both the dielectric and dynamic mechanical techniques were used to characterize these polymers, in addition to other thermal analysis investigations. It was observed that changing the chemical composition of the backbone for these engineering polymers did not effect the temperature at which the β transition was observed or the activation energy associated with this dispersion.

B. Background

A wide variety of engineering thermoplastic polymers have been examined over the last fifteen years. Due to their high thermal and hydrolytic stability, in addition to their excellent mechanical properties, these materials are being considered for many applications requiring high impact strength and as possible matrix resins for polymer composites. The commercialization of UDEL^{TM}, a polysulfone, and PEEK^{TM}, a poly(etheretherketone), has stimulated additional interest in the area.

Typically, these polymers have a strong low temperature β transition. It is believed that under high impacts (high frequency) the β transition shifts up in temperature to approximately room temperature in order to act as an energy absorbing mechanism. A quite intensive study was conducted on the quite similar poly(bisphenol-A carbonate) (91) in which the effects of thermal history, crystallinity, and solvent on the β and γ transitions was determined. These

factors all influence the impact strength of the material and change the mode of failure from ductile to brittle when it is also noted that these transitions are decreased in intensity.

C. Experimental

All polymers, except the UDEL, were all synthesized by Drs. James Hedrick and Dillip Mohanty in Professor J. E. McGrath's laboritories at Virginia Polytechnic Institute and State University (92,93). In general, the synthesis was similar for the poly(arylene ether sulfones) as it was for the poly(arylene ether nitriles).

1. Synthesis of Poly(arylene ether nitrile)

The poly(arylene ether nitrile) was synthesized using monomers 2,6-difluorobenzonitrile (and the chloro derivative) and bisphenol-A (see Figure 45a). The substituted benzonitrile was recrystallized from anhydrous ether and the bis-A from toluene. The monomers were added in a 1:1 mole ratio to a four-neck round bottom flask fitted with an overhead stirrer, gas inlet, thermometer, and a Dean-Stark apparatus fitted with a condenser with a drying tube. A total of 175 ml of N-methyl pyrrolidone was added. The polymerization was done under a N_2 atmosphere, a 40% molar excess of anhydrous K_2CO_3 was transfered to the reaction flask with 75 ml of toluene. The reaction flask was then heated to 160°C and water was removed by azeotropic distillation with toluene. Complete removal of water

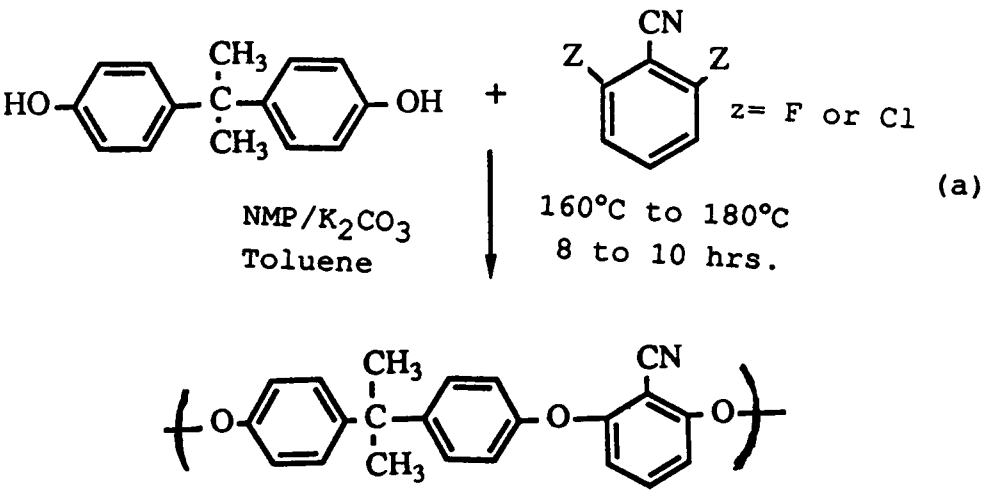

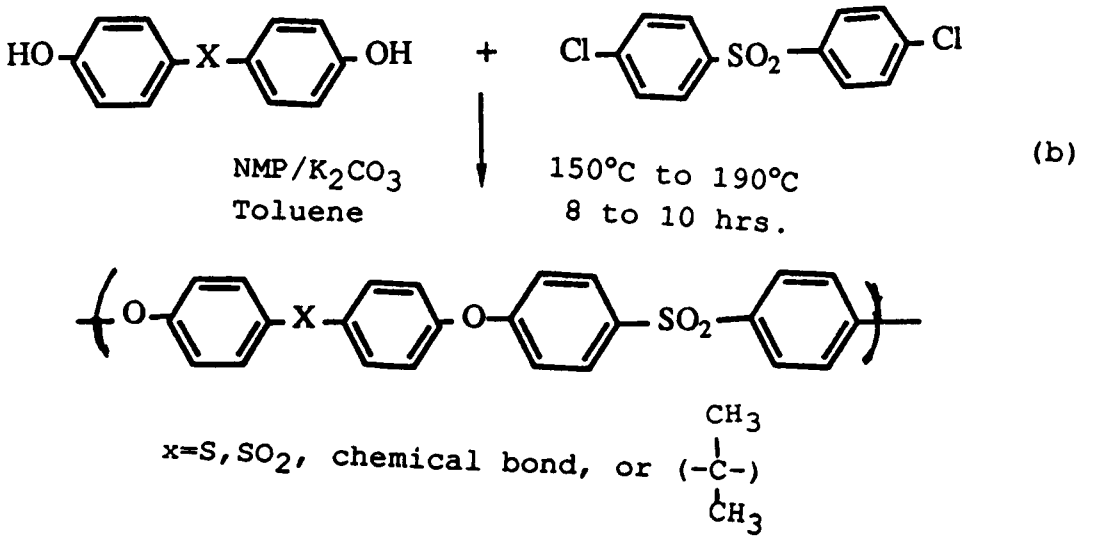

Figure 45. (a) Synthesis for poly(arylene ether nitrile)
(b) Synthesis for poly(arylene ether) sulfone

required 3 to 4 hours. The toluene was then removed and the reaction was held at 170°C for 8 to 10 hours. The cooled mixture was diluted with 300 ml of THF, filtered through a fritted funnel to remove any remaining salts. The polymer solution was acidified with glacial acetic acid to a pH of 7 and then precipitated in a 70/30 mixture of methanol/water, filtered and vacuum dried at 80°C for 10 hours.

A second 'clean-up' was done to insure complete removal of salts and NMP. This consisted of redissolving the polymer in THF, then filtering through a Buchner funnel. The solution was coagulated from a 50/50 mixture of methanol and water. The reprecipitated polymer was boiled in ethanol for 5 hours and then filtered and vacuum dried.

2. Synthesis of Poly(arylene ether)sulfones and ketones

The synthesis of the poly(arylene ether)sulfones and ketones is similar to that for the nitriles (Figure 44b). First the 4,4'-dichlorodiphenyl sulfone (or ketone), obtained from Union Carbide, was reacted with one or more of the recrystallized bisphenols in a 1:1 mole ratio. These monomers were added to a four-necked round bottom flask fitted with a nitrogen inlet, a thermometer, and a Dean-Stark trap fitted with a condenser. Distilled N-methyl-2-pyrrolidone (165 ml), anhydrous K_2CO_3, and 75 ml of toluene were added to the reaction flask. The reaction mixture was heated under reflux at 165°C until all the water was removed

via azeotropic distillation. The reaction mixture was cooled to 90°C and diluted with chorobenzene and filtered through a sintered glass funnel to remove any salts present. The filtrate was neutralized with glacial acetic acid. The polymer was precipitated from a methanol/water mixture and dried in a vacuum oven at 60°C.

A second 'clean-up' was done for complete removal of salts and NMP. This consisted of redissolving the polymer in THF (or methylene chloride), then filtering through a Buchner funnel. The solution was coagulated from a 50/50 mixture of methanol and water. The reprecipitated polymer was boiled in ethanol for 5 hours and then filtered and vacuum dried.

3. Instrumentation

The capacitance and dissipation factor measurements of these polymers were made on both the Polymer Laboratory Dielectric Thermal Analyzer (DETA), and the General Radio 1620A Capacitance Bridge assembly (see Chapter 2). The analyses were performed as a function of temperature over the frequency range of 100 Hz to 100 kHz and a temperature range of -100°C to 250°C.

The dynamic mechanical measurements were performed in the bending mode on the Polymer Laboratory Dynamic Mechanical Thermal Analyzer (DMTA) (see Chapter 2). A frequency of 1 Hz over a temperature range of -150°C to 200°C at 5°C/minute was utilized.

The glass transition (Tg) temperatures were determined on the Perkin Elmer Model 2 Differential Scanning Calorimeter (DSC-II) at a heating of 10°C/minute. In this work the glass transition temperatures quoted were determined from the midpoint of the observed transition. The Thermomechanical (TMA) and Thermogravimetric Analyses (TGA) were performed on the Perkin Elmer TMS-2and TGS-2. A heating rate of 10°C/minute in a nitrogen atmosphere was used.

The polymer's structure was confirmed in all cases using a Nicolet MX-1 Fourier Transform Infrared Spectrometer (FT-IR). Also a Varian FX-60-Q C-13 NMR spectrum of each polymer in $CHCL_3$ was obtained.

D. Results and Discussion

1. Poly(arylene ether nitrile)

This polymer was investigated primarily to determine what effect, if any, the polar nitrile group had on the transitions which had been observed dielectrically and mechanically in its absence. It was of interest to note that the pendant nitrile group should promote adhesion to metal substrates and would result in high intermolecular forces; this group may also represent a potential crosslinking site (94).

In the TMA scan (10 g load), shown in Figure 46, it is obvious that this polymer starts to soften at 170°C and that complete penetration occurs at 230°C. This is what would be

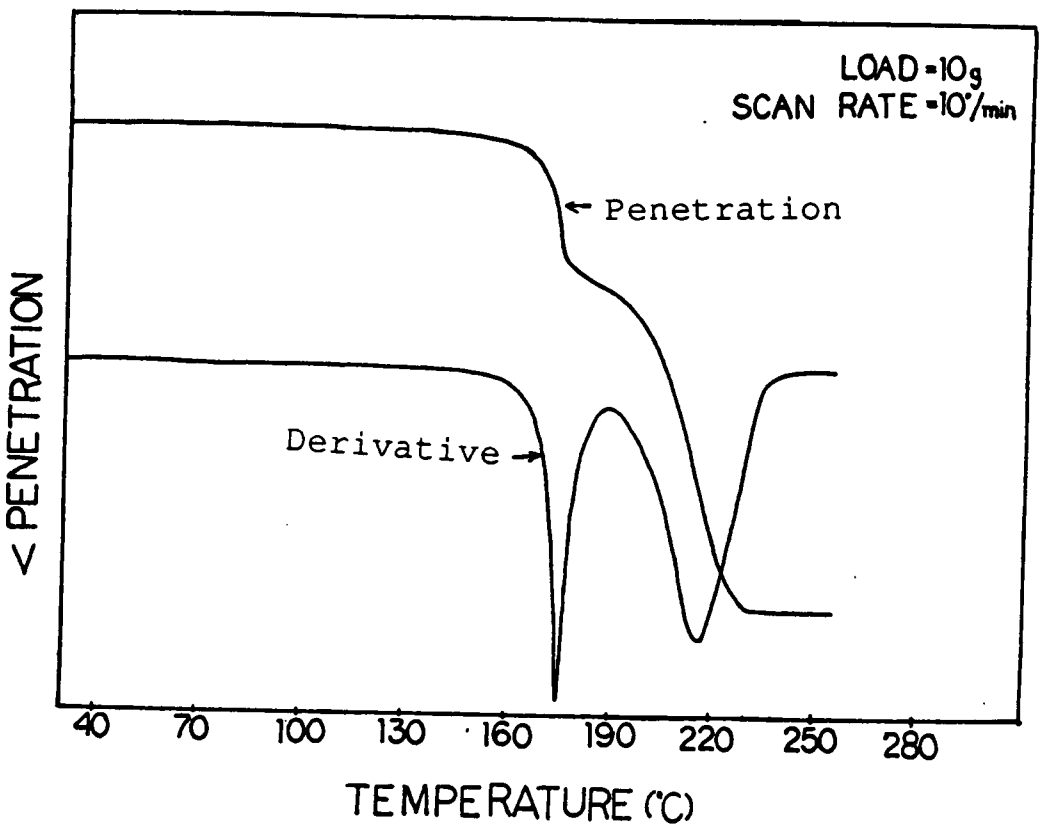

Figure 46. Thermal mechanical analysis of poly(arylene ether nitrile), 10°C/minute with a 10g load

expected considering the polymer has a Tg of 174°C.

The dynamic mechanical analysis performed in the two-point bend single cantelever beam mode at a constant strain and a frequency of 1 Hz is shown in Figure 47. The glassy modulus observed is slightly below the expected value of $1*10^9$ Pa due to the instrument's sensitivity to sample dimensions. The tan δ maximum at this frequency occurs approximately 4°C above the Tg and, as expected, the material appears to flow after it passes the glass transition temperature, with little rubbery plateau observed at these molecular weights.

Because the large electric dipole associated with the nitrile group, dielectric spectroscopy was considered. It was thought that this would be the only way to detect the specific intermolecular forces of association. It was postulated that if the bonding was strong enough a transition might be observed at a temperture above the Tg, where the dipole-dipole interactions break down. In Figure 48 the storage permittivity and tan δ values are plotted as a function of temperature at a frequency of 1000 Hz. A room temperature ϵ' value of 4.5 was observed for the poly(arylene ether nitrile), this is much higher then the value of 2.75 obtained for UDEL^{TM} measured in this lab at the same frequency. However, the value of 4.5 should be compared to the ϵ' value of 5.5 for poly(acrylonitrile) at 1 kHz (61). Of course poly(acrylonitrile) has a much higher concentration

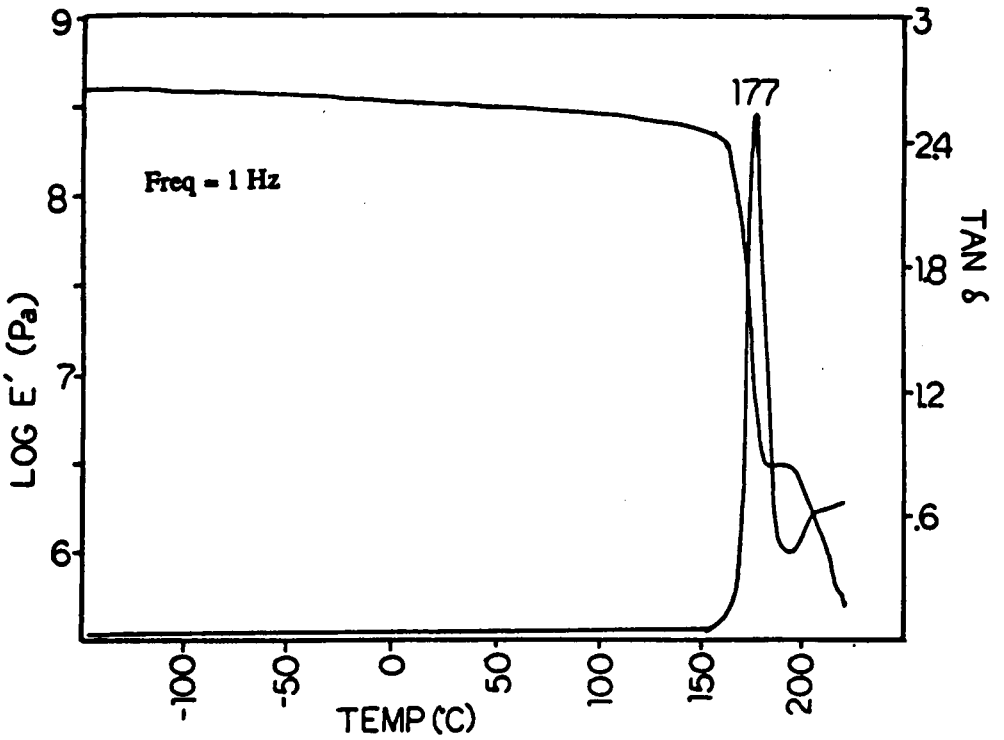

Figure 47. Dynamic mechanical thermal analysis of poly(arylene ether nitrile)

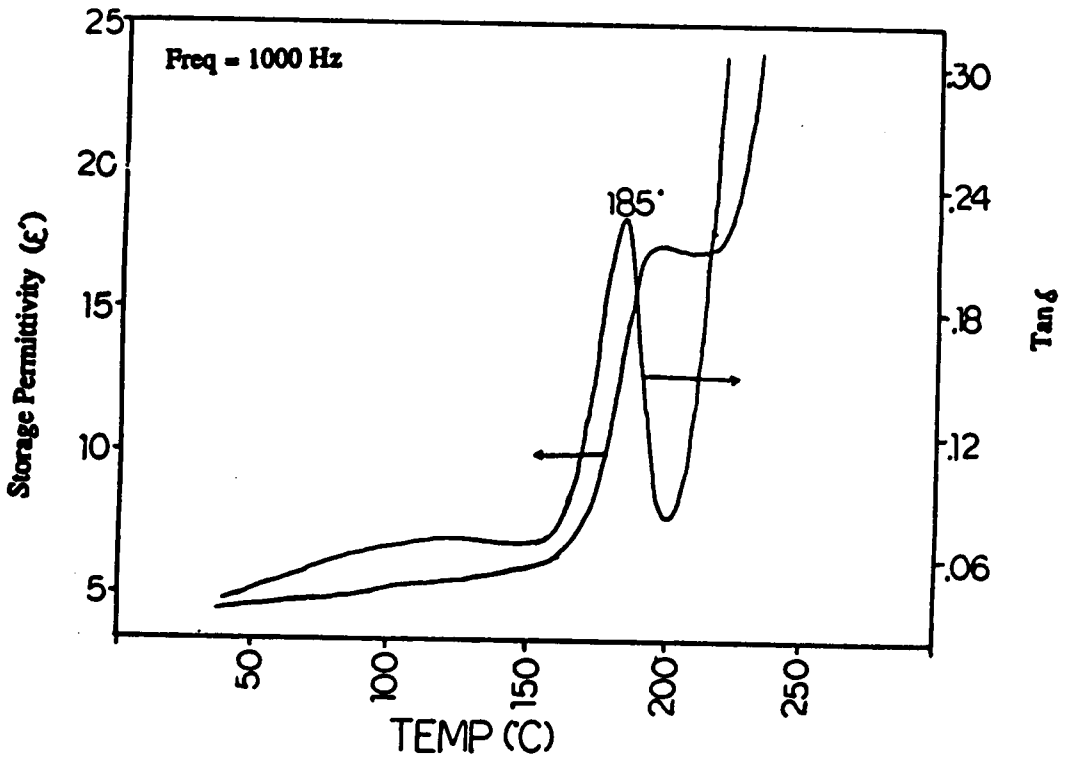

Figure 48. Dielectric thermal analysis of poly(arylene ether nitrile)

of nitrile groups per unit volume. In Figure 48 one can see a large change in the ϵ' with temperature, for this polymer ϵ' is approximately 12, whereas most nonpolar polymers show a ϵ' of about 3. This large change in the storage permittivity with temperature is possibly due to strong intermolecular forces, however, no transitions were observed above the Tg to indicate a breaking down of dipole-dipole interactions.

2. Poly(arylene ether) Sulfones and Ketones

In this part of the investigation a series of engineering homopolymers and copolymers, shown in Figures 43 and 44, were obtained as described above (95). The initial objective was to determine if systematic variations in the chemical structure influenced the β transition, with UDEL^{TM} to serve as a reference for the whole series. The low temperature dielectric results for UDEL^{TM} at three frequencies are shown in Figure 49. This transition is very broad, approximately 60°C, and calculations give an activation energy of 13 kcal/mole. This activation energy compares very well with the literature value of 12 kcal/mole (89). When Ea was determined for the β transition on the DMTA and DETA the same value was obtained; however, the dielectric transition was observed 30°C lower in temperature than the dynamic mechanical transition at the same frequency. In contrast, when the α transition was observed on the two instruments they were detected at appoximately the same

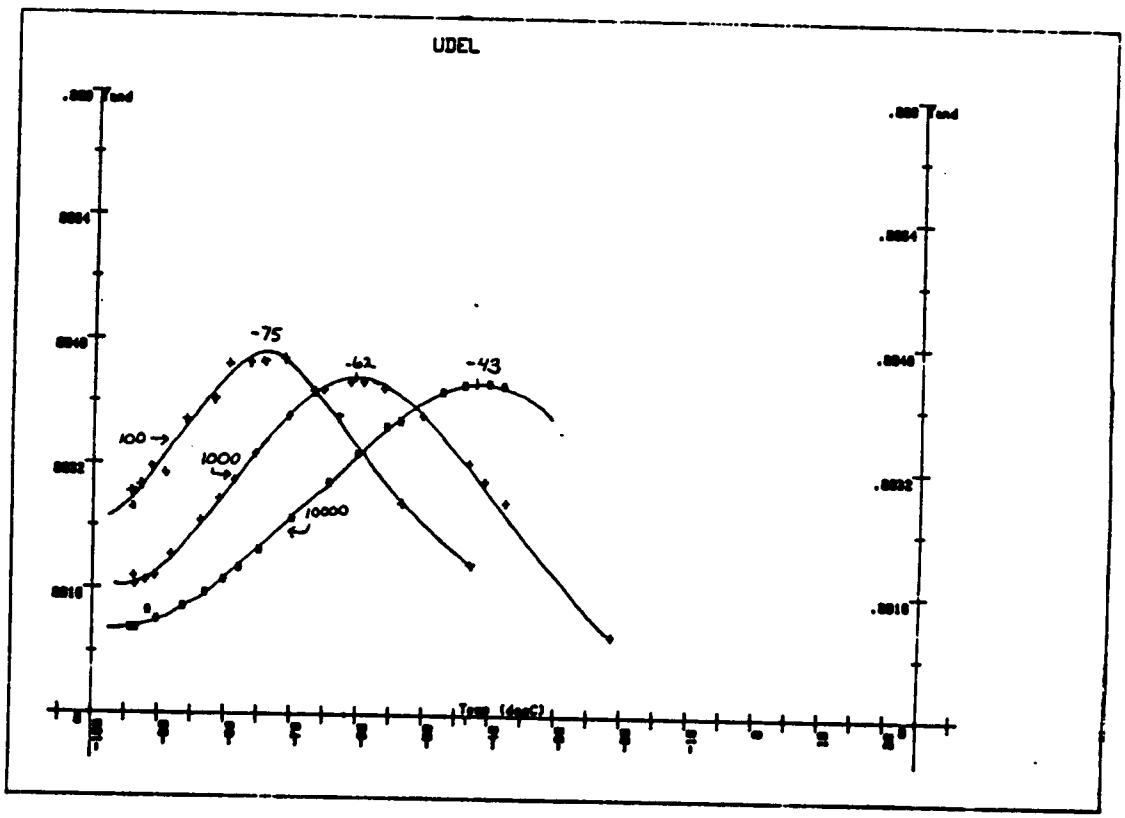

Figure 49. Low temperature dielectric scan of UDEL at three frequencies

temperature for the same frequency. Therefore, it appears that the molecular motions which are monitored at low temperature are more localized when observed with the dielectric experiment. The motions of the α transition seem the same for both experiments.

A very important factor in the performance of these engineering polymers is their ability to sorb water. The effect of water on UDEL^{TM} has been discussed by a number of scientists who feel water directly influences the magnitude of the β transition, by bonding to the SO_2 groups (90,95). In Figure 50 the presence of moisture in the material clearly has a direct effect on the magnitude of the transition.

Also in this study the effect of fillers on the dielectric response was investigated. As shown in Figure 51, filling the UDEL^{TM} with a Ti alloy filler at 15% by weight has shifted the transition up in temperature and broadened it. Here the polymer/filler interactions appear to be restricting the mobility of the groups responsible for the β transition.

Table 11 shows a summary of all of the polymers studied here. It appears that the β transition does not shift much in temperature with changes in the chemical composition of the polymer backbone. Only the Bis-A polyetherketone material has a β transition slightly higher in temperature than UDEL^{TM}, possibly due to the absence of the SO_2 groups. The activation energy for the β transition does not change

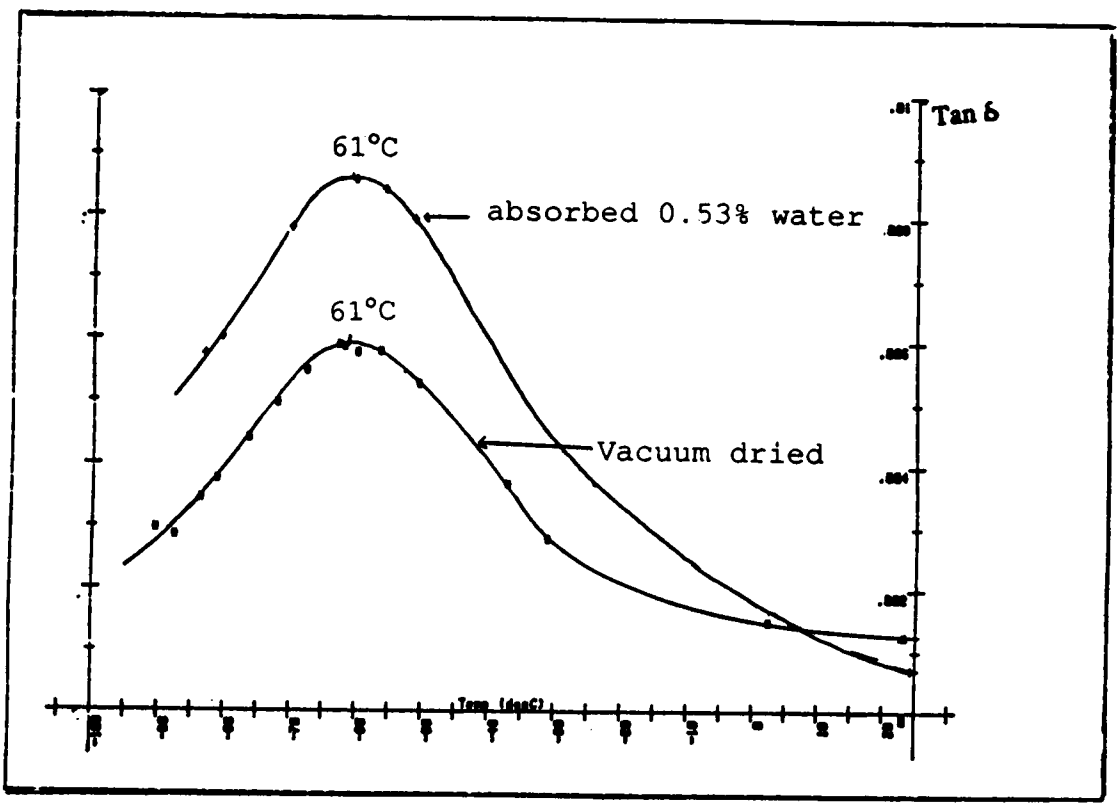

Figure 50. Effect of moisture on the β transition in UDEL polysulfone 1 kHz

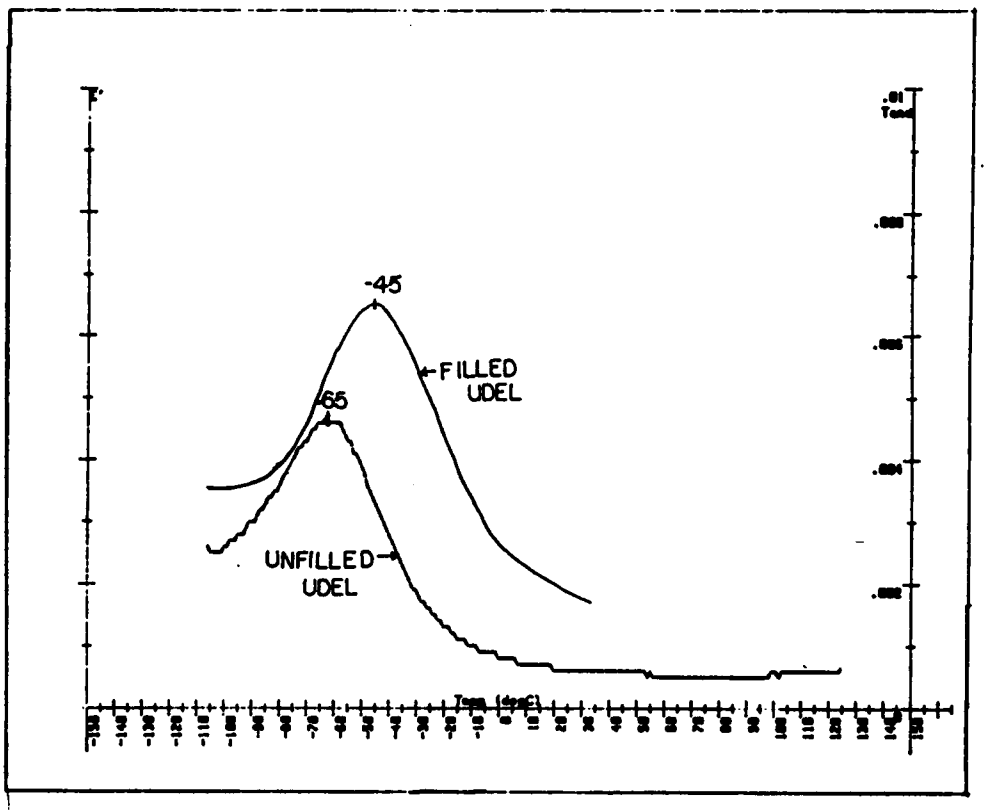

Figure 51. Effect of Ti filler on the β transition in UDEL polysulfone 1 kHz, 4°C/min

TABLE 11

SAMPLE	Temp. of Tan δ max.*	Ea(kcal/mol)	Tg
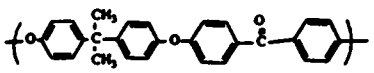	-41°C	12.3	160°C
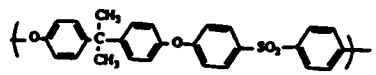	-61°C	13	190°C
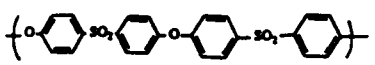	-60°C	12.2	180°C
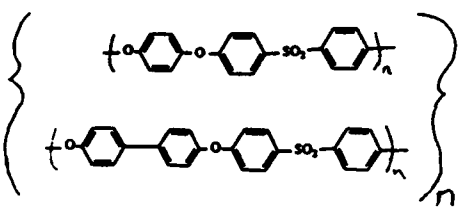	-57°C	11.5	217°C
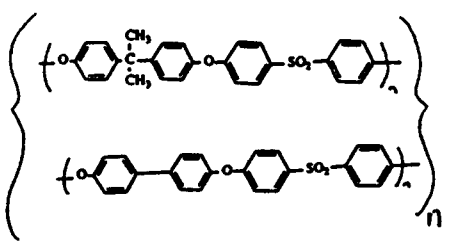	-60°C	11.9	—

*Dielectric experiment at 1000 Hz

for any of these polymers even though their structures are different.

E. Conclusions

In this study it appears that a few conclusions can be drawn. In the poly(arylene ether nitrile) analysis the high dipole detected results in a high dielectric constant; however, no dipole-dipole interactions were detected. The poly(arylene ether) sulfone and ketone investigations showed that the β transition does not shift much with structure and the activation energies do not change at all over a wide variation of backbone architectures. However, moisture and fillers play an important role on the magnitude and temperature of the β transition.

REFERENCES

1. R. T. Bailey, A. M. North, and R. A. Pethrick, *Molecular Motion in High Polymers*, Oxford University Press, New York, 1982.

2. N. G .McCrum, B. E. Read, and G. Williams, *Anelastic and Dielectric Effects in Polymeric Solids*, Wiley, New York, 1967.

3. P. Hedvig, *Dielectric Spectroscopy of Polymers*, Wiley, New York, 1977.

4. F. E. Karasz, *Dielectric Properties of Polymers*, Plenum Press, New York, 1972.

5. Y. Ishida, *J. Polym. Sci.: A-2*, 7, 1835 (1969).

6. R. H. Boyd, "Electrical Methods", in *Polymers, Methods in Experimental Physics*, R. A. Fava, (ed.), Academic Press, New York, 1980, p. 379.

7. C. P. Smyth, *Dielectric Constant and Molecular Structure*, J. J. Little and Ives Company, New York, 1931.

8. H. Frohlich, *Theory of Dielectrics, Dielectric Constant and Dielectric Loss*, Oxford University Press, New York, 1958.

9. J. J. Aklonis, W. J. MacKnight, *Introduction to Polymer Viscoelasticity, 2nd Ed.*, Wiley, New York, 1983.

10. J. D. Ferry, *Viscoelastic Properties of Solid Polymers, 3rd Ed.*, Wiley, New York, 1983.

11. I. M. Ward, *Mechanical Properties of Solid Polymers, 2nd Ed.*, Wiley, New York, 1983.

12. R. E. Wetton, M. R. Morton, and A. M. Rowe, *American Laboratory*, 18(1), 96 (1986).

13. T. G. Parker, "Dielectric Properties, II" in *Polymer Science*, Vol. II, A. D. Jenkins, (ed.), North-Holland Publishing Company, New York (1972), p.1298.

14. J. Heijboer, *Br. Polym. J.*, 1, 3 (1969).

15. H. Elias, *Macromolecules Vol. 1, Structure and Properties*, 2nd. Ed., Plenum Press, New York 1984.

16. F.A. Bovey and F. H. Winslow, *Macromolecules, An Introduction to Polymer Science*, Acedemic Press, New York, 1979.

17. Z. Arrhenius, *J. Phys. Chem.*, 4, 226 (1889).

18. R. H. Cole and K. S. Cole, *J. Chem. Phys.*, 9, 1484 (1941).

19. D. W. Davidson and R. H. Cole, *J. Chem. Phys.*, 9, 341 (1941).

20. S. Havriliak and S. Negami, *J. Polym. Sci. C*, No. 14, 99 (1966).

21. S. Havriliak and S. Negami, *Polymer*, 8, 161 (1967).

22. S. Negami, R. J. Ruch, and R. R. Myers, *J. Colloid Interf. Sci.*, 90, 117 (1982).

23. General Radio Company, "Instruction Manual for GenRad Type 1620-A Bridge", 1979, General Radio Co., Concord, MA.

24. W. E. Vaughan, C. P. Smyth, and J. G. Powles, "Determination of Dielectric Constant and Loss" in *Techniques of Chemistry*, Vol. 1, Part IV, A. Weissenberger, (ed.), Wiley-Interscience, New York, 1972, p. 351.

25. Gillian and Company, "Instruction Manual for LD-3 Research Cell", 1983, Gillian and Company, Watertown, MA.

26. ASTM-D-150-80 (1980).

27. Personal communication with Polymer Laboratories personel.

28. Polymer Laboratories, "Dielectric Thermal Analyzer Provisional Instruction Manual", 1985, Polymer Laboratories Ltd, Loughborough, Leicestershire, England.

29. Polymer Laboratories, "Dynamic Mechanical Thermal Analyzer Instruction Manual", 1983, Polymer Laboratories Ltd, Loughborough, Leicestershire, England.

30. R. E. Wetton, T. G. Croucher, and J. W. M. Fursdon, in *Polymer Characterization*, D. Craver, ed., ACS Symposium Series, #203, ACS, Washington DC, (1983).

31. A. Noshay and J. E. McGrath, *Block Copolymers: Overview and Critical Survey*, Academic Press, New York, 1977.

32. S. L. Cooper and G. M. Estes (eds.), *Multiphase Polymers*, Advances in Chemistry Series, 176, American Chemical Society, Washington D. C., 1979.

33. I. Goodman in *Developements in Block Copolymers*, Vol. 1 Applied Science, New York, 1982.

34. D. J. Meier, *J. Polym. Sci. Part C*, 26, 81 (1969).

35. D. J. Meier in *Block and Graft Copolymers*, J. J. Burke and V. Weiss, Eds, Syracuse University Press, NY (1973).

36. O. Olabisi, L. M. Robeson, and M. T. Shaw, *Polymer -Polymer Miscibility*, Acaemic Press, New York, 1979.

37. V. A. Kaniskin, A. Kaya, A. Ling, and M. Shen, *J. Appl. Polym. Sci.*, 17, 2695 (1973).

38. M. Shen, V. A. Kaniskin, K. Biliyar, and R. H. Boyd, *J. Polym. Sci., Polym. Phys.*, 11, 2261 (1973).

39. R. T. Jamieson, V. A. Kaniskin, A. C. Ouano, and M. Shen, "Viscoelastic and Dielectric Properties of A-B-A Type Block Copolymers", in *Adv. in Polym. Sci. and Eng* .,Plenum Press, New York (1972).

40. J. C. Maxwell, *Electricity and Magnetism*, 1, 452, Clarendon Press, Oxford (1892).

41. R. W. Sillars, *J. Inst. Elect. Engineers*, 80, 378 (1937).

42. K. W. Wagner, *Arch. Electrotech.* 2, 378, (1914).

43. A. M. North and J. C. Reid, *Eur. Polym. J.*, 8, 1129 (1972).

44. L. K. H. van Beek, "Dielectric Behavior of Heterogeneous Systems" in *Progress in Dielectrics*, Vol. 7, CRC Press, Cleveland (1967).

45. A. M. North, R. A. Petrick, and A. D. Wilson, *Polymer*, 19, 913 (1978).

46. A. M. North, R. A. Pethrick, and A. D. Wilson, *Polymer*, 19, 923, (1978).

47. J. M. Hoover, T. C. Ward, and J. E. McGrath, *Polym. Preprints*, 26(1), 253 (1985).

48. J. M. Hoover, T. C. Ward, and J. E. McGrath, Rubber Division (ACS), L.A. Meeting, April, 1985.

49. M. M. Sheridan, J. M. Hoover, T. C. Ward, and J. E. McGrath, *Polym. Preprints*, 26(1), 186 (1985); M. M. Sheridan, Ph.D. Thesis, Virginia Polytechnic Institute and State University, Dec. 1985.

50. P. K. Das, J. M. Hoover, T. C. Ward, and J. E. McGrath, *Polym. Preprints*, 25(2), 96 (1984).

51. J. Scott, M.S. Thesis, Virginia Polytechnic Institute and State University, Dec. 1986.

52. A. M. Walstrom, J. M. Hoover, T. C. Ward, and J. E. McGrath, *Polym. Preprints*, 26(1), 193 (1985).

53. J. E. Hoover and J. E. McGrath, *Polym. Preprints*, 27(2), 150 (1986).

54. D.B. Alward, D. J. Kinning, E. L. Thomas, and L. J. Fetters, *Macromolecules*, 19, 215 (1986).

55. D. J. Kinning, E. L. Thomas, D. B. Alward, L. J. Fetters, and D. L. Handlin Jr., 19, 1288, (1986).

56. Polymer Laboratory, "Dynamic Mechanical Thermal Analyzer Instruction Manual", 1983, Polymer Laboratories Ltd., Loughborough, Leicestershire, England.

57. D. G. Fesko and N. W. Tschoegl, *J. Polym. Sci.*, Part C, 35, 51(1971).

58. M. L. Williams, R. F. Landel, and J. D. Ferry, *J. Amer. Chem. Soc.*, 77, 3701 (1955).

59. D. W. Van Krevelen, *Properties of Polymers*, Elsevier Scientific, New York, 1976, p. 142.

60. L. E. Nielsen, *Predicting the Properties of Mixtures: Mixture Rules in Science and Engineering*, Mercel Dekker, Inc., New York, 1978.

61. J. Brandrup and E. H. Brandrup, *Polymer Handbook*, 2nd Edition, John Wiley and Sons, New York, 1978.

62. J. D. Stroupe and R. E. Hughes, *J. Am. Chem. Soc.*, 80, 2341 (1958).

63. S. Bywater and P. M. Toporowski, *Polymer*, 13, 94 (1972).

64. F. E. Karasz and W. J. MacKnight, *Macromolecules*, 1, 53 (1968).

65. S. S. Roger and L. Mamdelkern, *J. Phys. Chem.*, 61, 985 (1957).

66. G. P. Mikhaelov and T. I. Borisova, *Polym. Sci., USSR*, 2, 387 (1961).

67. Y. Ishida, S. Togami, and K. Yamafuji, *Kolloid. Zeit.* 222, 16 (1968).

68. Y. Ishida, S. Togami, and K. Yamafuji, *Polym. Letters*, 5, 745 (1967).

69. J. Heijboer, *Makromol. Chem.*, 35A, 86 (196).

70. Y. Tanabe, J. Hirose, K. Okano, and Y. Wada, *Polym. J.*, 1, 107 (1970).

71. K. Shimizu, O. Yana, and Y. Wada, J. Polym. Sci.: Polym. Phys., 23, 1297 (1985).

72. J. L. G. Ribelles and R. D. Calleja, *J. Polym. Sci.: Polym. Phys.*, 23, 1297 (1985).

73. M. A. Desando, M. A. Kashem, M. Siddiqui, and S. Walker, *J. of Chem. Soc. of London, Trans. Fara. Soc.*, 747 (1984).

74. T. E. Long, R. Subramanian, T. C. Ward, and J. E. McGrath, *Polym. Preprints*, 27(2), 259 (1986).

75. T. E. Long, R. D. Allen, and J. E. McGrath, *Polym. Preprints*, 27(2), 54 (1986).

76. R. D. Allen, T. E. Long, and J. E. McGrath, in *Advances in Polymer Synthesis*, Vol. 13, B. M. Culbertson and J. E. McGrath (eds.), Plenum Pub. Corp., New York, 1985, p. 347.

77. T. E. Long, R. D. Allen, and J. E. McGrath, "Controlled Synthesis of Various Poly(alkyl methacrylates) by Anionic Techniques", NATO Meeting, Bandor, France, Feb. 2-6, 1987; submitted for publication, 1987.

78. M. Morton, *Anionic Polymerization: Principles and Practice*, Academic Press, New York, 1983.

79. R. D. Allen, T. E. Long, and J. E. McGrath, *Polym. Bulletin*, 15, 127 (1986).

80. Z. Grubisic, P. Rempp, and H. Benoit, *Polym. Letters*, 5, 759 (1967).

81. A. M. Walstrom,R. Subramanian, T. E. Long, J. E. McGrath, and T. C. Ward, *Polym. Preprints*, 27(2), 135 (1986).

82. H. Yuki, K, Hatada, K. Ohta, and Y. Okamoto, *J. Macromol. Sci.-Chem.*, A9(6), 983 (1975).

83. W. Graessley, "Viscoelasticity and flow on Polymer Melts and Concentrated Solutions" in *Physical Properties of Polymers*, J.E. Mark, A. Eisenberg, W. Graessley, L. Mandelkern, and J. L. Koenig (eds.), ACS, Washington DC (1984).

84. M. A. Haney, *J. Appl. Poly. Sci.*, 30, 3023 (1985).

85. M. A. Haney, *J. Appl. Poly. Sci.*, 30, 3037 (1985).

86. H. Elias, *Macromolecules Vol. 1, Structure and Properties*, 2nd Ed., Plenum Press, New York (1984).

87. R. D. Deanin, *New Industrial Polymers*, ACS Symposium Series #4, ACS, Washington, D.C., (1972).

88. C. I. Chung and J. A. Sauer, *J. Polym. Sci.*: A-2, 9, 1097 (1971).

89. M. Baccaredda, E. Butta, V. Frosini, and S. De Petris, *J. Polym. Sci.*: A-2, 5, 1296 (1967).

90. G. Allen, J. McAinsh, and G. M. Jeffs, *Polymer*, 18, 85 (1971).

91. K. Varadarajan amd R. F. Boyer, *J. Polym. Sci.: Polym. Phys. Ed.*, 20, 141 (1982).

92. J. L. Hedrick, Ph. D. Thesis, Virginia Polytechnic Institute and State University, March 1986.

93. D. K. Mohanty, Ph. D. Thesis, Virginia Polytechnic Institute and State University, June 1983.

94. D. K. Mohanty, A. M. Walstrom, T. C. Ward, an McGrath, *Polymer Preprints*, 27(2), 147(1986).

95. D. K. Mohanty, J. L. Hedrick, K. Gobetz, B. C. Johnson, I. Yilgor, E. Yilgor, R. Yang, and J. E. McGrath, *Polymer Preprints*, 23(1), 284 (1982).

96. J. R. Fried and H. Kalkanoglu, *J. Polym. Sci.: Polym. Letters Edition*, 20, 381 (1982).

Appendix A. Comparison of Data Obtained from the GenRad Bridge and the Polymer Lab's DETA

Portions of the dielectric data, accumulated in this dissertation, were obtained on the General Radio Bridge and some on the Polymer Lab's Dielectric Thermal Analyzer (DETA). Typically no discrimination was made when one was used versus the other because the two instruments were in good agreement.

Figure A1 shows the tan δ curves at 1000 Hz for S-PEMA obtained from the two instruments. Both give the same tan δ peak maximum temperature and the same general shape. The magnitutes of the tan δ peaks do not coincide, but typically in this analysis the magnitude is not reproducible. To do this one needs to normalize all the tan δ values relative to the maximum value.

In Figure A2 the tan δ curves for the syndiotactic PMMA-PTBMA block copolymer from both instruments are shown. It is important to note that the GenRad curve was obtained at 100 Hz whereas the DETA curve was obtained at 200 Hz and therefore is shifted up in temperature. The shapes of the two curves are almost identical with the α transition being only a shoulder of the β transition.

The last comparison is in the calculated activation energies for isotactic PTBMA. The GenRad Bridge gave a value of 37.9 kcal/mole and the DETA instrument gave a value of 36.1 kcal/mole, these values are within the expected experimental error of approximately $\pm$ 3 kcal/mole.

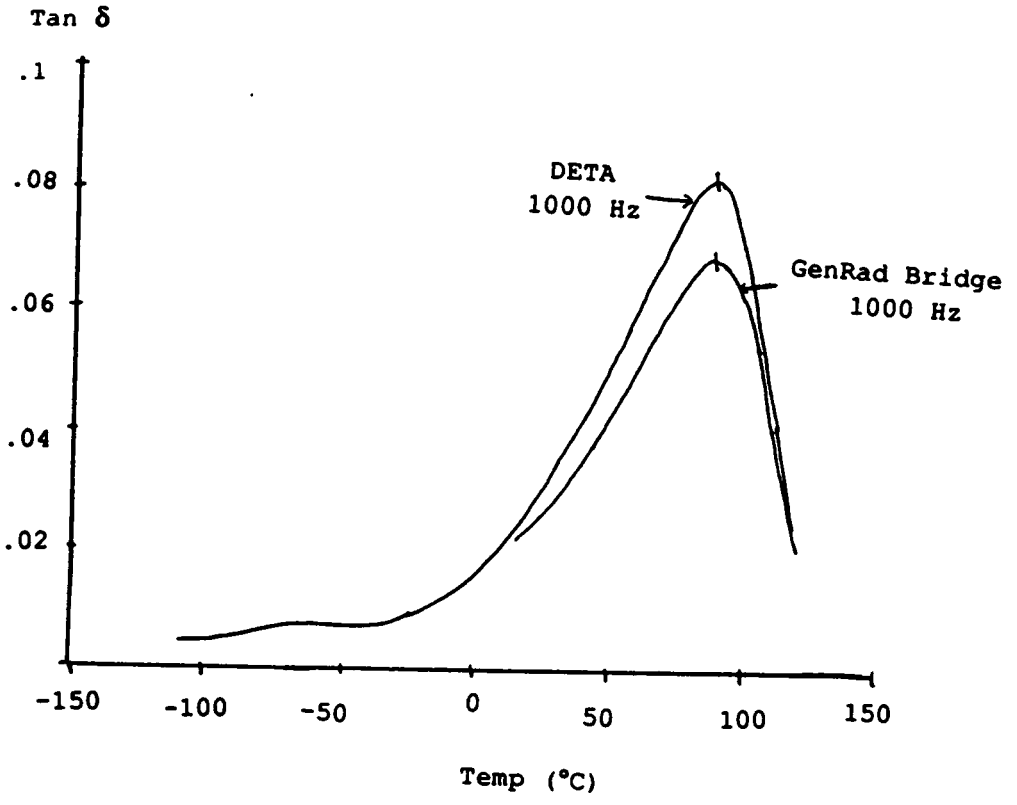

Figure A1. Comparison of Polymer Labs' DETA and the GenRad Bridge for syndiotactic PEMA

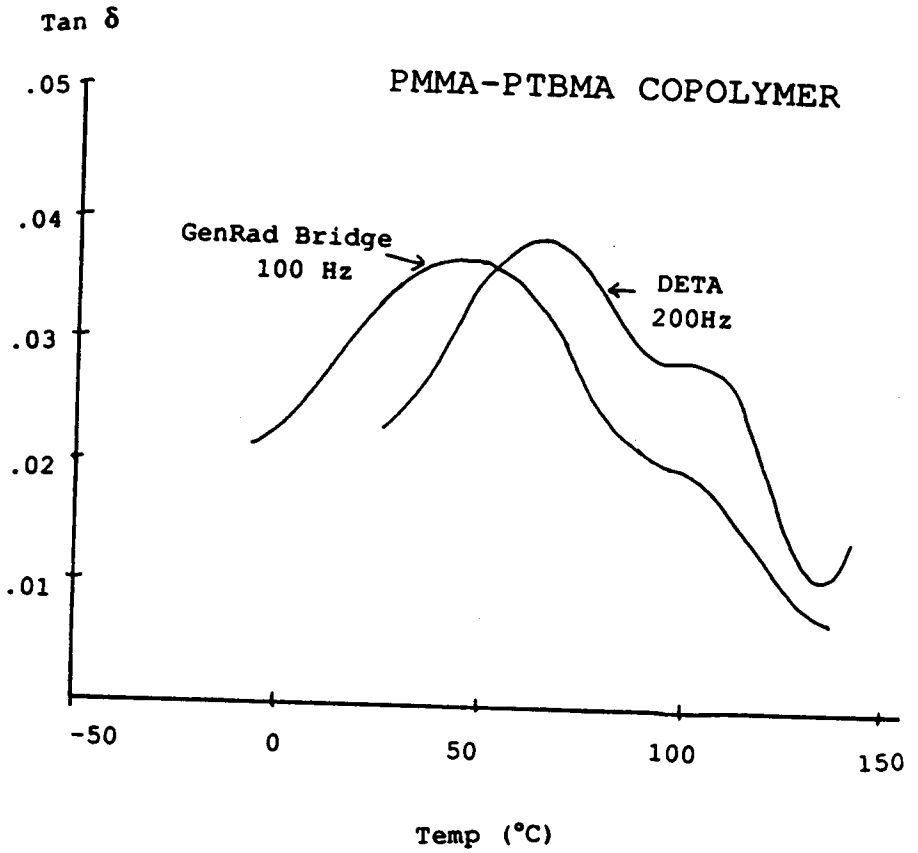

Figure A2. Comparison of Polymer Labs' DETA and the GenRad Bridge for PMMA-PTBMA block copolymer

Appendix B. DETERMINATION OF HAVRILIAK-NEGAMI PARAMETERS

The following is a detailed description of how to calculate the parameters of the Havriliak-Negami equation. Also discussed is the calculation of theoretical values of ϵ' and ϵ''. These will check the accuracy of the graphically determined parameters and also give data outside the range of the instrument (20,21).

1. Plot ϵ' versus ϵ'' values at each frequency examined for a given temperature, preferably a temperature which gives data over the entire relaxation spectrum region.

2. Graphically estimate the high frequency value ϵ_u and the low frequency value ϵ_R; both are the intercepts of the arc at $\epsilon''=0$.

3. Determine the limiting angle, ϕ_L, that the high frequency data make with the real axis ϵ'. It's bisector, $\phi_L/2$, will intersect the arc at a frequency which is equal to $1/\tau_0$ (the relaxation time^{-1}), (See Figure 8b).

4. Once the above values have been established, α can be calculated by the following equation:

$$\frac{1}{\phi_L} \log\left(\frac{R}{\epsilon_R - \epsilon_u}\right) = -\frac{1}{\pi(1-\alpha)} \log\left(2+2\sin\frac{\pi\alpha}{2}\right)$$

$$R=[\epsilon''^2(\omega\tau_0=1)+\{(\epsilon'(\omega\tau_0=1)-\epsilon_u)^2\}]^{1/2}$$

5. Once α is known β can be calculated from the following equation:

$$\phi_L=(1-\alpha)\beta\pi/2$$

6. Now any theoretical values of the modified Cole-Cole type plot can be calulated for any frequency using the following four equations:

$$\epsilon'(\omega)=\epsilon_u+r^{-\beta/2}*(\epsilon_R-\epsilon_u)\cos(\beta\theta)$$

$$\epsilon''(\omega)=r^{-\beta/2}*(\epsilon_R-\epsilon_u)\sin(\theta\beta)$$

$$r=\{1+(\omega\tau_0)^{(1-\alpha)}\sin\alpha\pi/2\}^2 + \{(\omega\tau_0)^{(1-\alpha)}\cos\alpha\pi/2\}^2$$

$$\theta=\text{ArcTan}\frac{(\omega\tau_0)^{(1-\alpha)}\cos\alpha\pi/2}{1+(\omega\tau_0)^{(1-a)}\sin\alpha\pi/2}$$

7. A computer program for the HP9816 was written in BASIC to do the above mentioned calculations for ϵ' and ϵ'' at any frequency:

```
100 PRINTER IS 1
101 ! E0 IS LOW FREQ STORAGE PERM
102 ! E1 IS HIGH FREQ STORAGE PERM
105 ! CALC THEOREDICAL VALUES FOR COLE-COLE PLOT FOR ANY
FREQ
108 ! A IS ALPHA, B IS BETA, T IS RELAXATION TIME
110 PRINTER IS 701
115 PRINT "   FREQ(HZ)   STORAGE PERM    LOSS PERM"
120 PRINTER IS 1
125 INPUT "E0,E1,A,B,T",E0,E1,A,B,T
130 INPUT "W",W
135 IF W=0 THEN GOTO 180
140  R=(1+((W*T)^(1-A))*(SIN(A*PI/2)))^2+(((W*T)^(1-
A))*(COS(A*PI/2)))^2
145  L=ATN((((W*T)^(1-A))*COS(A*PI/2))/(1+((W*T)^(1-
A))8SIN(A*PI/2)))
150 STORAGE_PERM=E1+((R^(-B/2))*(E0-E1)*COS(L*B))
155 LOSS_PERM=(R^(-B/2))*(E0-E1)*SIN(L*B)
160 PRINTER IS 701
165 PRINT USING IM1;W,STORAGE_PERM,LOSS_PERM
170 IM1: IMAGE 3X,DDDDDDD,9X,DD.DDDD,9X,D.DDDD
175 GOTO 130
180 END
```

The vita has been removed from the scanned document